Doctoral Dissertation

Human-like Haptic Assistance: Performance-based Haptic Assistance Using Neural Networks for Driving Skill Enhancement and Training

Hojin Lee (이 호 진)

Department of Computer Science and Engineering

Pohang University of Science and Technology

2019

인간-유사 햅틱 어시스턴스:
운전 기능 향상 및 교육을 목적으로
인공 신경망을 사용한
성능-기반 햅틱 어시스턴스

Human-like Haptic Assistance:
Performance-based Haptic Assistance
Using Neural Networks
for Driving Skill Enhancement and Training

Human-like Haptic Assistance: Performance-based Haptic Assistance Using Neural Networks for Driving Skill Enhancement and Training

by

Hojin Lee

Department of Computer Science and Engineering

Pohang University of Science and Technology

A dissertation submitted to the faculty of the Pohang University of Science and Technology in partial fulfillment of the requirements for the degree of Doctor of Philosophy in the Computer Science and Engineering

Pohang, Korea

12. 19. 2018

Approved by

Seungmoon Choi (Signature)

Academic advisor

Human-like Haptic Assistance: Performance-based Haptic Assistance Using Neural Networks for Driving Skill Enhancement and Training

Hojin Lee

The undersigned have examined this dissertation and hereby certify that it is worthy of acceptance for a doctoral degree from POSTECH

12. 19. 2018

Committee Chair   Seungmoon Choi   (Seal)

Member   Sung H. Han   (Seal)

Member   Minsu Cho   (Seal)

Member   Hwangjun Song   (Seal)

Member   Seokhee Jeon   (Seal)

DCSE   이 호 진. Hojin Lee

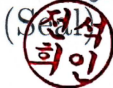20100825   Human-like Haptic Assistance:

           Performance-based Haptic Assistance

           Using Neural Networks

           for Driving Skill Enhancement and Training,

           인간-유사 햅틱 어시스턴스:

           운전 기능 향상 및 교육을 목적으로

           인공 신경망을 사용한

           성능-기반 햅틱 어시스턴스

           Department of Computer Science and Engineering , 2019,

           118p, Advisor :   Seungmoon Choi. Text in English.

ABSTRACT

A driving skill is a routine sensorimotor skill, regarded as a fascinating but a challenging research target in the area of sensorimotor skill control and learning. In this thesis, we propose human-like haptic assistance, an advanced data-driven framework using artificial neural networks and performance-based haptic feedback, for driving skill enhancement and training.

As an initial study, we conducted a training experiment to show the feasibility of hybrid haptic assistance that combines two haptic assistance methods (haptic guidance and disturbance) for virtual steering task. In the hybrid scheme, haptic guidance is used in the initial phase of learning, but it is progressively turned into haptic disturbance as the learner's performance improves. Experimental

results indicate some advantages of hybrid scheme, but did not show statistically significant differences in any retention tests.

To extend the prior work to practical driving, we developed a haptic driving training simulator which can provide realistic driving experiences. We recruited experienced drivers and recorded their driving data by using the simulator. Then, we trained neural networks with the collected data to obtain the optimized skill models which can predict the expert drivers' steering and pedaling behavior. We tried to show the validity and applicability of our modeling approach in human experiments. In results, our approach was valid to extract expert driving skills. However, only the steering model was applicable to performance-based haptic feedback.

Therefore, we implemented an autopilot algorithm using both expert skill models instead of performance-based haptic feedback, and conducted a test of autopilot runs on various paths. In results, the autopilot algorithm utilized by expert skill models can complete driving on every path. Further, we found the simulator can shows a steering control similar to human behavior due to the models trained by human expert drivers. Therefore, we named our framework as human-like haptic assistance, and we implemented human-like haptic guidance under this framework.

We conducted a final training experiment comparing two performance-based, progressive haptic assistance methods for steering skill: human-like haptic guidance and conventional robotic haptic guidance. In results, human-like haptic guidance showed a better performance improvement than robotic haptic guidance in both the accuracy and stability, because it mirrors an intrinsic nature of human steering skill. In conclusion, our human-like haptic assistance can be

effective on driving skill enhancement and training, and also it can be extendable to other sensorimotor skills such as trajectory-following.

Contents

List of Tables

List of Figures

I. Introduction

1.1 Preface: Research Motivation

Humans like us always make movements (motions). We breathe, walk and run to move to other locations, we play games and sports to have a fun, and we manipulate tools and objects to perform everyday functions. There are two main forms of human movements: one form is based on inherited, intrinsic movements such as eye blinking and breathing, and another form is based on learned movements [69]. In this thesis, the author is focusing on the later one, the learned movements.

Most of those movements have a specific goal; often we call a such goal as a task. A *sensorimotor task* requires the process of (1) perceiving various sensory information such as visual, auditory, haptic sensations and (2) reacting through movements. To achieve a better outcome of sensorimotor tasks, humans perceive environmental information from sensory channels beforehand, and then they intentionally move their body (muscles and joints) to perform voluntary actions. After the sufficient experience (or, practice) for the sensorimotor task, we learn; our cognitive reactions and behavioral movements become optimized according to the environmental states. The optimized behavioral control strategy against a sensorimotor task is usually called a *sensorimotor skill*. See this definition of the skill: "the ability to bring about some end result with maximum certainty and minimum outlay of energy or of time and energy" [25]. A sensorimotor skill, hence, includes human movements with increased efficiency of temporal and special movements without inefficient consumption of physical energy in a particular task circumstance.

In previous decades, experimental psychologists have investigated the behavioral nature of sensorimotor skill control and learning. In this area, controlling an automobile (so-called *driving*) is regarded as a fascinating research domain for several reasons. First, driving a car is routine in this era; automobiles are common, and individuals know what the driving skill is. Therefore, understanding the nature of driving has a high potential to contribute to the society, because it is a general and practical research domain. Second, driving is a representative sensorimotor skill composed of learned movements such as steering and pedaling. With simple limbs movements on mechanical manipulators (a steering wheel, accelerator and brake pedals), humans can control an automobile to move to other locations. Therefore, by measuring the kinematic and dynamic parameters of the manipulators, limb movements can be easily quantified to obtain the numerical task performance. Third, nevertheless, driving is a more challenging research target, compared to conventional targets like reaching/walking tasks. The dynamic and complex controls and movements of human bodies underlie in the driving skill. It requires a high cognitive load of visual-motor coordination to take a correct and safe action. Further, to control a nonholonomic vehicle, the skill requires simultaneous operations of manipulators based on a coordinated motion of limbs. However, this nature of driving frequently makes novice drivers feel unfamiliar and frustrated before their skill levels become mature.

We still face to a lot of research demands to understand the principles on human control and learning for the driving skill. To this end, as a research continuum and a solution to those demands, the author introduces *human-like haptic assistance*, a novel approach to (1) enhance human driving execution and (2) educate the driving skill to novice drivers. The idea includes a robot-mediated framework conflating various technologies such as artificial neural networks and haptic assistance.

1.2   Research Goal

Our framework mainly includes two main ideas.

First, artificial neural networks have been utilized to model an expert driving behavior under considerations of human skill strategies. We collected execution data of experienced drivers using a driving simulator, and then obtained a expert skill model using the neural networks trained by the recorded data. Because our model has been established by experienced human drivers, our performance-based haptic assistance has a human-like driving behavior. We hypothesize that this characteristics of our approach can induce unique effects for human drivers (learners).

Therefore, second, the model has been applied to performance-based haptic assistance, which embraces every form of robot-mediated training that utilizes haptic feedback based on human task performance. In this thesis, we conducted consecutive human experiments utilizing haptic feedback to show the modeling validity and the effectiveness of our approach for driving skill enhancement and training. The rest of this chapter contains a summarized contributions and an overview of this research.

1.3   Contributions

The major contributions of this thesis are as follows:

1. Review of related works

2. Initial study: hybrid haptic assistance for virtual steering task

   - A concept of hybrid haptic assistance: combining different performance-based haptic assistance (haptic guidance and disturbance)

   - Detailed design and implementation of hybrid haptic assistance

- User study for the training effectiveness of hybrid haptic assistance

3. Development of haptic driving training simulator

    - Integration of hardware and software for virtual driving simulation

    - Detailed design and development of haptic accelerator/brake pedals

    - Implementation of realistic torque feedback

4. Driving Skill modeling using neural networks for performance-based haptic assistance

    - Utilization of neural networks and its parameters

    - Detailed design of expert skill model using neural networks for steering/pedaling

    - Human experiment for validity of modeling

    - Human experiment for applicability to driving skill enhancement

5. Human-like haptic assistance for car steering task

    - A concept of human-like haptic assistance: performance-based haptic assistance using neural networks

    - Detailed design and implementation of human-like haptic assistance

    - Autopilot test using human-like haptic assistance

    - Human experiment for training effectiveness of human-like haptic assistance

1.4   Organization

To understand the overall framework of human-like haptic assistance, the background literature about haptics, human-robot interaction, sensorimotor skill control and learning, and neural networks is introduced in Chapter II. As an initial

study, this thesis involves a study on hybrid haptic assistance for training on a virtual steering skill. The concept and implementation of hybrid haptic assistance and the training results of human experiments are introduced in Chapter III.

Next from here, the author explains the main study of this thesis to extend the basic idea and overcome the limitations in the initial study. In Chapter IV, the author introduce a haptic driving training simulator, our apparatus for all of implemented algorithms and human experiments, In Chapter V, the detailed modeling procedure to capture an expert driving skill using neural networks, and its validation and applicability to performance-based haptic feedback through user studies are explained. Finally, in Chapter VI, the overall framework of human-like haptic assistance for skill learning is introduced, and validated through an autopilot test and a human experiment to show training effectiveness.

Then, possible recommendations and suggestions acquired from the previous chapters to generalize the study on the human-like haptic assistance are discussed in Chapter VII. In Chapter VIII, we summarize all findings and remaining future works as the finale of this thesis.

II. Background

In this chapter, the author presents previous literature necessary to understand the main topic of this thesis. Our interdisciplinary study is closely related to various research fields, including haptics, human-robot interaction, sensorimotor control and learning, and neural networks.

2.1 Context of Driving Skill

Controlling an automobile is a representative sensorimotor task which requires continuous executions of sub-tasks via various driving interfaces including mechanical manipulators. For example, automobile drivers manipulate a steering wheel to control the heading of a vehicle (steering), steps on accelerator, brake and clutch pedals to accelerate/decelerate the velocity of a vehicle (pedaling). Also in any particular driving events and scenarios, the drivers can change gears or interact with interface buttons manually. However, in this thesis, the context of a driving skill is narrowed down with only steering and pedaling skills using the mechanical manipulators, because they are only concurrent sub-tasks with full contact with limbs which providing haptic information can be efficiently contributed.

2.2 About Sensorimotor Control and Learning

Basically, to understand how our framework can contribute to both enhancement and training of the driving skill (in our context), it is necessary to remark several previous studies about sensorimotor skill control and learning, which a number of experimental psychologists have been studying on.

2.2.1 Motor Program

One of the most influential theories that account for control and learning of sensorimotor skills is Schmidt's schema theory [69, 67]. The schema is a rule developed by lifetime practice and experience, describing a relationship between the outcomes achieved on past attempts at running a *motor program*, and the parameters of the motor program are chosen on those attempts [67]. Here a motor program is an abstract representation which can initiate the production of a coordinated action sequence, and it is called a *generalized motor program* (GMP) when the program is generalized by several parameters and provides altered actions depending on the choice of the parameters [69].

According to the schema theory, a learner develops two schemas during motor learning: the *recall* and *recognition* schema. The recall schema is concerned with movement production, and it represents the abstract relationship between parameters of the motor program and movement outcome, including the initial conditions of the movement. Learning a motor task requires cognitive processing to establish a mental model called a motor program, and its building process is called *motor programming* [69, 34]. The motor program provides a reference for reproducing the motor task according to the current task context. A sensorimotor skill is a human behavioral control strategy against a sensorimotor task, which requires the process of perceiving various sensory information such as visual, auditory, and tactile senses and reacting through movements from the motor program stored in memory. In the case of a beginner, a motor program is not well-parameterized yet, and through learning or a self-practice, the motor program becomes improved.

Therefore, traditionally, the sensorimotor skill learning have been facilitated by human-to-human interaction; human instructors transfer assistive information to help human learner developing their own GMP. This process is called a *training*,

and the assistive information is usually called augmented feedback.

2.2.2   Intrinsic and Augmented Feedback

In the control and learning of sensorimotor skills, during the action, human learners receive two types of feedback: *inherent feedback* and *augmented feedback* [69]. The former feedback is also-called task-intrinsic feedback [42]. The feedback is automatically generated during task execution in any forms of sensory stimuli, and can be delivered to learners while paying attention (such as observation) to their own movements and the interaction with task environments. However, in usual learning situations, the inherent feedback is not easily recognizable for learners and also hard to be usefully evaluated for their own practice.

The contrast type of the inherent feedback is augmented feedback, which literally *augments* the inherent feedback. A number of studies about sensorimotor skill learning suggest that the learning process can be expedited by augmented feedback, which involves external assistive information. Therefore, a more effective skill learning can be established through a training which provides augmented feedback which refers to the knowledge pertaining to a learner's performance (e.g., instructions by a coach). Augmented feedback is categorized into two classes: *knowledge of results* (KR) and *knowledge of performance* (KP) [69]. KR is information about the resulted outcome of task execution, that is usually descriptive, terminal feedback about achievements after task completion. In contrast, KP is information about the nature of task performance, also descriptive but able to be concurrently given during task execution.

2.2.3   Haptic Augmented Feedback and Haptic Assistance

Many trainers, coaches, scientists and researchers already have utilized and studied various classes of augmented feedback to understand human behaviors

and to increase effectiveness of practice. Especially, recent advances of haptics technology has enabled haptics researchers offer an opportunity of designing special class of augmented feedback in the form of tactile or kinesthetic stimuli or both, in addition to visual and auditory stimuli, i.e., *haptic augmented feedback*. Tactile feedback is generally useful for transmitting relative simple movement information such as timing and spatial destination [71, 30, 37]. In contrast, kinesthetic feedback can deliver mechanical momentum and move the limbs of interest, providing more direct, detailed, continuous information on the desired movement as KP. The efficacy of kinesthetic augmented feedback as KP has been investigated in various applications, e.g., writing [26, 70, 9, 17], sports [74, 19], and rehabilitation [59, 33, 43].

2.3   About Haptic Assistance

The work we present in this thesis is also concerned with kinesthetic augmented feedback, providing KP for the driving skill. To this end, the term *haptic assistance* in this thesis is a generalized expression of all strategic methods and algorithms providing haptic (kinesthetic) augmented feedback. General strategies of haptic assistance can be classified into *gross assistance* and *gross resistance* [62]. While the former provides the haptic assistance that facilitates execution of a motor task (reducing performance errors), the latter increases the difficulty of training by adding haptic stimuli that hamper movement (augmenting performance errors).

2.3.1   Gross Assistance and Haptic Guidance

The most representative approach in gross assistance is *haptic guidance*, where external haptic stimuli, either active or passive, are provided to the learner concurrently during training in order to communicate information on the desired

movement. Haptic guidance has been expected to reduce the learner's unfamiliarity with a new motor skill and transfer the ideal skill to the trainee, thereby increasing the speed at which the skill is learned. A considerable body of previous studies examined the efficacy of haptic guidance, e.g., for writing [26, 70], dynamic control [23], motion reproduction [20], and rehabilitation [40]. However, they have not yet clearly demonstrated the anticipated benefits of haptic guidance. The common result has been that skill performance improves with haptic guidance during training, but it degrades rapidly after training when haptic guidance is not provided, even to levels below those attained by training with no guidance. This general tendency may be attributed to the *guidance hypothesis*: excessive concurrent augmented feedback may make learners dependent on the feedback stimuli and reduce their focus during the training, rather interfering with retention of the learned skill [66, 68].

The aforementioned drawback of generic haptic guidance inspired the development of *progressive haptic guidance*, in which the amount of guidance is decreased over the course of training to lessen the learner's dependence on the guidance stimuli. In this method, strong guidance stimuli are provided at the initial stage of learning to enable the learner to experience the desired movement, then they are gradually weakened, ultimately allowing the learner to practice with no guidance in the final stage of training [9, 38]. However, this approach generally ignores individual differences in learning speed. A presumably better method is to adjust the degree of guidance *adaptively* to the learner's performance [10]. This performance-based progressive haptic guidance has been frequently adopted for training of various motor skills, such as walking [18], driving [45], and dynamic target hitting [31]. In particular, Marchal-Crespo et al. showed that performance-based progressive guidance can lead to faster improvement of steering skill than can fixed-gain guidance [45].

2.3.2 Gross Resistance and Haptic Disturbance

In gross resistance, *error amplification*, which provides the haptic stimuli that increase movement errors during training, has received the most attention. In error amplification, the learner practices a motor skill while being exposed to an external force field that amplifies the task error, e.g., a force field that opposes the desired movement. After practice using this method, the learner usually exhibits an aftereffect, which can help correct the learner's movement to become similar to the desired one. For instance, Emken and Reikensmeyer applied a viscous force field to the learner's leg during normal walk [18]. Adaptation to the force field was accelerated when larger amplification errors were induced in the initial phase of training. Patton et al. demonstrated the benefit of error amplification in a reaching task with post-stroke patients [59, 60]. Reisman et al. reported that the walking symmetry of post-stroke patients could be improved by amplifying the asymmetry of walking during practice [64]. Milot et al. compared the effects of haptic guidance and error amplification on a timing-based task using a pinball-like game [47]. Both methods enhanced skill performance, but training with error amplification led to better improvement. However, error amplification has the drawback that the learner can anticipate the feedback stimuli that will be provided because they are determined on the basis of the learner's current performance.

Haptic disturbance is an extension of error amplification encompassing elevated difficulty of training in any forms. In particular, haptic disturbance includes random, unpredictable force fields that do not allow the learner to anticipate the feedback stimuli. Our research group first proposed the idea of haptic disturbance in [38], for a trajectory-following task using a robotic arm. This study demonstrated that noise-type haptic disturbance can contribute to the better retention of a motor skill than progressive haptic guidance or training with no assistance.

A similar result was also obtained in the recent study of Powell and O'Malley [62]. They compared the efficacy of four haptic assistance paradigms for shared control with two tasks (dynamic target hitting and trajectory following). Random haptic disturbance generally outperformed the other assistance methods in the generalization test of the trajectory following task. The generalization test used a task slightly modified from the task used during the training. In [36], we investigated the usefulness of different haptic assistance methods in memorizing the selection orders of points scattered on a 2D plane. Haptic disturbance implemented as a viscous force field was shown beneficial for delayed recall of the selection orders.

2.4 About Driving Skill

Originally, the term cybernetics has a comprehensive definition of covering all of the scientific studies of control and communication in the animal and the machine. Humans always interact (intercommunicate) with other cognitive systems (or, agents), such as other human beings, animals, devices and machines; we live in a cybernetic world.

Even in driving, a user agent (driver) and a machine agent (automobile) interact with each other in a cybernetic framework. Information flows in both directions between two agents via mechanical contact on mechanical manipulators. First, the automobile driver can motorize an action via manipulators, and the automobile then reflects the corresponding action. Second, information about driving states resulted by current driving environments is provided to automobile drivers through force and torque signals via manipulators to the limbs of the driver, as an intrinsic feedback of driving. After perceiving the feedback about environmental states, the driver can react through better cognitive behavior. Therefore, driving is a human-machine cooperative task in shared control (also-called human-machine shared control; HSC) [50].

2.4.1 Haptic Assistance for Driving Skill Enhancement

Recent technological advances have also enabled advanced interaction with artificial machine agents having cognitive capabilities, usually so-called *robots*. As a division of cybernetics, the studies of control and communication between humans and robots are called Human–robot interaction (HRI); by definition, HRI is a field of study for understanding, designing, and evaluating robotic systems for use by or with humans [24]. In HRI, using any cybernetic interface, both a human agent and a robot can communicate essential information to each other, via various sensory channels.

Nowadays, intelligent vehicles (i.e., robotic vehicles) where automated, cognitive systems are involved are emerging as an alternative to traditional automobiles. In these intelligent vehicles, the usual feedback loop of HSC can be augmented; Especially, the robot agent can intelligently alters and delivers haptic feedback to influence current driver's skill maneuver. Usually, this type of augmented HSC is also called haptic shared control [4, 5], which is mostly designed to support driving skill execution.

In this thesis, we define haptic assistance as a goal-oriented expression of haptic HSC to assist humans to enhance or to improve skill performance. A haptic assistance system plays the role of a *collaborator* that encourages humans, mostly by demonstrating appropriate maneuvers and correcting their driving performance. To this end, the human driver and the system share a common goal, i.e., successful driving, where both agents perform an effective, safe, and robust driving control. Hence, haptic assistance is considered as a bridge to automated driving with improved performance and reduced effort [48]. Various automobile companies have investigated haptic assistance as advanced driver-assistance systems (ADAS) [61], such as lane-keeping assistance systems (LKAS), intelligent parking assistance systems (IPAS), and adaptive cruise control (ACC).

In haptic HSC, both the user and the haptic assistance system communicate in real-time to achieve the optimum control of the shared goal. The system continuously watches and analyzes a current user's performance, and then exerts personalized haptic feedback, regarding a certain baseline of task performance, i.e., the ground truth. To this end, to design haptic assistance systems, the process of quantifying a skill performance as a desired reference to a user's current performance to generate suitable feedback (which is usually called a *modeling* process) should be always preveniently required.

To enhance the task performance, the most representative and effective form of haptic assistance is haptic guidance (often called haptic shared control), where external haptic stimuli are provided to the user in order to communicate control information on the desired movement. Several studies have demonstrated that haptic guidance can enhance the task performance of steering [72, 21, 65] and pedaling skills [6, 49, 32] by transferring useful information via haptic channels.

2.4.2 Haptic Assistance for Driving Skill Training

Traditionally, sensorimotor skill training has been usually facilitated by human-to-human interaction. Substituting the role of a human trainer by a human-robot shared interface, a *robot-mediated training* on sensorimotor skills has been developed and gained a high research interests [27]. Like human teachers, a robot-mediated training system can provide appropriate augmented feedback that pertains to the results of the trainee's motor action through various kinds of sensory information, often with reduced cost. Further, a robot-mediated training also allows safe practice in simulated scenarios, especially those including risky situations, in virtual environments [76]. The educational efficacy of a robot-mediated training has been tested for various applications (e.g., sports and rehabilitation), and these previous studies demonstrated that a well-designed robotic assistive

scheme can even improve the quality of learning, such as learning rate and the final skill level of trainees [63].

Therefore, haptic assistance is more widely utilized in motor learning and training, as well as rehabilitation applications. Using a number of strategies, including haptic guidance and other algorithms, haptic assistance was investigated to determine its training efficiency for various tasks [63, 46]. Here, a haptic assistance system should play the role of a *skill trainer*; while a driving skill learner tries to drive properly, the system checks the current learner's performance and provides haptic augmented feedback that transfers information about KP. Thus, the feasibility of haptic assistance, in which the system is aware of human performance errors in order to continually generate KP [27], lies in the special benefits to driving skill training. The effectiveness of haptic assistance under the continuous observation of a learner's driving control was shown for several driving tasks, especially for curve-tracing and lane-keeping tasks [45] as well as the reverse parking task [29].

2.5   Remarks

Most of the previous studies examined the effectiveness of performance-based kinesthetic feedback to arms or legs for a steering task [45, 44] or a pedaling task [6, 49, 32], as a sub-skill of driving. In those studies, the task and the skill model to learn steering or pedaling was manually abstracted into simple deterministic forms. However, these abstraction of tasks were usually different from real driving which requires simultaneous manipulation of the steering wheel and pedals for lane-keeping and velocity control. This is what the work we present in this paper focuses on: a framework of (1) building a proper skill model and (2) utilizing the model for haptic assistance.
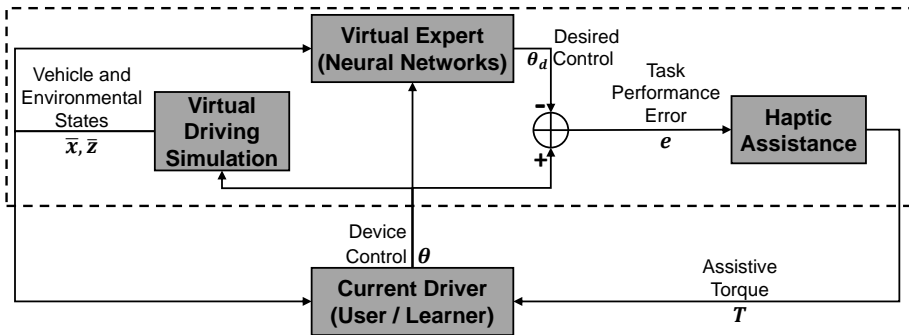
Figure 2.1: Framework of driving skill modeling for haptic assistance.

2.5.1 Framework

In this thesis, the author introduces a *data-driven*, robot-mediated framework for enhancement and training on a driving skill, that (1) models a proper expert driving skill from experienced drivers, and (2) utilizes the model for haptic assistance, to perform a freeway driving (lane-keeping with maintaining the same velocity) task (Figure 2.1). Our approach is to record how experienced drivers execute driving successfully without haptic assistance, and then to train an adequate continuous model (representing a virtual expert) of associated variables from the collected data, which was obtained from virtual environments.

A promising way is to record how expert drivers execute driving tasks and then learn an adequate continuous model of associated variables from the collected data. However, this important domain of data-driven skill modeling has not been researched intensively. We face an immediate demand for reasonable modeling methods of complicated driving skills, which is a prerequisite of competent skill transfer systems.

2.5.2 Neural Networks

Specifically, we introduce a useful methodological solution that extracts a behavioral model of experienced drivers using (artificial) neural networks. A neural network (NN) is generally used to find a nonlinear function that explains

an input/output relationship, and to identify a structure beneath a complex dynamic system, e.g., a human driving behavior. Zhang et al. showed that the characterization of driving skill levels (expert, typical, and low-skill) is possible, by analyzing individual driving manuvers using several pattern recognition algorithms [77]. Also, various researchers presented the feasibility of NN-based model of human driving skills for feedforward steering control [39, 22].

In a similar way, we extend and apply those model to the freeway driving task which requires simultaneous manipulation of the steering wheel and pedals to generate and provide assistive torque feedback for haptic assistance. Previously, Nechyba and Xu used neural networks to model a human driving strategy from driving data collected under simplified driving simulation using a mouse interface [54, 55, 56]. Their neural network model could produce a predictive trajectory based on an individual motor behavior using experimental states and environmental variables as inputs. However, their study did not involve realistic driving hardware, so the usability of their behavioral model for a pragmatic driving training has not been validated yet. In this study, we complete their NN-based modeling approach in a virtual driving simulator, and validate the suitability of our framework via consecutive human experiments.

III. Initial Study: Hybrid Haptic Assistance On Virtual Steering Task

The literature about the classification of haptic assistance (Section 2.3) has suggested that haptic guidance may accelerate the learner's acquisition of a unfamiliar motor skill in the early stage of training, whereas haptic disturbance can be effective in further improving the motor skill in the later stage of training [38, 63]. The present initial study investigated the validity of the following hypothesis: *Combining haptic guidance and disturbance into hybrid haptic assistance may improve the effectiveness of motor learning.* To this end, we carried out a human subjects study using a simulated steering task. As previously stated, steering is essential part of driving skill that most people learn, and it has been the subject of many prior studies [21, 45, 44, 13]. We designed a hybrid haptic assistance method for the steering task and then evaluated its efficacy compared to that of progressive haptic guidance and haptic disturbance.

3.1 Methods

3.1.1 Training System and Task

For training and tests, we used a commercial steering wheel (Logitech G27 Racing Wheel; rotation angle range 900°) that has torque feedback capability and a 27-inch LCD monitor. Torque feedback was updated at $200\,\mathrm{Hz}$ using the DirectInput library. The range of feedback commands was between -10,000 and 10,000. The actual values of this torque range were unavailable from the manufacturer, but we confirmed that the range was sufficient to provide distinct feedback. Visual scenes were displayed on the screen at a $60\,\mathrm{Hz}$ refresh rate using OpenGL.

The trainees were allowed to adjust the distance (0.5 and 0.8 m) between the driver's seat and the monitor to have both comfortable driving posture and clear visual perception.

A driving path was drawn using three parallel white lines (Figure 3.1): a centerline that indicated the desired path and two side lines that represented the boundaries of the driving lane, each 1 m apart from the centerline. Green buildings were also placed outside the two sidelines (10 m away from the centerline) to facilitate depth perception. The height of each building and the distance between buildings were randomly chosen between 1 and 4 m and between 10 and 13 m, respectively. The vehicle position was displayed as a red arrow instead of a car shape, similarly to [21], to clearly visualize its position and orientation with respect to the centerline.
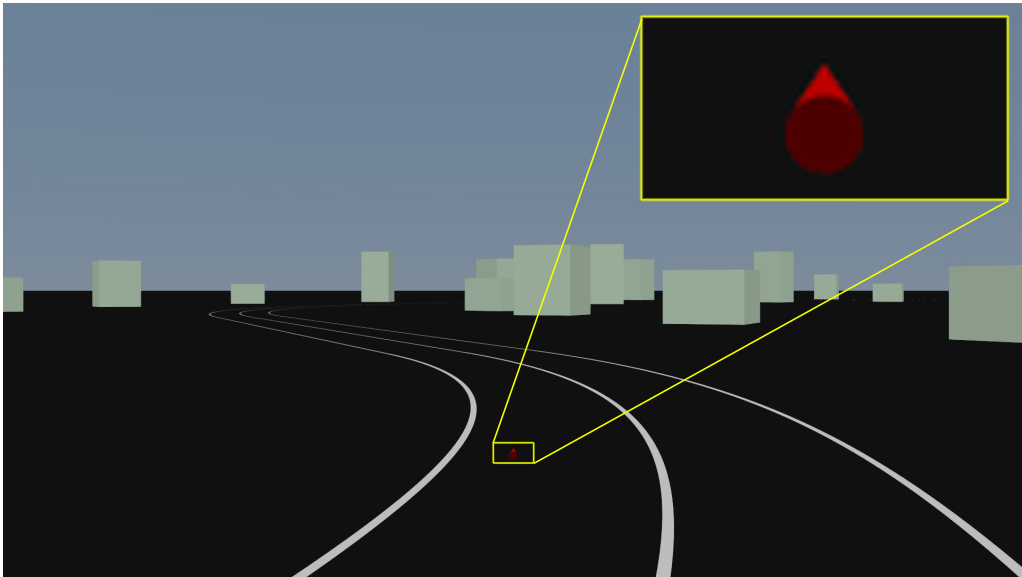
Figure 3.1: Visual scene. The top-right inset shows a magnified view of the vehicle.

Participants' task was to control the simulated vehicle to track the centerline of a displayed path by turning the steering wheel. The velocity of the vehicle was fixed at $v = 4\,\mathrm{m/s}$ to eliminate the need for accelerator and brake pedals.

3.1.2 Driving Paths
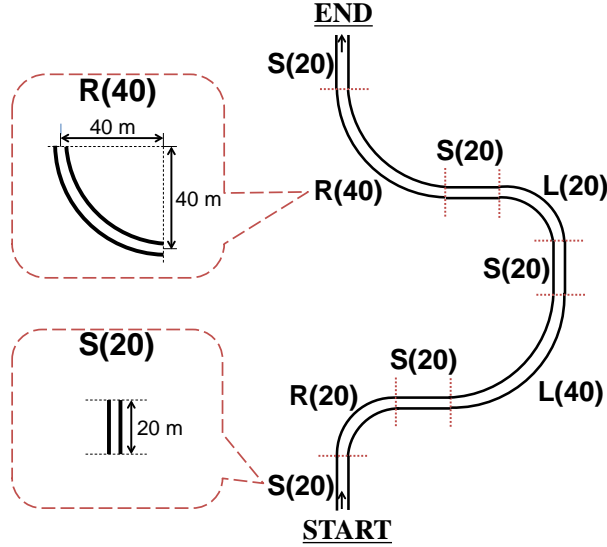
Figure 3.2: Example driving path (P_1). Notation is described in the text.

We designed four driving paths to use in the experiment by combining straight and curved segments. All curves were right-angle turns, so their radius is the only factor that controls the difficulty of driving on them. The four paths were:

$$P_1: \quad S(20) \to R(20) \to S(20) \to L(40) \to S(20)$$
$$\to L(20) \to S(20) \to R(40) \to S(20)$$

$$P_2: \quad S(20) \to L(40) \to S(20) \to R(20) \to S(20)$$
$$\to R(40) \to S(20) \to L(20) \to S(20)$$

$$P_3: \quad S(20) \to R(40) \to S(20) \to L(20) \to S(20)$$
$$\to L(40) \to S(20) \to R(20) \to S(20)$$

$$P_4: \quad S(20) \to L(20) \to S(20) \to R(40) \to S(20)$$
$$\to R(20) \to S(20) \to L(40) \to S(20)$$

where $S(l)$ denotes a straight path with length l (m); $R(r)$ and $L(r)$ represent a

right and a left curve with radius r (m), respectively. All paths had the same total length of 288.5 m (straight path: 100.0 m; curved path: 188.5 m). An example is provided in Figure 3.2.

These paths were designed to be reasonably difficult by making the four curved segments have different lengths and directions. The task performance for each path was represented by the mean absolute tracking error:

$$\mu = \frac{1}{N} \sum_{i=0}^{N-1} |e[i]|, \tag{3.1}$$

where $e[i]$ is the distance between the vehicle and the centerline in the i-th sample (recorded at 200 Hz) (Figure 3.3).

3.1.3   Haptic Assistance Design

We tested four haptic assistance methods, including the control condition of no assistance. The other three haptic assistance methods are described in this subsection.

Progressive Haptic Guidance

As reviewed earlier, the performance-based progressive haptic guidance is regarded as the most effective guidance scheme, especially for steering tasks [45, 44, 43]. Thus, we implemented the guidance algorithm presented in [45, 43] for our experiment.

This guidance algorithm is based on the observation that a driver determines his/her driving based on prediction, not on the current situation. Therefore, we considered two error terms: the look-ahead direction error e_{ang} and the look-ahead distance error e_{dis} (Figure 3.3). In our simulation, $d = v\Delta t$ and $\Delta t = 1$ s is the look-ahead time. The same $\Delta t = 1$ s was used in [21].

The desired angle θ_d of the steering wheel and the guidance torque τ_G to make the current steering wheel angle θ converge to θ_d are determined by the
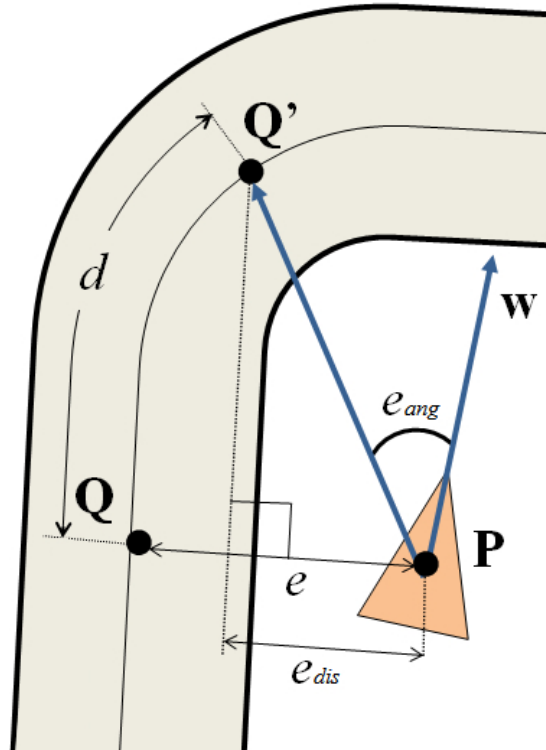
Figure 3.3: Variable definitions. **P**: current vehicle position; **Q**: point nearest to **P** on the centerline; **Q′**: look-ahead point on the centerline with a path length d from **Q**; **w**: vector that indicates the orientation of the vehicle; e_{ang}: look-ahead direction error (angle from **w** to **PQ′**); e_{dis}: look-ahead distance error (distance between **P** and the point projected from **Q′** onto **PQ**.

following PD control-based rules:

$$\theta_d = G_{ang}e_{ang} + B_{ang}\dot{e}_{ang} + G_{dis}e_{dis} + B_{dis}\dot{e}_{dis}, \tag{3.2}$$

$$e_\theta = \theta - \theta_d, \tag{3.3}$$

$$\tau_G = G_G e_\theta + B_G \dot{e}_\theta, \tag{3.4}$$

where $G_{ang} = 80$, $B_{ang} = 2\,\mathrm{s}$, $G_{dis} = 10$ degree/m, $B_{dis} = 0.25$ degree·s/m, $G_G = 10$ degree^{-1}, and $B_G = 0.1\,\mathrm{s}$/degree. These gains allow e_θ to converge to 0 when the vehicle is autonomously driven along the four paths using haptic guidance only, without a driver.

For progressive guidance, the guidance torque must be adjusted adaptively according to the driver's performance. First, we consider the performance changes *within* a training trial. During each trial, the two torque gains G_G and B_G are updated at each sampling time i following the rule presented in [18]:

$$\tau_G[i] = K[i]\left(G_G e_\theta[i] + B_G \dot{e}_\theta[i]\right), \tag{3.5}$$

$$K[i+1] = f_K K[i] + g_K |e_\theta[i]|, \tag{3.6}$$

where $K[1] = 1$. f_K is the forgetting factor that decreases the guidance torque over time, and g_K is the learning factor that increases the guidance torque in proportion to the absolute tracking error. In the experiment, $f_K = 0.9996$ and $g_K = 0.00004\,\mathrm{m}^{-1}$.

Second, we consider the performance variations *across* the training trials. An across-trial gain $\alpha[j]$ of the j-th trial is computed as

$$d\left(\mu[j], \mu_{good}\right) = \begin{cases} \mu[j] - \mu_{good} & \text{if } \mu[j] \geq \mu_{good} \\ 0 & \text{otherwise} \end{cases}, \tag{3.7}$$

$$\alpha[j+1] = f_\alpha \alpha[j] + g_\alpha d\left(\mu[j], \mu_{good}\right) \tag{3.8}$$

where $\alpha[1] = 1$. f_α and g_α are the across-trial forgetting and learning factors, respectively. μ_{good} is a reference for high performance and set to be a small value

that the learner rarely outperforms. In the experiment, $\mu_{good} = 0.02\,\text{m}$, $f_\alpha = 0.8$, and $g_\alpha = 0.65\,\text{m}^{-1}$. It is noted that $\alpha[j]$ is not updated if the participant's performance is poor ($\mu > 0.04\,\text{m}$) in both of the two previous trials.

Combining the two adjustments, the final guidance torque at the sampling time i during the j-th trial is

$$\tau[i] = \alpha[j]\tau_G[i]. \tag{3.9}$$

Using this guidance rule, we conducted a pilot experiment with three participants to determine the number of trials necessary for training. The participants finished 20 trials each, and their across-trial gain $\alpha[j]$ decreased to be lower than 0.1 after the 17th or 18th trial (Figure 3.4). Such small gains do not result in perceptible torque feedback, so the number of training trials was determined to be 16.

Haptic Disturbance

For haptic disturbance, noise-like torque feedback was produced by the steering wheel to elevate the difficulty of the task. The torque command was computed by

$$\tau[i] = \tau_D[i] = D_D PN[i], \tag{3.10}$$

where D_D is the disturbance gain and PN is the Perlin noise function as used in [38]. In our implementation, PN approximated a Gaussian distribution with an almost zero mean (0.0225) and a standard deviation of 0.4608 (both measured empirically). The same distribution was used in all trials.

D_D was determined in such a way that the distribution of τ_D is comparable to that of τ used in the first training trial of progressive guidance ($\tau[1] = \tau_G[1]$ in (3.9)). For this purpose, we collected samples of τ in the first trials of the three participants in the pilot experiment described in Section 3.1.3. These samples
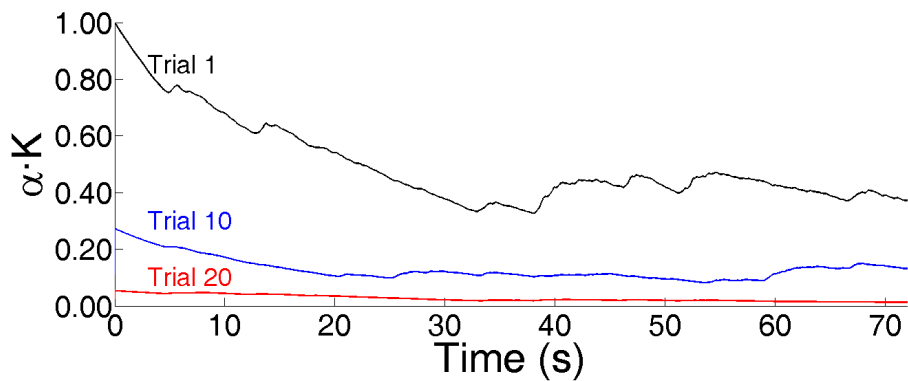
(a) Within-trial gain $K[i]$ (scaled by $\alpha[j]$)
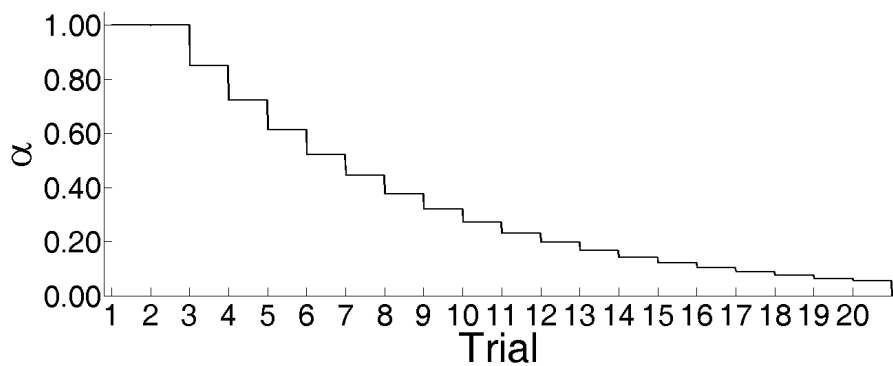
(b) Across-trial gain $\alpha[j]$

Figure 3.4: Guidance gains of one participant observed in the pilot experiment.

followed a Gaussian distribution with an almost zero mean and a standard deviation 2645.8. Thus, we set D_D to 5000 to make the standard deviations of both distributions to be very similar, with that of $\tau_D[i]$ being 2304.0 for all i.

Hybrid Haptic Assistance

Hybrid haptic assistance combines haptic guidance and disturbance according to the learner's performance. In our progressive guidance algorithm, the across-trial gain $\alpha[j]$ is decreased during training to reduce the guidance torque. To determine the amount of disturbance torque, we define another across-trial gain $\beta[j]$ as

$$\beta[j] = 1 - \alpha[j] \tag{3.11}$$

Then the hybrid assistance torque at time i during the j-th trial is computed by

$$\tau[i] = \alpha[j]\tau_G[i] + \beta[j]\tau_D[i]. \tag{3.12}$$

If a trainee performs better in the current trial j than in the previous trial, $\alpha[j]$ is decreased but $\beta[j]$ is increased in the subsequent trial. Hence, the guidance component in the feedback torque $\alpha[j]\tau_G[i]$ is decreased, but the disturbance component $\beta_j\tau_D[i]$ is increased. With this hybrid assistance scheme, we expected that participants could practice with haptic guidance in early trials while experiencing the desired wheel operations. Then, the participants would be challenged with disturbance torque in later trials, which may stimulate them to further improve their skill that they acquired as a result of previous training facilitated by haptic guidance.

The initial values were $\alpha[1] = 0.9$ and $\beta[1] = 0.1$, and $\alpha[j]$ and $\beta[j]$ were expected to be close to 0.1 and 0.9 in the last (16th) trial ($\alpha[j]$ was about 0.1 after training was completed in the pilot experiment described earlier in Section 3.1.3).

3.1.4 Participants

To recruit participants, we tried to control their gender, age, and driving skill level. Gender and age are generally regarded as important factors for motor learning, especially for steering tasks [63]. Eligible participants were those who did not have a driving license, or had not driven a car or motorcycle in the previous two years[1]. As a result, 40 eligible participants (all male; 18–25 years old; M 21.03; SD 2.19) participated in the experiment. They were paid KRW 15,000 ($\simeq$ USD 15) after the experiment.

3.1.5 Procedure

Ten participants were randomly assigned into each of four groups in a between-subjects design. The three groups were: no assistance (N), haptic guidance (G), haptic disturbance (D), and hybrid haptic assistance (H). Within-subjects designs were inappropriate because the degrees of learning were different among the three methods.

The experiment was conducted on two consecutive days. On day 1, each participant finished three sessions for pre-practice (S-PP), training (S-TR), and an immediate retention test (S-IR). On day 2, 24 hours after the onset of day 1, each participant completed another session for a delayed retention test (S-DR).

In S-PP, the participant freely drove a 60 m straight path only once. The purpose was to familiarize the participant with our driving simulator, while minimizing their improvement of driving skills before actual training. Three participants asked to conduct an additional practice trial, and they were allowed to do so.

S-TR was for main training and consisted of 16 trials. Torque feedback was provided according to the training method assigned to the participant. The four

---

[1]In Korea, many young people who have passed a driving license do not own a car. Their driving skills remain very low.

driving paths $P_1 - P_4$ were grouped into one block with the fixed order within each block, and four such blocks of trials were repeated. The participant was required to rest for 1 min between blocks to prevent fatigue.

After S-TR, the participant rested for 1 min and then proceeded to S-IR that was included to assess their performance improvement immediately after training. In S-IR, each participant finished one block of the same four trials using $P_1 - P_4$ with no haptic assistance.

After S-IR, the participant was asked to answer the following five questions on a 7-point Likert scale: (1) Was the training easy/difficult to follow? (Easiness); (2) Was the training effective? (Effectiveness); (3) Was the training comfortable/uncomfortable? (Comfort); (4) Was the training fun? (Fun); and (5) Do you think the training helped to improve your skill? (Helpfulness). The first-day experiment took about one hour per participant.

On day 2, S-DR was conducted. It had the same procedure as S-IR. The purpose of S-DR was to evaluate the long-term effectiveness of each training method. This session took about 10 min for each participant.

3.2 Results

3.2.1 Learning Curves in Training Session

Figure 3.5 shows the mean absolute tracking errors μ defined in (3.1) that were averaged across the participants of each group for each experimental trial. The control condition N, training with no haptic assistance, resulted in a typical learning curve. Compared to the N group, the haptic guidance group G exhibited smaller μ during training (in S-TR). The haptic disturbance group D showed the steepest learning curve, with the highest μ in S-TR. These results of μ are consistent with the nature of each assistance method [38].

The results of the hybrid assistance group H were more complex. In the
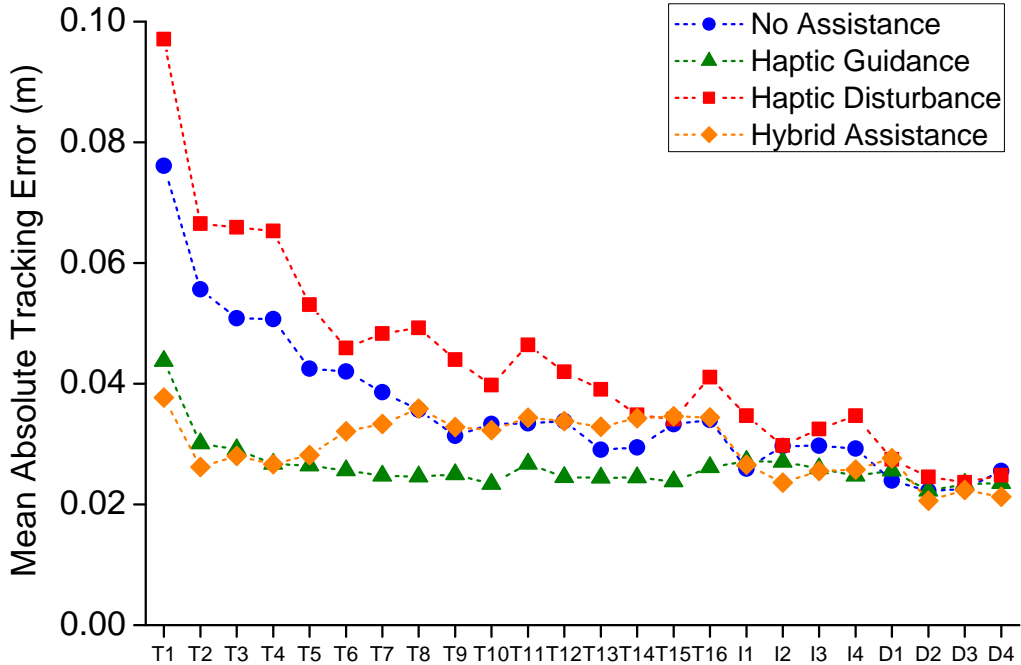
Figure 3.5: Means of the absolute tracking errors for each trial. T1–T16, I1–I4, and D1–D4 denote the trials in session S-TR, S-IR, and S-DR, respectively.

early trials of S-TR, μ's of this group were low and rapidly decreased, similar to group G. However, μ began to increase with further trials (after T4 in Figure 3.5) and stabilized after T8 until the end of S-TR, similar to group D. This tendency clearly demonstrates the hybrid nature of this assistance method.

3.2.2 Mean Absolute Tracking Errors for Entire Path

This subsection reports the results of the two post-training retention test sessions S-IR and S-DR. Each session consisted of one block of four trials, and the mean tracking errors of each participant group for each trial were averaged over the four trials. The results are shown in Figure 3.6a. For statistical analysis, we applied a mixed-factor two-way ANOVA with participant group (haptic assistance method) as a between-subjects factor and path (P_1–P_4) as a within-subject factor.

In S-IR, the ranking of the average μ's was: H < G < N < D. No statistically
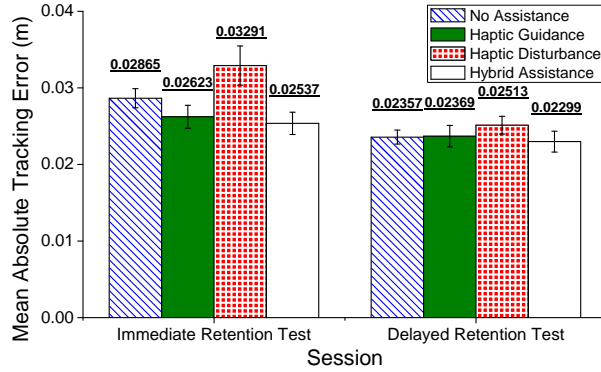
(a) Entire path
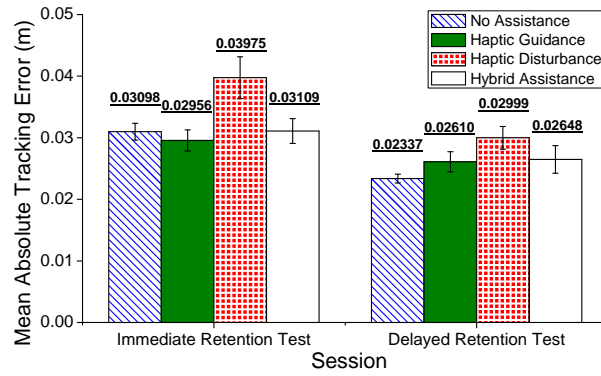
(b) Straight segments only
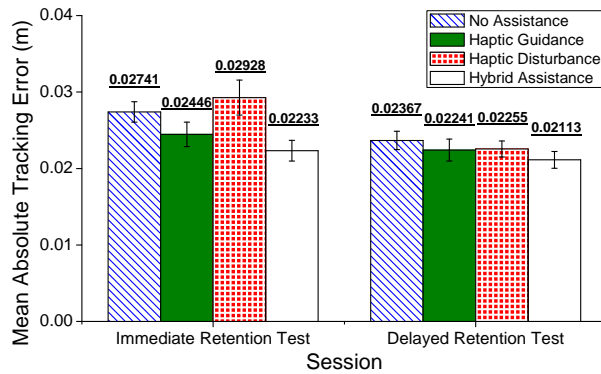
(c) Curved segments only

Figure 3.6: Mean absolute tracking errors μ measured in the two test sessions. Error bars represent standard errors.

significant differences were found among the participant groups ($F(3, 36) = 1.00$, $p = 0.4035$) or among the paths ($F(3, 108) = 0.44$, $p = 0.7272$). In S-DR, the ranking was changed to: H < N < G < D. Statistically significant differences were observed among the paths ($F(3, 108) = 5.35$, $p = 0.0018$), but not among the participant groups ($F(3, 36) = 0.18$, $p = 0.9103$). As shown in Figure 3.5, the first trial using P_1 in S-DR resulted in the highest tracking errors, likely due to the one day recess from the first day training.

3.2.3 Mean Absolute Tracking Errors for Straight and Curved Segments

The driving paths consisted of straight and curved segments, and we observed during the experiment that the required driving skill was dependent on the segment type. While the participants mainly relied on tracking the centerline on the straight segments, they had to rotate the steering wheel to a large degree in order to make turns on the curved segments. To distinguish the two cases, we computed the mean tracking errors separately for the straight and curved segments.

The mean absolute tracking errors for the straight segments, μ_s, are shown in Figure 3.6b. In S-IR, the ranking of the average μ_s's was: G < H < N < D. No statistically significant differences were found for either factor (participant group: $F(3, 36) = 1.22$, $p = 0.3163$; path: $F(3, 108) = 0.38$, $p = 0.7658$). In S-DR, the ranking was changed to: N < G < H < D. Only path was a statistically significant factor (participant group: $F(3, 36) = 1.03$, $p = 0.3890$; path: $F(3, 108) = 4.75$, $p = 0.0038$).

The mean absolute tracking errors for the curved segments, μ_c, are shown in Figure 3.6c. In S-IR, the ranking of the average μ_c's was: H < G < N < D. Neither factor was statistically significant for μ_c (participant group: $F(3, 36) = 0.97$, $p = 0.4198$; path: $F(3, 108) = 0.80$, $p = 0.4951$). In S-DR, the ranking

was: $H < G < D < N$. Only path was a statistically significant factor for μ_c (participant group: $F(3, 36) = 0.24$, $p = 0.8701$; path: $F(3, 108) = 5.59$, $p = 0.0013$).

3.2.4 Summary of Quantitative Results

In the immediate retention test, the two training methods that include guidance feedback, G and H, generally showed better tracking performance. The highest performance was achieved with H for the entire path, G for the straight segments, and H for the curved segments. However, training method did not have statistically significant effect on any of the three tracking errors. In the delayed retention test, the skills of the four participant groups seem to have improved to a similar level, without noticeable patterns or statistically significant differences. Therefore, our hypothesis of the present study, *combining haptic guidance and disturbance into hybrid haptic assistance may improve the effectiveness of motor learning*, remains inconclusive.
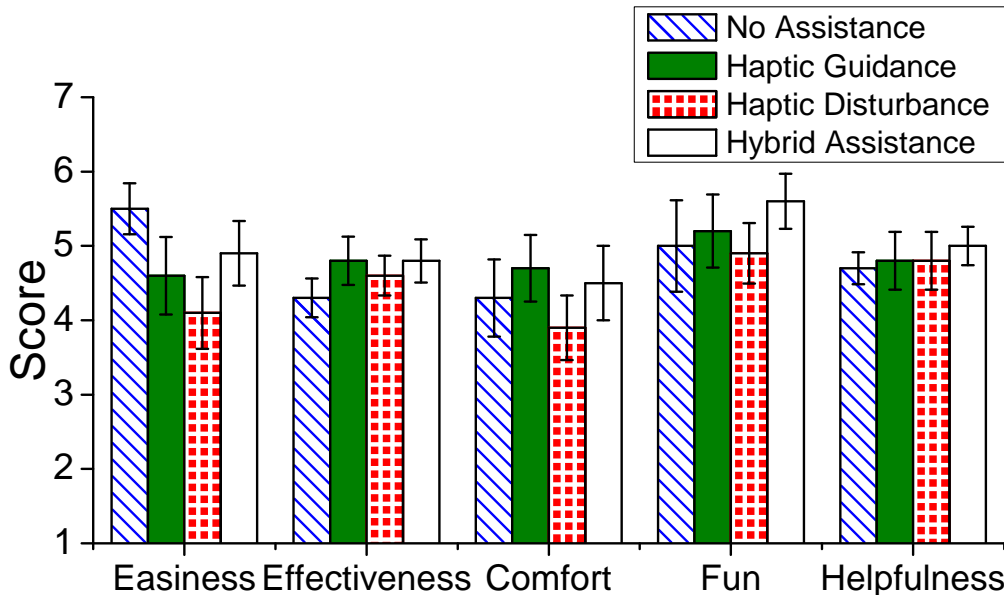
Figure 3.7: Subjective scores responded from the participants for the questionnaire (7-point Likert scale).

3.2.5 Subjective Questionnaire

The mean scores for the five subjective questions in the questionnaire are shown in Figure 3.7. The post-hoc Kruskal-Wallis test did not show any statistically significant difference for any of the five questions. Hence, only noticeable results are summarized in the following for each training method. Method N was ranked at the first on easiness, but at the lowest or second lowest on all other criteria. H was ranked the highest on all criteria except easiness and comfort. G was ranked the highest on effectiveness (a tie with H) and comfort. D was ranked the lowest or second lowest on all criteria except helpfulness.

3.3 Conclusions and Discussion

We designed a hybrid haptic assistance scheme for the learning of a steering skill by combining haptic guidance and disturbance. In this method, the feedback force provided to the learner initially guides the learner's movement by correcting errors, but the force is progressively changed to random disturbing force to improve the learner's skill level further. The effectiveness of this hybrid assistance method was investigated by a human subjects experiment in comparison to other three methods of no haptic assistance, progressive haptic guidance, and haptic disturbance, with emphasis on the retention performance. According to the experimental results, the methods that included guidance feedback, i.e., haptic guidance and hybrid haptic assistance, seemed to be generally advantageous for immediate retention of the learned skill, but its statistical significance was not supported. It is noted that individual performance differences were very large in our experimental data. The four methods also showed similar performance in the delayed retention test conducted one day later.

The steering task used in the present study requires simultaneous execution of two kinds of motor skills. One is the open-loop road tracking skill, which
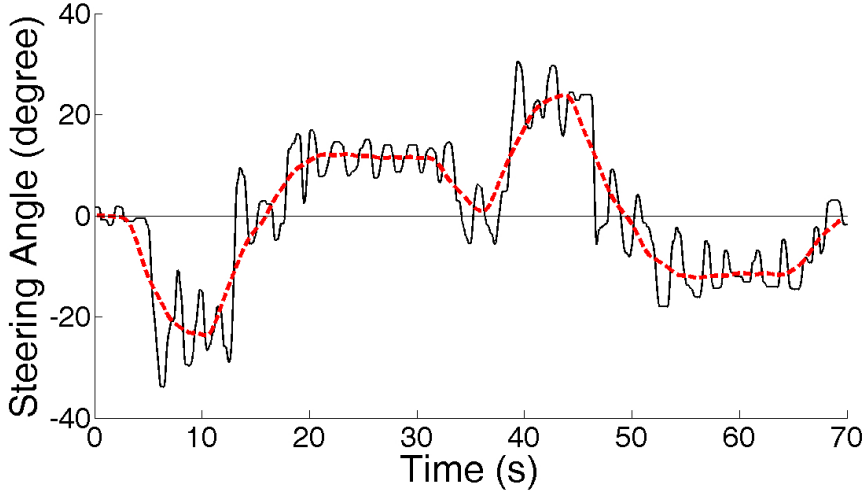
Figure 3.8: Example of the steering wheel trajectories of P_1 collected in S-IR. P_1 belonged to group N and showed median performance in S-IR within the group. A black solid line shows the raw data. A red dashed line represents the data obtained by applying a low-pass filter with 0.1 Hz cutoff frequency to the raw data.

is necessary to follow a road on the basis of the visually-perceived curvature of the road by rotating the steering wheel relatively slowly. The other is the error canceling skill, which is used to control the vehicle to stay on the centerline in a closed-loop by correcting small tracking errors with relatively fast wheel operations based on visual feedback. This classification is similar to that of point-to-point movements that generally consist of an open-loop transfer motion and smaller corrective movements [15]. We initially expected that the road tracking skill would be more important in curved segments, while the error canceling skill would be more critical in straight segments.

To gain more insights, we attempted to extract the participants' movement characteristics corresponding to each of the two skills from the experimental data. An example is given in Figure 3.8. We can regard smooth low-frequency movements in the figure as a representative of the road tracking skill, and the difference between the original and low-frequency trajectories as a representative of the er-

ror canceling skill. For further analysis, we applied a high-pass filter with $0.1\,\text{Hz}$ cutoff frequency to the steering angle data collected in S-IR and S-DR, which allowed us to isolate the trajectories for error canceling movements. Then we computed the energy of this trajectory and divided the energy by that of the original trajectory to find the normalized energy $\hat{E}_{EC}$ used for error canceling movements. Results are shown in Figure 3.9.

While driving on straight segments, the need for the error canceling skill can be greatly more significant than that for the road tracking skill. This anticipation is confirmed in Figure 3.9b; $\hat{E}_{EC}$ on the straight segments is greatly higher than $\hat{E}_{EC}$ on the entire path or the curved segments for each of the four training methods. We also expected that the noise-like disturbing forces provided by haptic disturbance or hybrid haptic assistance could contribute to further improving error canceling skills, but this expectation was not supported. This is against the positive results of haptic disturbance reported in two previous studies that used a similar path following task [38, 62]. Finding out reasons for this inconsistency will be one of our future research topics.

To follow a curved road, the need for the road tracking skill can be much higher, as can be seen from the low $\hat{E}_{EC}$ values in Figure 3.9c. The road tracking skill consists of a sequence of large-angle left/right rotations, and each of these rotations is close to an open-loop, discrete motor skill[2]. Thus, the road tracking skill is a serial motor skill, and its competent execution is likely to require a well-parameterized GMP. In this case, haptic guidance may help the learner develop a better general motor program during training by providing kinetic references to ideal movements. This trend can be observed in Figure 3.6c in which the haptic guidance and hybrid assistance group showed the better retention performance on

---

[2] A motor skill that has specific definitions of the start and end of that skill is called a discrete motor skill. A serial motor skill generally consists of a number of discrete motor skills that are executed one after another [42, 69].
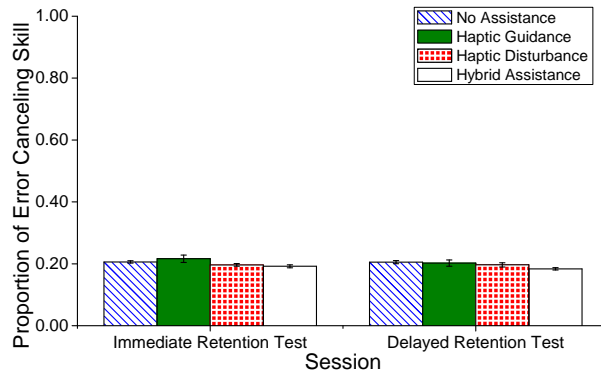
(a) Entire path
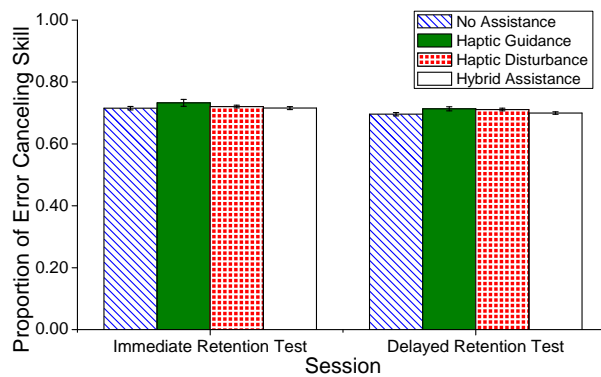
(b) Straight segments only
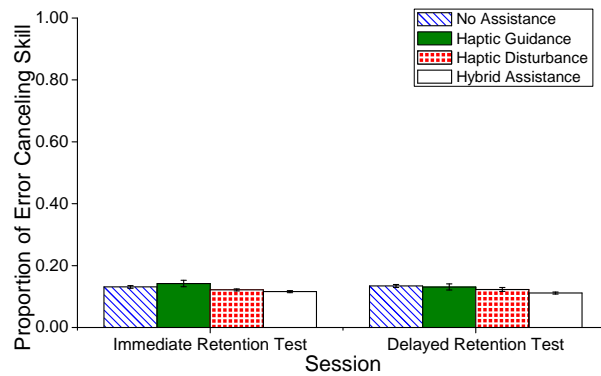
(c) Curved segments only

Figure 3.9: Energy used for error canceling movements normalized by the total energy. Error bars represent standard errors.

the curved segments. Seeking for stronger evidence for this conjecture is another line of research we can plan to pursue.

IV. Haptic Driving Training Simulator: An Extension to a Realistic Driving
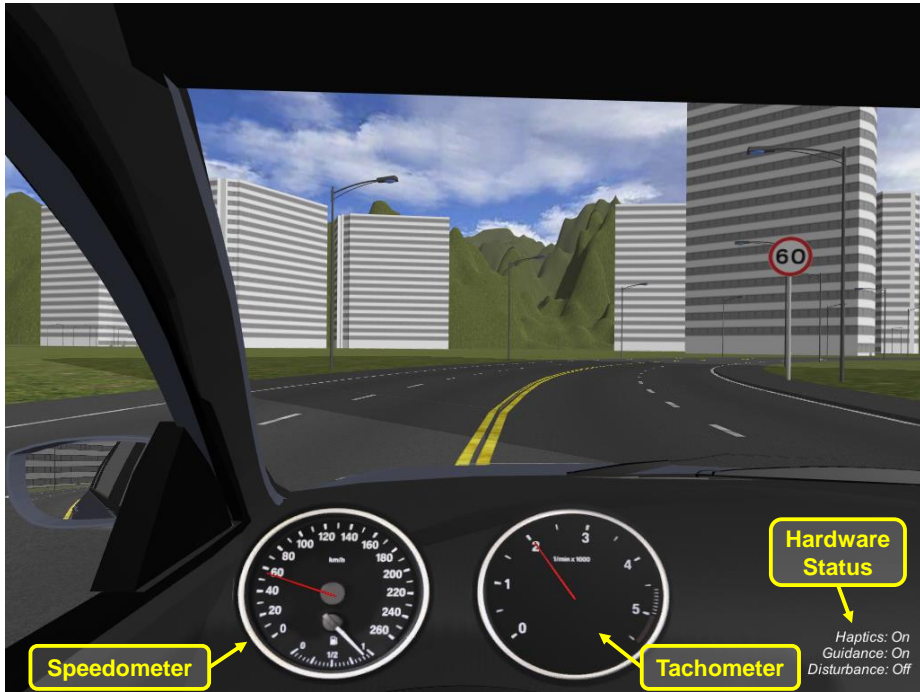
Figure 4.1: A visual scene of driving simulation.

This chapter describes the haptic driving simulator (Figs. 4.1 and 4.2) that we developed for two purposes:

1. Driving skill modeling: The simulator records the driving data of experienced drivers. It provides realistic driving experiences to acquire reliable data, including realistic torque feedback to the steering wheel and pedals; and

2. Haptic assistance: The simulator generates torque feedback in order to assist a current driver's driving skills with high fidelity.
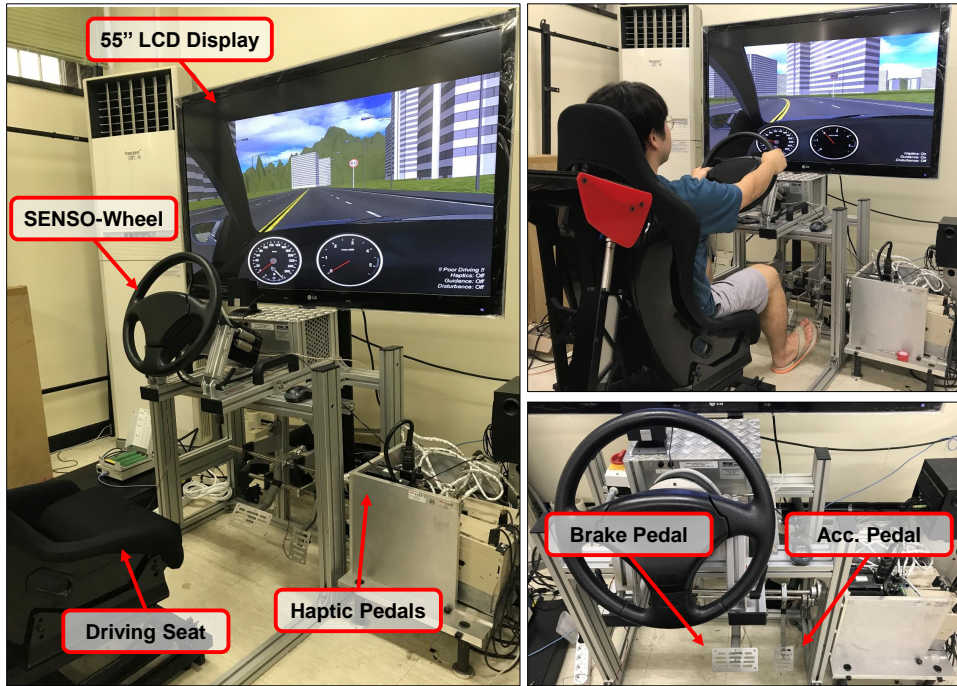
Figure 4.2: Haptic driving training simulator.

4.1 Hardware

The simulator consists of a large visual display, a steering wheel, an accelerator pedal, and a brake pedal (Figure 4.2). All devices are fastened to an aluminum frame to imitate a real driving seat. We used a 55-inch LCD (55LW6500, LG Electronics), and the distance from the display to the seat is about $1.2\,\mathrm{m}$ for a comfortable field of view of $60\,^{\circ}$. The simulator also uses a commercial steering wheel (SENSO-Wheel SD-LC, SensoDrive) to provide high-fidelity torque feedback. The maximum instantaneous torque and the maximum continuous torque are $16.58\,\mathrm{Nm}$ and $7.5\,\mathrm{Nm}$, respectively.

We have custom-designed and built the accelerator and brake pedals with appropriate torque feedback capability. Two sets of AC servo motor (SGMGV-20A, Yaskawa Electrics) and servo pack (SGDV-18011A, Yaskawa Electrics) were used to provide independent torque feedback. The communication between the

device and PC is done using a MechatroLink-II network control board (PCI-R1604-MLII, Ajinextek). The maximum instantaneous torque and the maximum continuous torque of each motor are 27.8 Nm and 10 Nm, respectively.

For compact housing, both motors should be mounted on the same side, maintaining the alignment of the two rotation axes of the pedals. For this reason, while the accelerator pedal is directly connected to the motor with a coupler, the brake pedal is connected to another motor through a four bar mechanism. The loop that is formed by the four-bar mechanism is designed to be a parallelogram for a simple kinematic relationship between the pedal and the motor. The steering wheel and the pedals are controlled with a sampling rate of 800 Hz.

4.2 Software

To achieve a realistic simulation, the simulator renders virtual driving environments including visual and auditory stimuli based on Vehicle Physics Pro (VPP [1]), which is a commercial vehicle physics engine running in the Unity 5 game engine (Figure 4.1) with an update rate of 50 Hz. The controller process (running in 800 Hz) and this simulation process are connected via shared memory and continuously exchange necessary variables and parameters.
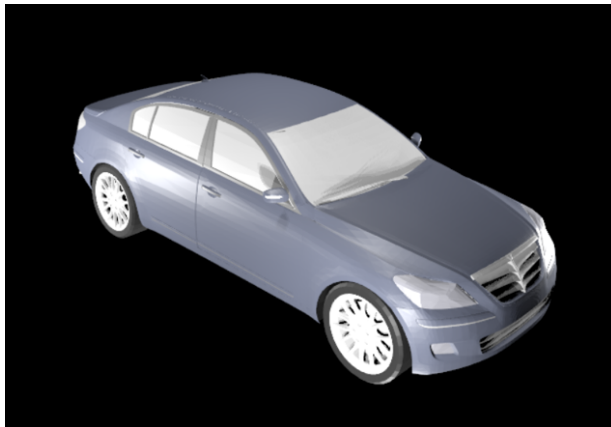
Figure 4.3: Visualization of 3D Vehicle Model.

(a) Reference engine curves [2] (b) Simulated engine curves
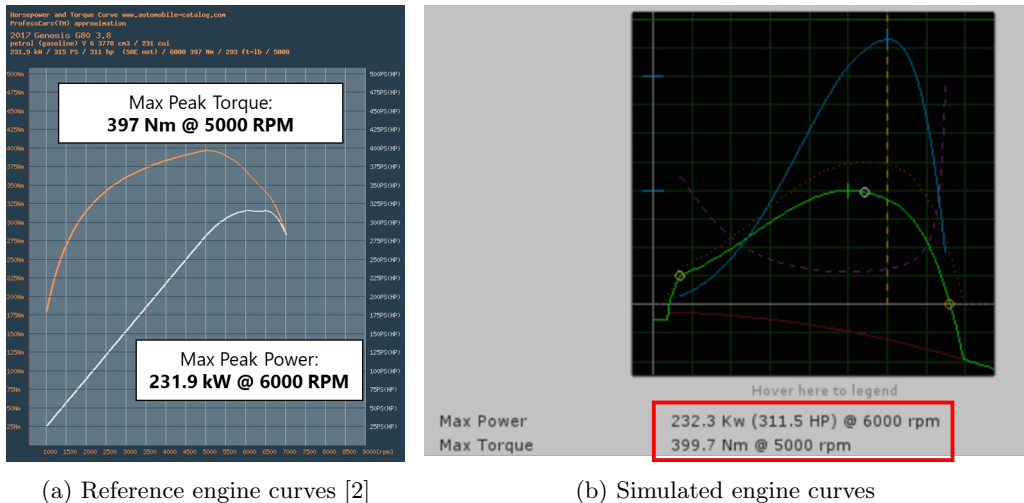
Figure 4.4: Comparison between real and simulated engine torque/power curves.

For the realistic simulation of car dynamics, a specific vehicle (Genesis G80, Hyundai Motors) was chosen to determine the physical parameters of VPP. Figure 4.3 represents a simulated vehicle in our driving simulator. Its size was $1.8\,\mathrm{m\,(W)} \times 5.0\,\mathrm{m\,(D)} \times 1.5\,\mathrm{m\,(H)}$, and its weight is $1900\,\mathrm{kg}$. Figure 4.4 shows a comparison between the real and simulated parameters of engine torque/power curves. We formed the simulated engine torque/power curves of the virtual vehicle engine to have a similar shape and peak values to the realistic reference [2]. Other physical parameters, such as tire parameters and gear ratios, were also carefully tuned for realistic simulation.

4.3 Realistic Torque Feedback Control

Table 4.1: Constants for Simulated Realistic Driving Torque Feedback

Steering Wheel		Accelerator/Brake Pedals	
G_{shaft} (m)	0.75	K_a, K_b (N·m/degree)	0.2
D_s (N·m·s/degree)	0.002	D_a, D_b (N·m·s/degree)	0.001
$T_{friction}$ (N·m)	0.1		

In our proposed system, the steering angle θ_s is between $\theta_{s,min} = -459°$ and $\theta_{s,max} = 459°$, and the steering ratio is 11.8:1. The driver cannot steer outside this range. The simulated steering torque T_s is implemented such that it is similar to the real torque transmitted from the driving shaft to provide useful information about the road and vehicle status, as follows:

$$T_s = T_{s,align} + T_{s,damping} + T_{friction}, \tag{4.1}$$

where $T_{s,align}$ is the self-alignment torque, and $T_{s,damping}$ and $T_{friction}$ are the viscous and Coulomb frictions from the car dynamics, respectively. In four-wheel drive, the steering reactive torque can be estimated [28] as follows:

$$T_{s,align} \approx G_{shaft} \cdot \frac{1}{2} \left(F_{fl} + F_{fr}\right), \tag{4.2}$$

where F_{fl} and F_{fr} are the lateral forces applied to the left and right front wheels obtained from VPP. G_{shaft} is the imaginary gain of the torque transmission from the shaft. $T_{s,damping} = D_s \dot{\theta}_s$, and $T_{s,friction}$ is constant, both in the opposite direction of the steering wheel rotation. From (4.2), a user can perceive driving-like sensations on a path with respect to the direction and velocity of the virtual vehicle.

Our haptic pedals are controlled using a spring-damper impedance control scheme. Let the accelerator angle be θ_a. If θ_a is between $\theta_{a,min} = 0°$ and $\theta_{a,max} = 10°$, it is normalized and sent to the throttle value of the virtual engine in VPP. The simulated torque to the accelerator is computed as follows:

$$T_a = T_{a,spring} + T_{a,max} + T_{a,damping} + g\left(\theta_a\right), \tag{4.3}$$

where $T_{a,damping} = D_a \dot{\theta}_a$ is a virtual damping torque and $g\left(\cdot\right)$ is a gravity-compensation term. The spring-like torque $T_{a,spring}$ is determined by

$$T_{a,spring} = K_a \left(\theta_a - \theta_{a,0}\right), \tag{4.4}$$

where K_a is the virtual spring coefficient, and $\theta_{a,0}(= \theta_{a,min} - 5° = -5°)$ is the initial position of the accelerator pedal. $T_{a,spring}$ pushes the driver's right foot upward to deliver information about how much s/he is pressing the pedal from $\theta_{a,0}$. $T_{a,max}$ is a unilateral feedback term to provide information regarding the maximum angle such that

$$T_{a,max} = \begin{cases} 0 & \text{if } \theta_a < \theta_{a,max} \\ K_{a,max} (\theta_a - \theta_{a,max}) & \text{if } \theta_a \geq \theta_{a,max} \end{cases}. \tag{4.5}$$

$T_{a,max}$ enables the driver to perceive the virtual endpoint at $\theta_{a,max} = 10°$. We used $K_{a,max} = 10 K_a$.

The simulated torque to the brake pedal, T_b, is computed similarly for the brake angle θ_b. The only difference was that the maximum brake angle $\theta_{b,max} = 5°$.

We carefully tuned all of the other parameters to achieve realistic experiences, and their values are specified in Table 4.1.

V. Part I: Driving Skill Modeling Using Neural Networks for Haptic Assistance

Usually, the optimal (desired) trajectory should be obtained to represent successful skill execution. In this chapter, we explain our data-driven modeling approach using neural networks to get the desired angles from experienced drivers' driving data. We conducted two human experiments (1) to validate our modeling strategy and (2) to show the feasibility of our strategy for driving skill enhancement.

5.1   Modeling Using Neural Networks

In [53], the dynamic nature of human control strategy is abstracted into a static mapping between the input and output using NNs. In fact, a dynamic system can be approximated using difference equations [51], such that

$$
\begin{aligned}
\boldsymbol{u}\left[k+\tau\right] = f[\boldsymbol{u}\left[k\right], \boldsymbol{u}\left[k-\tau\right], \cdots, \boldsymbol{u}\left[k-\left(D_{\boldsymbol{u}}-1\right)\tau\right], \\
\boldsymbol{x}\left[k\right], \boldsymbol{x}\left[k-\tau\right], \cdots, \boldsymbol{x}\left[k-\left(D_{\boldsymbol{x}}-1\right)\tau\right], \\
\boldsymbol{z}\left[k\right], \boldsymbol{z}\left[k-\tau\right], \cdots, \boldsymbol{z}\left[k-\left(D_{\boldsymbol{z}}-1\right)\tau\right]],
\end{aligned}
\tag{5.1}
$$

where $f\left[\cdot\right]$ represents a nonlinear map using NN, $\boldsymbol{u}\left[k\right]$ is the control vector, $\boldsymbol{x}\left[k\right]$ is the system-state vector, and $\boldsymbol{z}\left[k\right]$ is a vector that describes exogenous environmental features at time step k. Then, (5.1) can be rewritten as

$$
\boldsymbol{u}\left[k+\tau\right] = f\left[\bar{\boldsymbol{u}}\left[k\right], \bar{\boldsymbol{x}}\left[k\right], \bar{\boldsymbol{z}}\left[k\right]\right],
\tag{5.2}
$$

where $\bar{\boldsymbol{m}}\left[k\right] = \left[\boldsymbol{m}\left[k\right], \boldsymbol{m}\left[k-\tau\right], \cdots, \boldsymbol{m}\left[k-\left(D_{\boldsymbol{m}}-1\right)\tau\right]\right]^{T}$ for an arbitrary vector $\boldsymbol{m}$. The training of $f\left[\cdot\right]$ using the input-output of (5.2) optimizes a future value of $\boldsymbol{u}$ at τ-step later from the current and previous states of $\boldsymbol{u}$, $\boldsymbol{x}$, and $\boldsymbol{z}$.

Therefore, after the training, $f\left[\cdot\right]$ outputs

$$\hat{\boldsymbol{u}}\left[k\right]=f\left[\bar{\boldsymbol{u}}\left[k\right],\bar{\boldsymbol{x}}\left[k\right],\bar{\boldsymbol{z}}\left[k\right]\right],\qquad(5.3)$$

where $\hat{\boldsymbol{u}}\left[k\right]$ is a predictive control vector optimized by the future control vectors ($\hat{\boldsymbol{u}}\left[k\right]\simeq\boldsymbol{u}\left[k+\tau\right]$).

5.1.1 Data Acquisition

We designed 25 two-lane paths to collect driving trajectories and other important variables for skill modeling. Each path consists of three segments with a total length of 600 m. The first and third are a 200-m straight segment. The second segment is a curve with curvature $\kappa=\frac{1}{R}=\frac{|\phi|}{L}$, where R is the radius, L is the arc length, and ϕ is the angle in radians, as shown in Figure 5.1a. The value L of the second segment is 200 m, but each path has varying ϕ from -180° to 180° with 15° step (Figure 5.1b). Therefore, $\phi=0°$ results in a 600-m-long straight path.
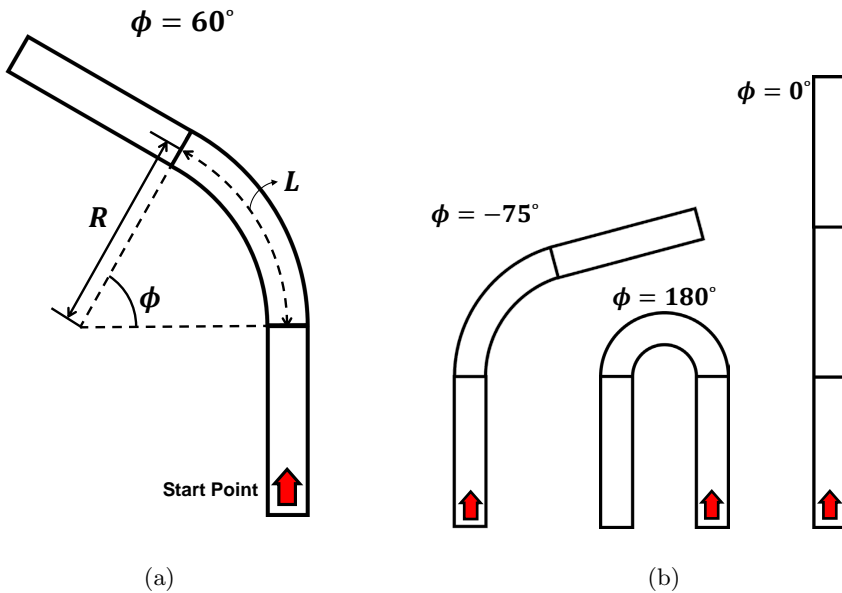
Figure 5.1: Driving paths. (a) Variable definitions. (b) Examples.

Table 5.1: Statistics of Driving Experts

Expert	Age (years)	Driving Experience (years)	Total # of Trajectory Samples in 50 Hz
E_1	30	6	282,265
E_2	25	5	286,263
E_3	51	30	282,210
E_4	39	19	286,386
E_5	44	16	299,473
M±SD	37.6±10.8	15.2±10.3	

Five experienced drivers (E_1–E_5; all males; age 25–51 years, M 37.6, SD 10.8; driving experience 5–30 years, M 15.2, SD 10.3) participated in the data acquisition(Table 5.1). In each trial, the driver was instructed to complete driving following a given path, while staying only in the first lane of the path and maintaining a velocity of 60 km/h using the speedometer. Each trial took about 36–40 s, and each driver completed six trials for each path (150 trials per driver).

5.1.2 Neural Network Design

We observed that the experienced drivers did not require the manipulation of the brake pedal for the lane-keeping task, so excluded θ_b from the control vector. In addition, we do not consider the interdependence between the controls of the steering wheel and accelerator pedal, and we train separate NNs for each. This allows us to use more compact networks with accurate modeling results. Hence, in the model for the steering wheel, $\boldsymbol{u} = \theta_s$, and in the model for the accelerator pedal, $\boldsymbol{u} = \theta_a$. For the vehicle state, we used $\boldsymbol{x} = [v \ \omega \ r]^T$, where v is the longitudinal velocity (m/s), ω is the angular velocity (degree/s), and r is the number of engine revolutions per minute (RPMs) of the virtual car.

To define the environmental features, we rely on d_i ($i = 1, \cdots, 5$; Figure 5.2), which is the two-dimensional (2D) Euclidean distance from the driver's position
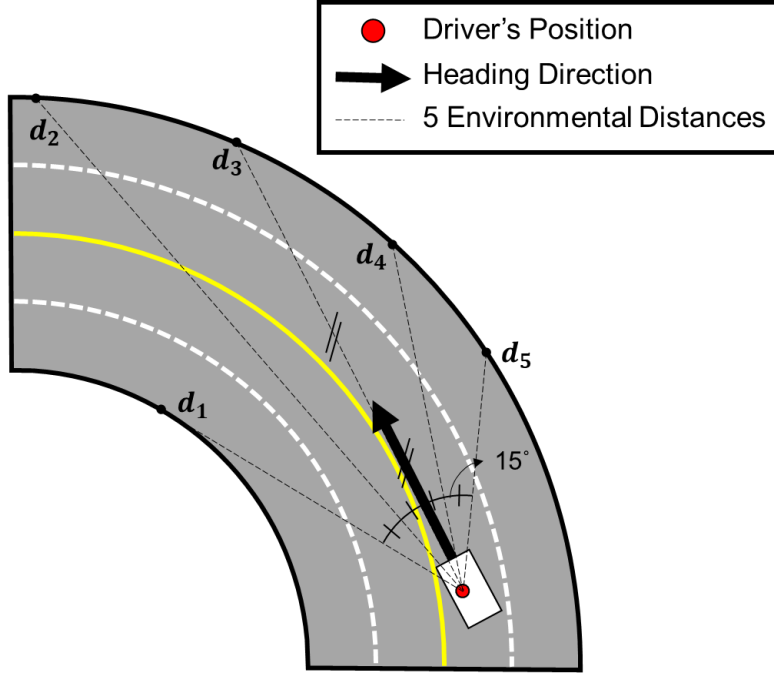
Figure 5.2: Five distances from the driver's perspective.

to the road boundary of the road in the direction of -30°, -15°, 0°, 15°, and 30° relative to the driver's frontal direction. The angular values of d_i were determined considering the driver's field of view (60°) within the simulated vehicle. The maximum value of d_i is set to 60 m. Then the environmental feature vector $\boldsymbol{z} = [z_1 \ z_2 \ z_3 \ z_4 \ z_5]^T$, where

$$z_i = \frac{1}{1 + d_i}. \tag{5.4}$$

z_i represents the future hazard of collision in the i-th direction.

Then the two NNs, i.e., f_s and f_a, for the steering wheel and the accelerator pedal, respectively, are trained using the input-output of the following equations:

$$\theta_s \left[k + \tau\right] = f_s \left[\bar{\theta}_s \left[k\right], \bar{\boldsymbol{x}} \left[k\right], \bar{\boldsymbol{z}} \left[k\right]\right], \tag{5.5}$$

$$\theta_a \left[k + \tau\right] = f_a \left[\bar{\theta}_a \left[k\right], \bar{\boldsymbol{x}} \left[k\right], \bar{\boldsymbol{z}} \left[k\right]\right]. \tag{5.6}$$

Therefore, the output variables $\hat{\theta}_s \left[k\right] \simeq \theta_s \left[k + \tau\right]$ and $\hat{\theta}_a \left[k\right] \simeq \theta_a \left[k + \tau\right]$ can respresent the predictive driving behavior of experienced drivers under the current

and previous states of θ_s, θ_a, $\boldsymbol{x}$, and $\boldsymbol{z}$.

Considering that the human motion bandwidth is less than $5\,\mathrm{Hz}$ [11], we used the same constants for all of the input vectors: $\tau = 10$ and $D_{\boldsymbol{u}} = D_{\boldsymbol{x}} = D_{\boldsymbol{z}} = 5$. Then all NNs predict $0.2\,\mathrm{s}$ future values of execution from the five current and previous variables in 50-Hz simulations. Before training, all input-output vectors, $\boldsymbol{u}$, $\boldsymbol{x}$, and $\boldsymbol{z}$ are normalized.

5.1.3 Training Results

We trained all networks using MATLAB (R2017a, MathWorks). The training used a network training function of gradient descent backpropagation with an adaptive learning rate and a transfer function of a hyperbolic tangent sigmoid. The initial learning rate was 0.5. Each NN consisted of four hidden layers with 32, 24, 16, and 8 nodes. We pooled the input-output data of all the experienced drivers for NN training. The data were partitioned into training, validation, and test sets in the proportion of 70%, 15%, and 15%, respectively. The training was terminated if the root mean-squared error (RMSE) of predicting a test set decreased, and was saturated into 1% and 4.5% for θ_s and θ_a, respectively. These values were determined by trial and error.

5.2 Experiment I: Validity of Driving Skill Modeling Using Neural Networks

To provide haptic assistance for trajectory-following tasks, an optimal (desired) trajectory should be given for the computation of task performance errors [46]. In our driving task, we denote the performance error vector $\boldsymbol{e}_\theta = \boldsymbol{\theta} - \boldsymbol{\theta}_d$, where $\boldsymbol{\theta} = [\theta_s\ \theta_a]^T$ is the current angle vector and $\boldsymbol{\theta}_d = [\theta_{s,d}\ \theta_{a,d}]^T$ is the desired angle vector. Therefore, we required a expert skill model that produces $\boldsymbol{\theta}_d$, representing appropriate actions of the steering wheel and the accelerator pedal that

depend on the current and the past driving situations.

Because the experienced drivers can produce appropriate actions [14], we considered the expert skill model as the NNs trained by experienced drivers. In other words, we set $\boldsymbol{\theta}_d = \hat{\boldsymbol{\theta}}$, where $\hat{\boldsymbol{\theta}} = \begin{bmatrix} \hat{\theta}_s & \hat{\theta}_a \end{bmatrix}^T$ is the output vector generated by two NNs. In Experiment I, we aim to provide logical evidence of setting $\boldsymbol{\theta}_d = \hat{\boldsymbol{\theta}}$, by validating whether the NN-based model can produce ideal driving trajectories with the following research questions: Q_1: *Can our model produce stable predictive outputs even in other general driving environments?*; Q_2: *Can our model distinguish two different driving skill levels (experienced/novice)?*; and Q_3: *Can we objectively prove that experienced drivers have enough expertise, compared to novice drivers?*

5.2.1 Data Acquisition

Our NN models were trained using the experienced drivers' data collected along the 25 simple paths (Section 5.1.1). The first goal of Experiment I was to validate whether the NN models can be applied to general, longer, and more complex driving environments. To this end, we designed a long path as a sequence of randomly generated straight and curved segments similar to that in [52].
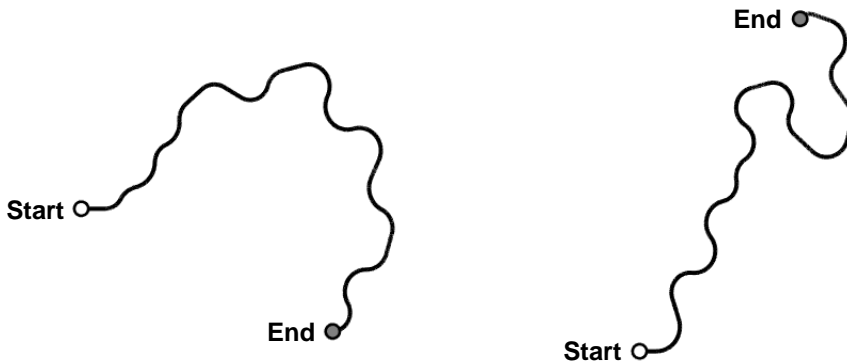
Figure 5.3: Driving paths used in Experiments I (left) and II (right).

Each straight segment had one parameter, length L. Each curved segment

had a radius of curvature R and its sweep angle ϕ as parameters. The parameters were randomly chosen from 100–150 m (L and R) and $\pm 45°$–$\pm 135°$ (negative for right curves) for each segment. A straight segment was followed by a left/right curve with equal probability 0.5. A left (right) curve was followed by a straight segment with probability 0.4 and a right (left) curve with probability 0.6. The total length of the path was 4 km. From many randomly generated paths, we selected two representative paths consisting of 23 and 22 segments for our experiments (Figure 5.3). Compared to the short, simple, predetermined paths used in the modeling (Section 5.1.1), the two paths in Figure 5.3 are long, arbitrary and complex, and randomized (L, R, and ϕ). Thus, we deem the two paths appropriate for our experiments.

The same five experienced (EX: E_1–E_5) and 18 new novice drivers (NO: N_1–N_{18}; all male; 18–28 years old, M 22.8, SD 3.0) participated in collecting new driving data. The latter participants either did not have driving licenses or had licenses but with very little driving experience, e.g., young individuals who had not owned or driven a car/motorcycle in the past two years. We controlled the novice drivers' gender and age as these are important factors for motor learning.

As in the practice, participants drove in three 600-m short paths ($\phi = -90°, 0°, \text{and } 90°$). Then, they completed driving in the 4-km long path while staying only in the first lane of the path at 60 km/h. The driving data of each participant was applied to the NN models (f_s and f_a) to obtain the trajectories of the predicted device angles ($\hat{\theta}_s$ and $\hat{\theta}_a$).

5.2.2 Performance Measures

Modeling Performance

For each participant, the NN outputs $\hat{\theta}_s$ and $\hat{\theta}_a$ represent the control action that the experienced drivers would make after τ steps given the control vectors

$\bar{\theta}_s$ and $\bar{\theta}_a$, the vehicle state $\bar{\mathbf{x}}$, and the environmental state $\bar{\mathbf{z}}$ of that participant; see (5.5) and (5.6). Hence, the following two errors indicate the difference in the participant's driving action relative to the predicted output of our model:

$$e_{s,p}[k] = \hat{\theta}_s[k] - \theta_s[k+\tau], \tag{5.7}$$

$$e_{a,p}[k] = \hat{\theta}_a[k] - \theta_a[k+\tau]. \tag{5.8}$$

Let $RMS(\tilde{m})$ be an operator that is used to compute the root mean square of all available samples of $m[k]$ in the sequence $\tilde{m}$. Then, the normalized RMSE, $\bar{E}_{s,p}$ and $\bar{E}_{a,p}$, for each individual driving data are defined by

$$\bar{E}_{s,p} = \frac{E_{s,p}}{\theta_{s,M} - \theta_{s,m}} = \frac{RMS(\tilde{e}_{s,p})}{\theta_{s,M} - \theta_{s,m}}, \tag{5.9}$$

$$\bar{E}_{a,p} = \frac{E_{a,p}}{\theta_{a,M} - \theta_{a,m}} = \frac{RMS(\tilde{e}_{a,p})}{\theta_{a,M} - \theta_{a,m}}, \tag{5.10}$$

where $\theta_{s,M}$, $\theta_{s,m}$, $\theta_{a,M}$, and $\theta_{a,m}$ are the maximum and minimum device angles obtained from the data of experienced drivers used for NN modeling (These values were also used for the training data normalization in Section 5.1.2). Thus, $\bar{E}_{s,p}$ and $\bar{E}_{a,p}$ quantify the similarity of the participant's driving skill relative to that of the experienced drivers captured in the NN models.

Objective Skill Performance

The driving skill of each participant is broken down into steering and pedaling performance. The steering performance is evaluated by a distance error e_d, and an angle error e_δ of the virtual vehicle, as defined in Figure 5.4. The distance error e_d is the distance between the current car position and the closest point on the (invisible) midline of the first lane. The angular error e_δ is the angle between the car heading direction and the road frontal direction at the closest point on the midline of the first lane. Then we use $E_d = RMS(\tilde{e}_d)$ and $E_\delta = RMS(\tilde{e}_\delta)$ as indicators of the steering performance.
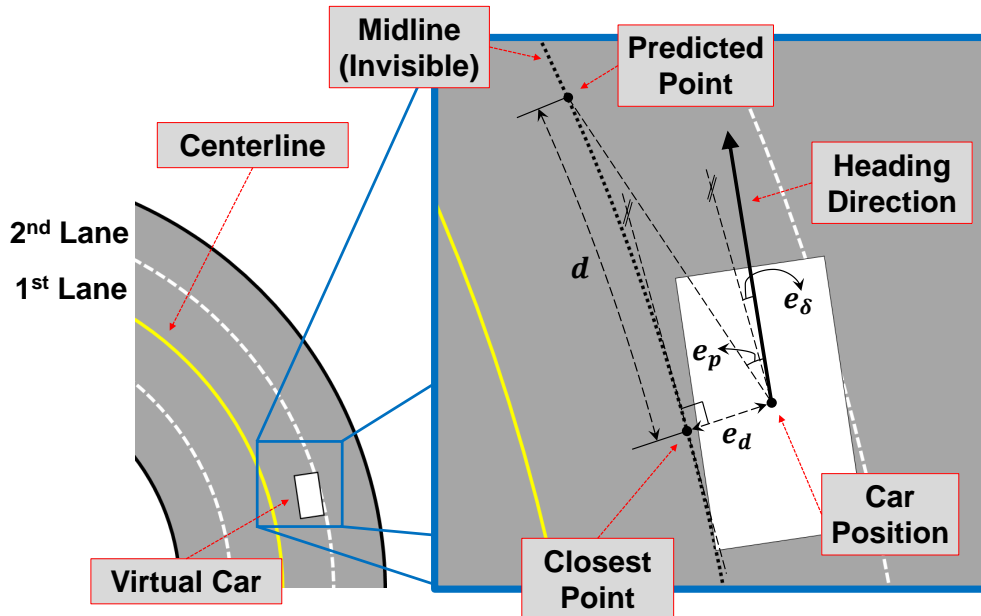
Figure 5.4: Driving errors (e_d, e_δ, and e_p) used in Experiments I and II. In our simulation, $d = v\Delta t$ and $\Delta t = 1\,\mathrm{s}$ is the look-ahead time.

For the pedaling performance, we first define a vehicle velocity error as $e_v\,[k] = v\,[k] - v_d$, where $v_d = 62.64\,\mathrm{km/h}$. In our simulator, the target speed $60\,\mathrm{km/h}$ imposed on the participants corresponds to the actual vehicle speed of v_d when the needle of the speedometer reaches $60\,\mathrm{km/h}$ from the driver's perspective. $E_v = RMS\,(\tilde{e}_v)$ is used as a measure of the pedaling performance. Because the initial vehicle velocity is $0\,\mathrm{km/h}$, E_v is computed using only the velocity samples obtained after the vehicle speed first reaches v_d. In addition, as a measure of the pedaling efficiency, we compute $\Omega_a = RMS\,(\tilde{\omega}_a)$, where $\omega_a\,[k] = |\dot{\theta}_a\,[k]\,|$, focusing on the pedaling speed. Ω_a increases if the participant operates the pedal more abruptly.
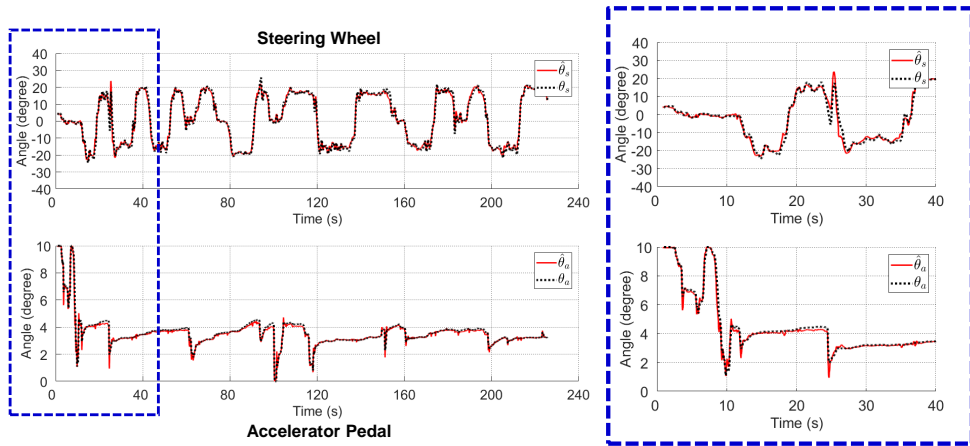
(a) Experienced E4, Right: magnified at $t =$0–40 (s).
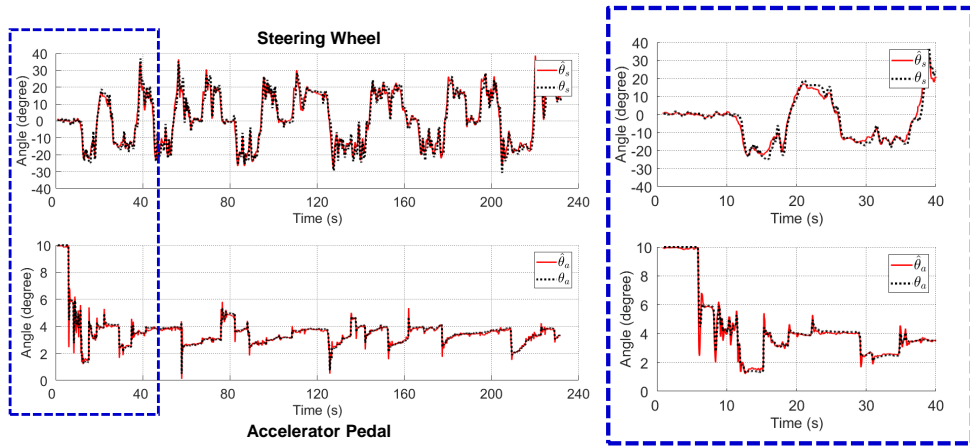
(b) Novice N11, Right: magnified at $t =$0–40 (s).

Figure 5.5: Examples of the recorded trajectory $\theta(t)$ (black, dotted) and the desired trajectory $\hat{\theta}(t)$ (red, solid) in Experiment I.
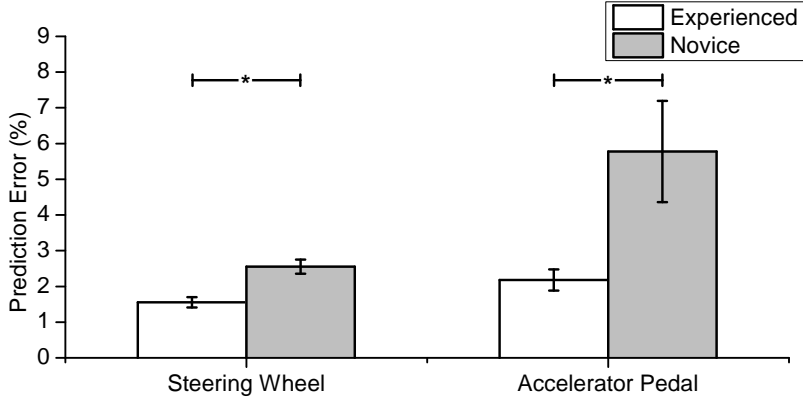
Figure 5.6: Mean $\bar{E}_{s,p}$ (left) and $\bar{E}_{a,p}$ (right). Error bars represent standard errors. Asterisks indicate statistically significant differences.

5.2.3 Results and Discussion

Figure 5.5 shows examples of an experienced (E_4) and a novice (N_{11}) driver who achieved a median performance of $\bar{E}_{s,p}$ and $\bar{E}_{a,p}$ from among the respective groups. The experienced driver's trajectories appear to be in better agreement with the desired trajectories.

The means of the six performance measures are shown in Figs. 5.6 and 5.7. We applied Welch's t-test (unequal sample sizes and unequal variances) to assess the effect of the participant group (EX and NO) on each measure. The results are: $\bar{E}_{s,p}$: EX$(1.55\,\%) <$ NO$(2.55\,\%)$, $t(17.99) = -4.08$, $p < 0.001$; $\bar{E}_{a,p}$: EX$(2.18\,\%) <$ NO$(5.78\,\%)$, $t(18.40) = -2.48$, $p = 0.023$; E_d: EX$(0.34\,\mathrm{m}) <$ NO$(0.46\,\mathrm{m}$, $t(5.67) = -2.20$, $p = 0.072$; E_δ: EX$(1.01\,^\circ) <$ NO$(1.45\,^\circ)$, $t(9.62) = -4.11$, $p = 0.002$; E_v: EX$(1.93\,\mathrm{km/h}) <$ NO$(2.18\,\mathrm{km/h})$, $t(4.82) = -0.63$, $p = 0.557$; and Ω_a: EX$(1.58\,\mathrm{degree/s}) <$ NO$(4.27\,\mathrm{degree/s})$, $t(18.77) = -2.53$, $p = 0.021$.

These results provide answers to our research questions.

Q_1

Our NN models (f_s and f_a) were trained using the experienced drivers' driving data on many simple paths, and the NN training ended when the RMSE
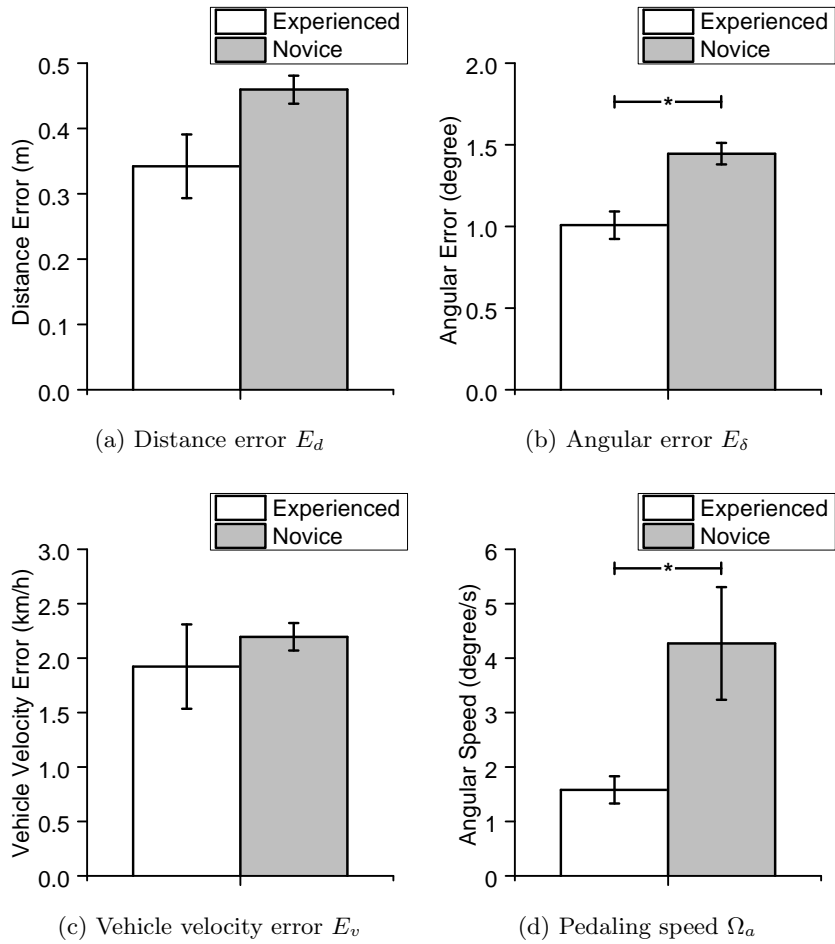
Figure 5.7: Mean objective skill measure for the steering wheel (a and b) and the accelerator pedal (c and d). Error bars represent standard errors. Asterisks indicate significant differences.

was less than 1% and 4.5% for f_s and f_a, respectively (Section 5.1.1). In this experiment, the predictive errors of our models for the same drivers' driving data on a more complicated and general path were also small with mean $\bar{E}_{s,p} = 1.55\%$ and mean $\bar{E}_{a,p} = 2.18\%$. Hence, our models can effectively predict their driving actions even for complicated paths composed of arbitrary curves and straight lanes.

Q$_2$

The experienced drivers showed smaller values of two predictive errors than the novice drivers with statistical significance. This result indicates that our models can represent the specific driving skills of experinced drivers, which are particularly different from those of other novice drivers.

Q$_3$

All the skill-performance measures (E_d and E_δ for steering and E_v and Ω_a for accelerator pedaling) showed better performance with the experienced drivers than with the novice drivers. The differences in E_δ and Ω_a were statistically significant. Thus, the driving skill of the experienced drivers captured by our NN models is more professional than novice drivers.

5.3   Experiment II: Applicability To Driving Skill Enhancement

We can design haptic assistance exerting feedback for supporting corrections of current movement, by utilizing the performance error vector $\boldsymbol{e}_\theta = \boldsymbol{\theta} - \boldsymbol{\theta}_d$, where $\boldsymbol{\theta}_d = \hat{\boldsymbol{\theta}}$ based on the behavior of expert (experienced) drivers. Of the various haptic assistance, the most representative approach is haptic guidance, where external haptic stimuli are provided to learners concurrently during training in

order to communicate information on the desired movement [23]. By transferring the desired movement via kinesthetic feedback in haptic guidance, we can hypothesize that a current driver's skill execution can be enhanced. To this end, we conducted an experiment comparing two performance-based haptic guidance approaches for a driving skill; one obtains $\boldsymbol{\theta}_d = \hat{\boldsymbol{\theta}}$ and the other conventionally formulates $\boldsymbol{\theta}_d$ from a fixed environments.

The followings are research questions: Q_1: *Can haptic guidance be implemented with our NNs?*; Q_2: *Can haptic guidance that is implemented with our NN provide the demonstration of experts' driving behavior?*; and Q_3: *Can haptic guidance that is implemented with our NN demonstrate the competitive driving skill performance competitively relative to conventional haptic guidance?*

5.3.1 Methods

Here, we report three different methods tested in this experiment.

N: No Haptic Guidance

A driver completes driving, receiving only realistic driving feedback (Section 4.3).

G: Haptic Guidance with Neural Networks

A driver completes driving, receiving assitive haptic feedabck using the NN-based expert model. First, $\hat{\theta}_s[k]$ and $\hat{\theta}_a[k]$ ($50\,\mathrm{Hz}$) have been smoothened to $\hat{\theta}_s(t)$ and $\hat{\theta}_a(t)$ by moving average filters to command semi-continuous feedback ($800\,\mathrm{Hz}$). Because $\boldsymbol{\theta}_d = \hat{\boldsymbol{\theta}}$, the PID-based steering feedback $T_{s,assist}$, which is required to deliver $\hat{\theta}_s$ can be computed as follows:

$$T_{s,assist}(t) = K_{pid}e_s(t) + I_{pid}\int_{t_0}^{t} e_s(t')\,dt' + D_{pid}\dot{e}_s \qquad (5.11)$$

$$e_s = \theta_s - \theta_{s,d} = \theta_s - \hat{\theta}_s, \qquad (5.12)$$

where t_0 is the recent time when e_s becomes zero. The whole steering feedback is replaced by

$$T_s = T_{s,assist} + T_{s,stable}, \tag{5.13}$$

where $T_{s,stable} = D_{stable}\dot{\theta}_s$ provides stable feedback with increased viscosity and without the Coulomb friction. $K_{pid} = 0.60\,\text{N·m/degree}$, $I_{pid} = 0.12\,\text{N·m·s}^{-1}\text{/degree}$, and $D_{pid} = 0.06\,\text{N·m·s/degree}$, and $D_{stable} = 5D_s$. From trial and error, the gains have been appropriately tuned for two purposes: (1) to exert the steering wheel feedback strongly so that the virtual vehicle can complete driving only with pedal manipulations (similar to autonomous steering), but also (2) to enable a driver to overcome the feedback to adjust device angles.

Because the driver's foot and the accelerator pedal are not in full contact in any time, for assistive pedaling feedback, a unidirectional torque is utilized rather than PID-based feedback. The $T_{a,assist}$ required to deliver $\hat{\theta}_a$ is as follows:

$$T_{a,assist}(t) = \begin{cases} 0, & \text{if } \theta_a(t) < \hat{\theta}_a(t), \\ K_{a,max} \cdot e_a(t), & \text{if } \theta_a(t) \geq \hat{\theta}_a(t), \end{cases} \tag{5.14}$$

$$e_a = \theta_a - \theta_{a,d} = \theta_a - \hat{\theta}_a, \tag{5.15}$$

which replaces $\theta_{a,max}$ in $T_{a,max}$ to $\hat{\theta}_a$. From (5.14), the accelerator pushes the driver's foot upwards when a driver pushes it more than $\hat{\theta}_a$. Then, whole pedaling feedback is altered to:

$$T_a = T_{a,assist} + T_{a,spring} + T_{a,damping} + g(\theta_a). \tag{5.16}$$

C: Conventional Haptic Guidance

A driver completes driving, receiving conventionally designed assitive haptic feedback. Compared with G, C determines $\boldsymbol{\theta}_d$ only from external environments. The same torque control equations (6.4) and (5.14) are adopted. For steering

feedback, predictive haptic guidance ([45]) was adopted. The predictive haptic guidance is based on the observation that a driver determines his/her driving based on a prediction. This method considers two error terms, a look-ahead direction error e_p and the distance error e_d (Figure 5.4), and determines the desired angle $\theta_{s,d}$, as follows:

$$\theta_{s,d} = K_p e_p + K_d e_d. \tag{5.17}$$

Using $K_p = 7.65$ and $K_d = 1.00\,\text{degree/m}$ and the same torque gains of G, this method can also support the vehicle to complete driving only with pedal manipulations.

For the accelerator, there exist several applicable algorithms [49, 32], but none of them guarantees training effectiveness. Hence, we implemented a simpler, deterministic feedback that only provides overspeed cues. Let $v_M = 66.0\,\text{km/h}$ be a criterion of overspeed. We computed $\theta_{a,d}$ as follows:

$$\theta_{a,d} = \begin{cases} \theta_{a,max}, & \text{if } v < v_M, \\ \theta_{a,min}, & \text{if } v \geq v_M, \end{cases} \tag{5.18}$$

From (5.18), the driver perceives an impulse-like feedback from the right foot when the vehicle velocity exceeds v_M.

5.3.2   Experimental Protocol

Every participant (the same in Experiment I) completed three different driving trials in a complicated path different from the path in Experiment I (Figure 5.3), by receiving corresponding assistive feedbacks. Since there are total $3! = 6$ possible permutations from three conditions, novices of three each were assigned to the same presentation order.

After each trial, the participant was asked to answer the following questions for both steering and pedaling feedback, respectively, on an 1 to 7 continuous

scale (a neutral score of 4): (1) Was the training effective for driving? (Effectiveness); (2) Was the training comfortable/uncomfortable? (Comfort); (3) Was the training fun? (Fun); (4) Do you think that a more extended training period under the corresponding feedback can help to improve your skill (Helpfulness). Thus, there was a total of 24 questions (4 questions × 2 devices × 3 conditions) for each participant. Each participant was paid KRW 15,000 ($\simeq$ USD 13) after the experiment.

5.3.3 Results and Discussion

This section reports the quantitative (the same metrics in Experiment I) and qualitative results of Experiment II. For the statistical analysis, we applied a repeated measures ANOVA, with methods (Section 5.3.1) as the within-subject factor. Tukey's HSD multiple testing was conducted as a post-hoc test to significant effects.

Behavioral Similarity

We computed the predictive errors ($\bar{E}_{s,p}$ and $\bar{E}_{a,p}$) for each resulting trajectory (Figure 5.8).

If a participant's driving behavior is similar to experts' behavior captured in NNs, then the errors decrease. The ranking of $\bar{E}_{s,p}$ is G (1.10 %) < C (1.42 %) < N (2.36 %). Because the assumption of sphericity was violated from the Mauchly's test ($\chi^2(2) = 29.04$, $p < 0.001$), the Greenhouse-Geisser estimate of sphericity ($\epsilon = 0.54$) was used to recompute the statistics. In results, there exists a significant difference ($F(1.09, 18.51) = 34.27$, $p < 0.001$), and in the post-hoc test, G < N ($t(34) = 11.27$, $p < 0.001$) and C < N ($t(34) = 8.39$, $p < 0.001$). The ranking of $\bar{E}_{a,p}$ is N (4.63 %) < C (6.32 %) < G (6.38 %), and the assumption of sphericity was not violated ($\chi^2(2) = 5.92$, $p = 0.052$). There exists a significant difference ($F(2, 34) = 5.55$, $p = 0.008$), and in the post-hoc test, N < G

$(t(34) = 4.15, p = 0.016)$ and $\mathsf{N} < \mathsf{C}$ $(t(34) = 4.01, p = 0.020)$. Two haptic guidance methods showed significant differences from N.
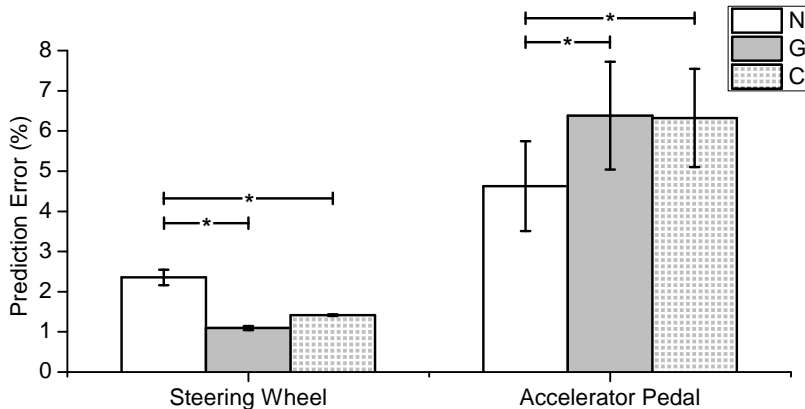
Figure 5.8: Mean $\bar{E}_{s,p}$ (left) and $\bar{E}_{a,p}$ (right) for each method. Error bars represent standard errors. Asterisks indicate statistically significant differences.

Objective Skill Performance

We computed the objective skill measures (E_d, E_δ, E_v, and Ω_a) for each resulting trajectory (Figure 5.9). The ranking of E_d is $\mathsf{N}\,(0.46\,\mathrm{m}) < \mathsf{G}\,(0.50\,\mathrm{m}) < \mathsf{C}\,(0.56\,\mathrm{m})$, and the assumption of sphericity was not violated ($\chi^2\,(2) = 1.74$, $p = 0.418$). There exists a significant difference ($F(2, 34) = 4.73$, $p = 0.015$), and in the post-hoc test, $\mathsf{N} < \mathsf{C}$ $(t(34) = 4.35, p = 0.011)$. The ranking of E_δ is $\mathsf{C}\,(0.94\,^\circ) < \mathsf{G}\,(1.12\,^\circ) < \mathsf{N}\,(1.35\,^\circ)$. Because the assumption of sphericity was violated ($\chi^2\,(2) = 25.68$, $p < 0.001$), the Greenhouse-Geisser estimate of sphericity ($\epsilon = 0.56$) was used for recomputation. In results, there exists a significant difference ($F(1.11, 18.90) = 30.60$, $p < 0.001$), and in the post-hoc test, $\mathsf{G} < \mathsf{N}$ $(t(34) = 6.37, p < 0.001)$, $\mathsf{C} < \mathsf{N}$ $(t(34) = 11.02, p < 0.001)$, and $\mathsf{C} < \mathsf{G}$ $(t(34) = 4.65, p = 0.007)$.

The ranking of E_v is $\mathsf{C}\,(1.62\,\mathrm{km/h}) < \mathsf{G}\,(1.91\,\mathrm{km/h}) < \mathsf{N}\,(2.25\,\mathrm{km/h})$, and the assumption of sphericity was not violated ($\chi^2\,(2) = 1.24$, $p = 0.538$). There exists a significant difference ($F(2, 34) = 5.74$, $p = 0.0071$), and in the post-hoc

(a) Distance error E_d

(b) Angular error E_δ

(c) Vehicle velocity error E_v

(d) Pedaling speed Ω_a
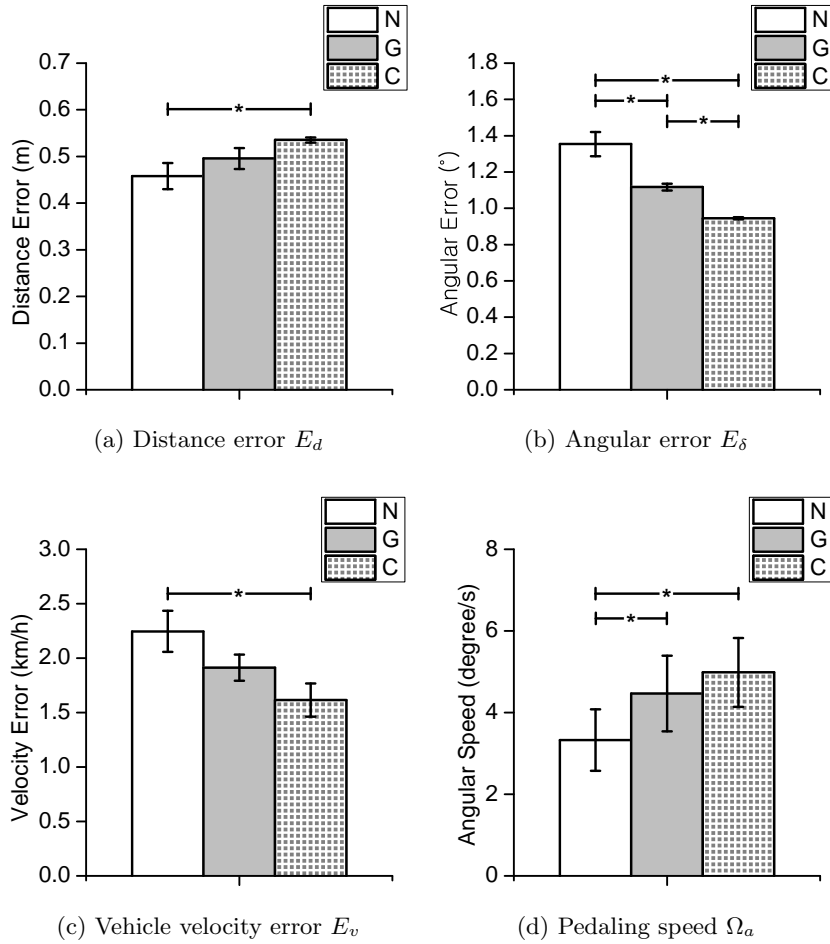
Figure 5.9: Mean objective skill measure for the steering wheel (a and b) and the accelerator pedal (c and d). Error bars represent standard errors. Asterisks indicate significant differences.

test, $C < N$ ($t(34) = 4.79$, $p = 0.005$). The ranking of Ω_a is N ($3.33\,\text{degree/s}$) $<$ G ($4.47\,\text{degree/s}$) $<$ C ($4.98\,\text{degree/s}$), and the assumption of sphericity was not violated ($\chi^2(2) = 3.15$, $p = 0.207$). There exists a significant difference ($F(2, 34) = 8.08$, $p = 0.001$), and in the post-hoc test, $N < G$ ($t(34) = 3.82$, $p = 0.028$), and $N < C$ ($t(34) = 5.56$, $p = 0.001$). In summary, G exhibited a better performance of E_δ, but a worse performance of Ω_a than N. C showed better performances of E_δ and E_v, but worse performances of E_d and Ω_a than N. Comparing the two haptic guidance methods, C achieved better performance than G in E_δ. However, they have no differences with respect to in other measures.

Qualitative Results

We computed the mean scores for each subjective question (Figure 5.10). For the steering wheel, the ranking of effectiveness score is N (3.84) $<$ G (5.87) $<$ C (6.05). Because the assumption of sphericity was violated ($\chi^2(2) = 10.87$, $p = 0.004$), the Greenhouse-Geisser estimate of sphericity ($\epsilon = 0.67$) was used for recomputation. In results, there exists a significant difference ($F(1.34, 22.77) = 22.53$, $p < 0.001$), and in the post-hoc test, $N < G$ ($t(34) = 7.85$, $p < 0.001$), and $N < C$ ($t(34) = 8.55$, $p < 0.001$). The ranking of comfort score is N (4.23) $<$ C (4.70) $<$ G (5.52), and the assumption of sphericity was not violated ($\chi^2(2) = 0.09$, $p = 0.957$). There exists a significant difference ($F(2, 34) = 3.41$, $p = 0.045$), and in the post-hoc test, $N < G$ ($t(34) = 3.65$, $p = 0.037$). The ranking of fun score is C (3.93) $<$ G (4.77) $<$ N (5.09). Because the assumption of sphericity was violated ($\chi^2(2) = 7.41$, $p = 0.025$), the Greenhouse-Geisser estimate of sphericity ($\epsilon = 0.73$) was used. In results, there exists a (marginally) significant difference ($F(1.46, 24.81) = 3.73$, $p = 0.051$), and in the post-hoc test, $C < N$ ($t(34) = 3.73$, $p = 0.032$). The ranking of helpfulness score is C (3.65) $<$ G (4.60) $<$ N (5.18). Because the assumption of sphericity was violated ($\chi^2(2) = 6.28$, $p = 0.043$),
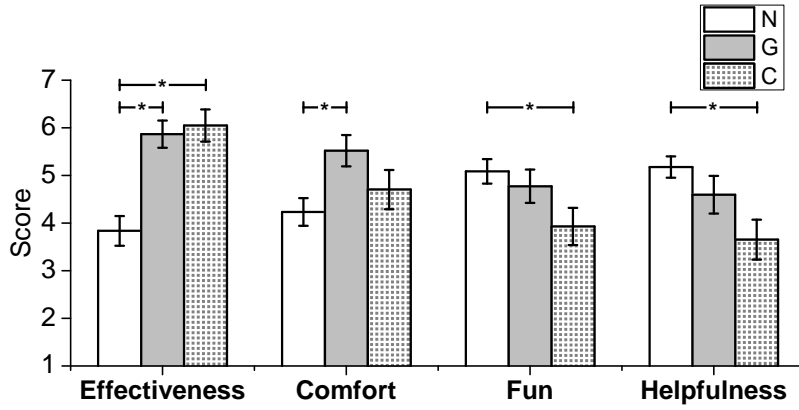
(a) Steering Wheel
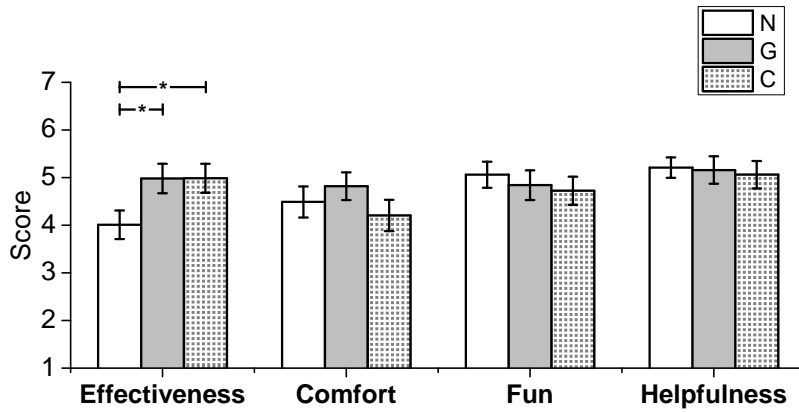
(b) Accelerator Pedal

Figure 5.10: Subjective score responses obtained from questionnaires (1–7 continuous scale). Error bars represent standard errors. Asterisks indicate significant differences.

the Greenhouse-Geisser estimate of sphericity ($\epsilon = 0.76$) was used. In results, there exists a significant difference ($F(1.51, 25.67) = 6.06$, $p = 0.012$), and in the post-hoc test, C $<$ N ($t(34) = 4.88$, $p = 0.004$). The significant differences are observed in the every score of the steering feedback. In the post-hoc test, the participants reported that two haptic guidance methods are more effective than N. However, they reported that only G appears to be more comfortable, and C appears to be less fun and helpful than N.

For the accelerator pedal, the ranking of effectiveness score is N (4.01) $<$ G (4.98) $<$ C (4.99), and the assumption of sphericity was not violated ($\chi^2(2) = 1.19$, $p = 0.550$). There exists a significant difference ($F(2, 34) = 5.38$, $p = 0.009$), and in the post-hoc test, N $<$ G ($t(34) = 4.01$, $p = 0.020$), and N $<$ C ($t(34) = 4.02$, $p = 0.020$). The participants reported that two haptic guidance methods are more effective than N. The rankings of comfort, fun, and helpfulness scores are C (4.21) $<$ N (4.49) $<$ G (4.82), C (4.73) $<$ G (4.84) $<$ N (5.06), C (5.06) $<$ G (5.16) $<$ N (5.21), respectively. However, there were no significant differences in comfort, fun, and helpfulness scores.

Summarized Answers

These results provide answers to our research questions.

Q_1: We successfully implemented haptic guidance which involves the performance-error vector $\boldsymbol{e}_\theta = \boldsymbol{\theta} - \boldsymbol{\theta}_d$, utilizing $\boldsymbol{\theta}_d = \hat{\boldsymbol{\theta}}$, which is a predicted output of NNs.

Q_2: By receiving the steering feedback based on the NNs, the novices could steer the vehicle with smaller predictive errors ($\bar{E}_{s,p}$), which indicates that the novices could make similar steering behavior to experts. However, upon receiving the pedaling feedback, the novices moved the accelerator with an increased value of predictive errors ($\bar{E}_{a,p}$), which indicates that the novices had awkward pedaling behavior distinct from experts. Therefore, while the steering feedback was able

to effectively transfer experts' predictive actions, this was not possible with the pedaling feedback.

Q_3: Both haptic guidance methods helped the novices to achieve better steering performance of E_δ than driving without guidance, which implies that the guidance methods can be adequately applied to the skill transfer. The predictive haptic guidance improved the performance of E_δ, but vitiated performance of E_d, compared to haptic guidance with NN. Hence, it is inconclusive to assert which method is the better. The qualitative results also show that two guidance methods have competitive effectiveness. The effectiveness of the two methods may vary depending on the implementation details, e.g., tuning the parameters.

In contrast, our implementation of the pedaling guidance using NN was inappropriate for the skill transfer. Only the pedaling feedback providing overspeed cues achieved better pedaling performance of E_v, whereas haptic guidance with NN failed to show an improvement. Both haptic guidance methods resulted in an increased Ω_a, which indicates that the novices abruptly moved the accelerator pedal when the assistive feedback was given.

In this study, we selected haptic guidance of among the variety of types of performance-based haptic assistance. However, haptic guidance has a disadvantage which is referred to as the *guidance hypothesis*: excessive concurrent augmented feedback may make learners dependent on the feedback and reduce their focus during the training, interfering with the retention of the learned skill [68]. In Experiment II, the novices reported that they believe that the concurrent haptic feedback may not be suitable for longer training, which is an attribution to the guidance hypothesis.

VI. Part II: Human-like Haptic Assistance: Data-Driven Haptic Assistance Using Neural Networks for Training on Car Steering Task

In the previous chapter, we introduced a NN-based modeling strategy of driving skills in terms of two sub-skills, steering and pedaling and tested the applicability for skill enhancement. However, because our task needed a high cognitive capacity on simultaneous execution of both sub-skills in driving (steering and pedaling), the novice drivers could not recognize the optimized skill model of pedaling.

Therefore, in this chapter, we focus on a steering skill only; we investigated the training effectiveness of haptic assistance methods for a steering skill. Before we go deeper, we should understand the characteristics of a steering skill.

6.1 Steering Characteristics

In practice, *Fitts' law* is a famous approach measuring the performance of manual accuracy tasks numerically [41]. As an extension to Fitt's law, Accot and Zhai have divided a whole path into infinite number of short point-based segments to derive an index of difficulty (ID) of trajectory-based steering tasks; it is called the *steering law* [7] . The steering law has been a widely accepted theoretical model that interprets and predicts human trajectory-following tasks and skills.

Driving is a typical example of trajectory-following tasks in continuous movements. Usually for a simple trajectory-following task, usually a visual reference is given to the trainee to show the current performance error e. However, for

steering in a wide-banded path with only displaying boundaries as in practical driving scenarios like ours, the performance error e (and the desired angle θ_d) cannot be easily recognized.
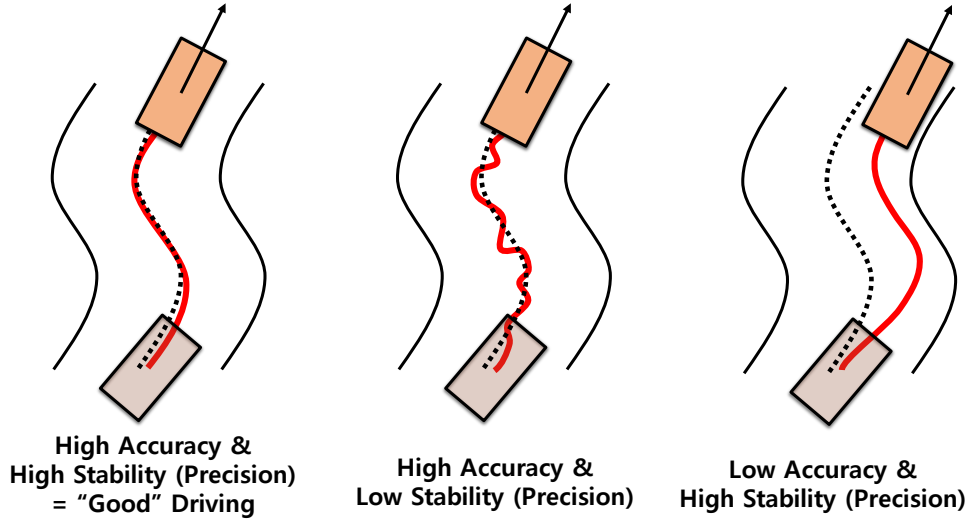
Figure 6.1: Various driving styles in terms of accuracy and stability (precision).

One successful way of to determine the task performance is either measuring both the accuracy and the precision simultaneously during the task execution [35]. Usually, point-to-point human movements consist of a gross, less accurate transfer motion with slower responses and fine, more accurate corrective movements with faster responses [12, 15], in a speed-accuracy tradeoff. Hence, because our steering task is a type of point-to-point trajectory-following task, the steering skill can be regarded a mixture of two sub-skills: error canceling and curve initiation. Error canceling skill incorporates a human ability to make accurate movements to minimize current errors. On the other hand, the purpose of the curve initiation skill is to cope with the vehicle's future status with respect to appropriate prediction of heading direction. Therefore, it incorporates a human ability to make precise movements to optimize vehicle motions, efficiently without mistakes.

Figure 6.1 demonstrates different styles of automobile movements, which

can be resulted by accurate precise steering skill performance. With accurate steering movements, the automobile also can move accurately to an invisible midline. Also, with precise steering movements, the automobile can move stably without large variability.

In the previous chapter, we suggested two error metrics which can be measured from vehicle movements: $E_d = RMS(\tilde{e}_d)$ and $E_\delta = RMS(\tilde{e}_\delta)$. The distance error E_d indicates accurate vehicle motions referencing to the midline; if the vehicle runs close to the midline during the execution, E_d becomes smaller. In contrast, the angular error E_δ indicates stable vehicle motions placing the car's heading direction to the curvature of the path; if the vehicle runs parallel to the path, E_δ becomes smaller.

Therefore, they can represent objective steering skill performance, with respect to two sub-skills in accurate and precise steering control. The numerical error measure E_d reflects the better performance of error canceling skill with accurate steering movements. The numerical error measure E_δ reflects the human sub-skill performance of curve initiation with precise steering movements under human prediction. In the previous experiment described in Section 5.2, the experienced drivers showed small E_d and E_δ resulted in both fine steering performance of the accuracy and the stability. Therefore, in this chapter, we designed an autopilot test to compare the driving styles which two different skill models in each haptic assistance method can produce.

6.2 Experiment I: Automated Driving (Autopilot) Test

We have designed two different haptic assistance methods utilizing different steering models: the first one utilizes a data-driven, NN-based model to generate human performance errors whereas the second one utilizes a conventional model which guides the vehicle to the determined predictive position on the path [45].

In the previous experiment, because the driver's foot and the accelerator pedal are not in full contact in any time, for assistive pedaling feedback, a unidirectional torque was utilized instead of PID-based feedback. However, the result showed that providing the amount of performance errors (as performance-based haptic feedback) might not efficiently enhance the pedaling performance. Therefore, we decided not to use our pedaling skill model for training purpose; instead, we utilized the pedaling skill model to automated control of an accelerator pedal, in order to demonstrate the optimal execution of pedaling. With automated pedaling, it is possible to measure the performance of the steering task objectively.

To this end, we introduce two autopilot modes which have the same implementation to haptic assistance (i.e., haptic guidance) to human drivers: human-like haptic guidance (HG) and robotic haptic guidance (RG). They share the same automated control methods of steering and pedaling. However, they only differ in the steering skill model which provides the desired steering wheel angle. We hypothesized that each autopilot mode may result different steering characteristics.

6.2.1 Automated Control of Accelerator Pedal

In the previous experiment, we used the same configuration of $\tau = 10$ $(0.2\,\mathrm{s})$ for both NNs (f_s and f_a), which provides desired information based on 0.2-s prediction. However, the sensing accuracy and dexterity of lower limbs are often regarded as being less than those of the hands [73]. Moreover, the simultaneous nature of driving which requires the manipulation of both steering and pedaling, requires learners to learn either one of them. Therefore, compared with f_s, f_a may require assistive feedback that is less frequent, resulting in ineffective skill transfer (enhancement). Thus, we considered that an NN with $\tau > 10$, which leads to less frequent feedback, may result in better control efficiency.

Therefore, we trained a new version of $f_a^{(25)}$ using the configuration of $\tau = 25$ (0.5 s) with the same data-set. Then, using the new predictive output, PID control of automated pedaling was utilized as follows:

$$T_{a,auto}(t) = K_{a,pid}e_a(t) + I_{a,pid}\int_{t_0}^{t} e_a(t')\,dt' + D_{a,pid}\dot{e}_a \qquad (6.1)$$

$$e_a = \theta_a - \theta_{a,d} = \theta_a - \hat{\theta}_a^{(25)}, \qquad (6.2)$$

where t_0 is the recent time when e_p becomes zero, and $\hat{\theta}_a^{(25)}$ is an predicted output of the new skill model, $f_a^{(25)}$, i.e., $\theta_{a,d} = \hat{\theta}_a^{(25)}$ $K_{a,pid} = 0.008\,\text{N·m/degree}$, $I_{a,pid} = 0.24\,\text{N·m·s}^{-1}\text{/degree}$, and $D_{a,pid} = 0.0008\,\text{N·m·s/degree}$. Then, the whole accelerator torque for automated control is altered to:

$$T_a = T_{a,auto} + g(\theta_a), \qquad (6.3)$$

where $g(\cdot)$ is a gravity-compensation term. We applied this automated pedaling method to HG and RG.

6.2.2 Automated Control of Steering Wheel

Both HG and RG share the same PID control as follows:

$$T_{s,auto}(t) = K_{s,pid}e_s(t) + I_{s,pid}\int_{t_0}^{t} e_s(t')\,dt' + D_{s,pid}\dot{e}_s \qquad (6.4)$$

$$e_s = \theta_s - \theta_{s,d}, \qquad (6.5)$$

where t_0 is the recent time when e_s becomes zero. $K_{s,pid} = 0.60\,\text{N·m/degree}$, $I_{s,pid} = 0.12\,\text{N·m·s}^{-1}\text{/degree}$, and $D_{s,pid} = 0.06\,\text{N·m·s/degree}$. Then, the whole steering torque for automated control is replaced by

$$T_s = T_{auto} + T_{stable}, \qquad (6.6)$$

where $T_{stable} = D_{stable}\dot{\theta}_s$ provides stable feedback. $D_{stable} = 5D_s$. As previously mentioned, two autopilot modes only differ in the steering skill model which provides the desired steering wheel angle $\theta_{s,d}$.

Data-driven Approach: Human-like Haptic Guidance

In the previous chapter, we obtained an NN-based steering model whose output is a predicted steering angle of experienced drivers. Therefore, in this mode, we set the desired angle in the rule[1]:

$$\theta_{s,d} = \hat{\theta}_s, \tag{6.7}$$

where $\hat{\theta}_s = f_s\left[\cdot\right]$, the output of the NN-based expert model of steering (f_s).

Because the NN-based model is trained by the data of human experienced drivers, we expected that the driving style using this data-driven mode should be in a human-like style. Therefore, we named this autopilot mode as *human-like haptic guidance* (HG).

Model-driven Approach: Robotic Haptic Guidance

This method considers two error terms, a look-ahead direction error e_p and the distance error e_d (Figure 5.4), and determines the desired angle $\theta_{s,d}$, as follows: converge to θ_d are determined by the following PD-based rule[2]:

$$\theta_{s,d} = K_p e_p + K_d e_d, \tag{6.8}$$

where $K_p = 7.65$ and $K_{dis} = 1.00\,\text{degree/m}$.

This method is based on the observation that a driver determines his/her driving based on prediction, not on the current situation. We named this mode as *robotic haptic guidance* (RG) as an opposite term to HG, because it is a conventional method used in robot-mediated strategies.
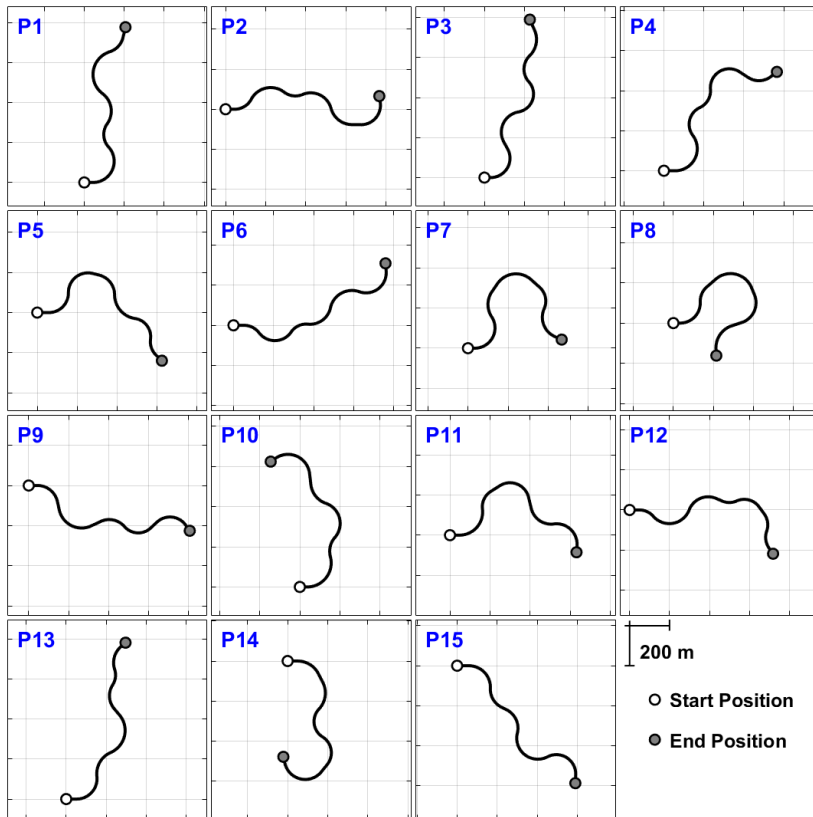
Figure 6.2: Fifteen different 1-km roads used for the autopilot test.

6.2.3 Experimental Protocol

In order to analyze respective driving styles where two autopilot modes can demonstrate, we conducted an autopilot experiment that involves repeated driving trials on a number of various paths. Therefore, for this autopilot test, we designed 15 different paths (P1–P15; Figure 6.2). Each straight segment had one parameter, length L. Each curved segment had a radius of curvature R and its sweep angle ϕ as parameters. The parameters were randomly chosen from 30–60 m (L), 90–120 m (R) and $\pm 45°$–$\pm 135°$ (negative for right curves) for each segment. A straight segment was followed by a left/right curve with equal probability 0.5. A left (right) curve was followed by a straight segment with probability 0.4 and a right (left) curve with probability 0.6. The total length of the path was shortened to 1 km.

We conducted five test-run trials for each path in respective autopilot modes. Therefore, total 150 test-run trials (15 paths × 2 modes × 5 trials) were performed.

6.2.4 Results and Discussion

Both autopilot modes performed nice examples of driving in every test-run trial. Figure 6.3 depicts example trajectories obtained in a test-run trial on P8, and Figure 6.4 is an example trace from top-view in the same trial. The vehicle did not fell outside of the path and successfully stayed in the first lane of the path in most of the time (Figure 6.4a), and the accelerator pedal was automatically controlled to maintain the same desired velocity $v_d = 62.64$ km; i.e., the autopilot of pedaling executed the pedaling task efficiently in both steering modes.

---

[1]It is the same implementation to G which had been used in the previous experiment.

[2]It is the same implementation to C which had been used in the previous experiment. The actual driving style in terms of accuracy and precision can be varied from setting of values of K_p and K_d. However, finding appropriate values needs an additional effort for haptic assistance designer. Therefore, we used the same parameters in the previous experiment.
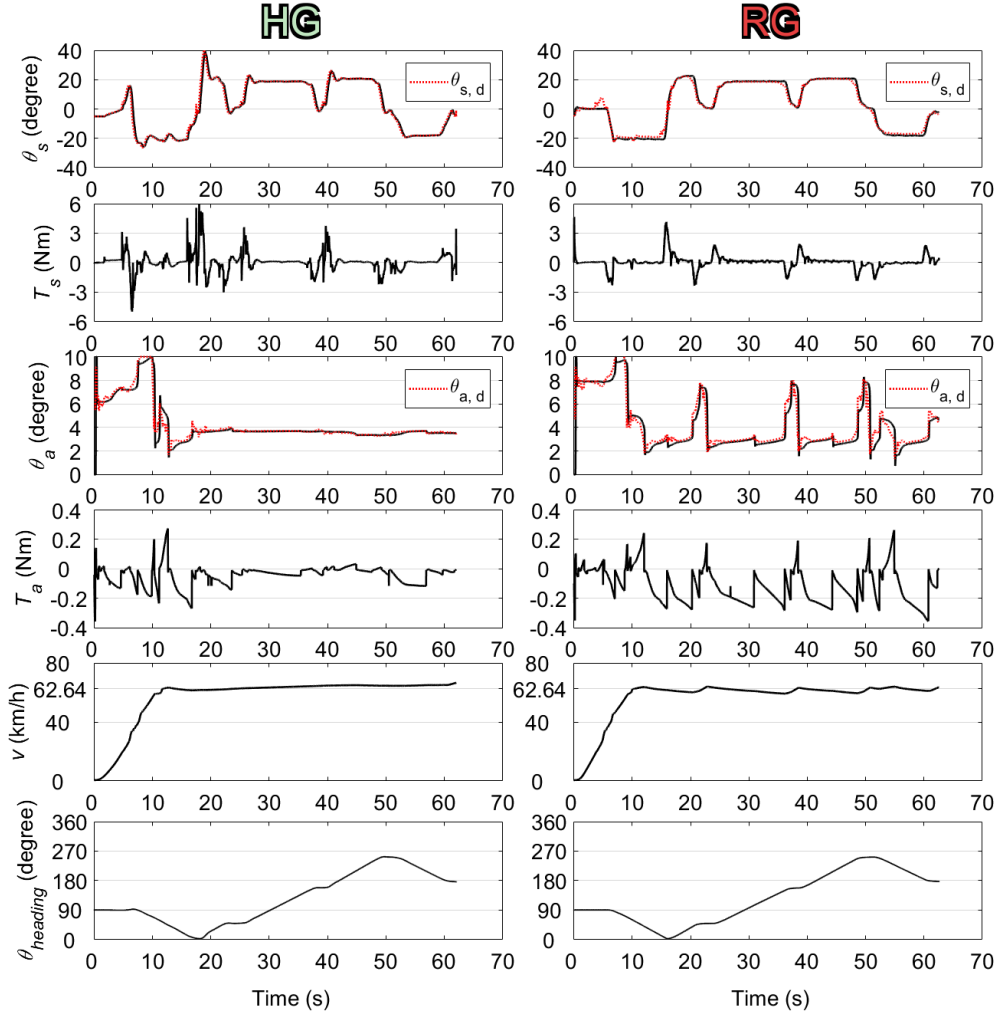
Figure 6.3: Example trajectories as a function over P8 (left: HG, right: RG). From top: measured and desired steering wheel angle (θ_s and $\theta_{s,d}$), and generated steering wheel torque (T_s); measured and desired accelerator angle (θ_a and $\theta_{a,d}$) and generated accelerator torque (T_a); car velocity (v) and heading angle ($\theta_{heading}$).
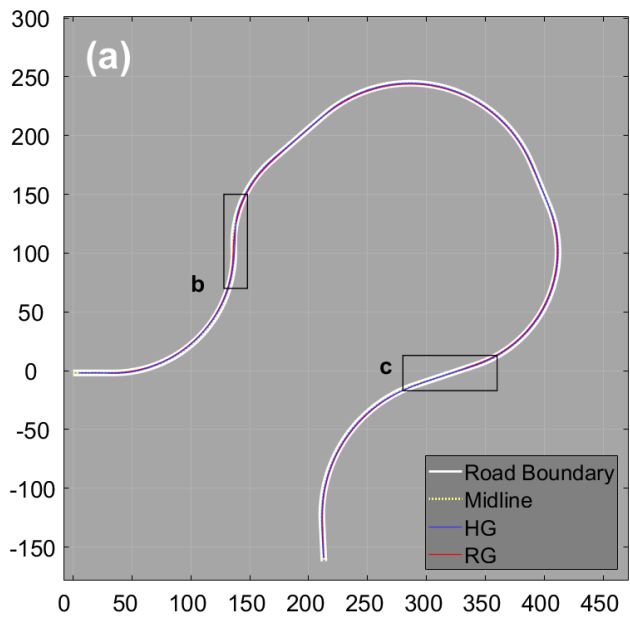
(a)
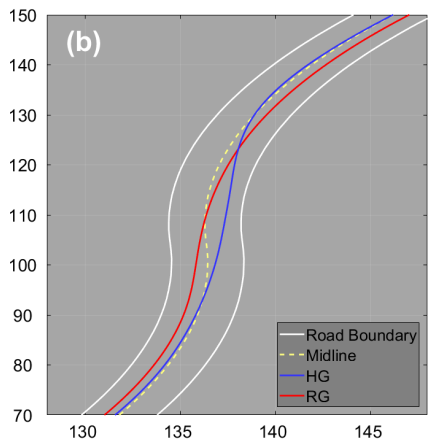
(b)
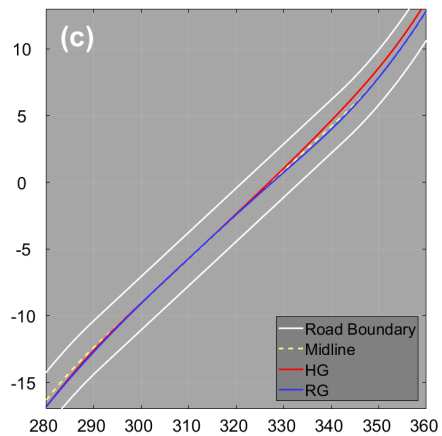
(c)

Figure 6.4: Examples of autopilot runs over P8 (the unit of each axis: m).

However, the driving style that each mode has shown differ in detail. HG showed more variance of steering movements with frequent force generations, whereas RG showed little variance without frequent movements. In RG, steering torque is generated mostly when the vehicle enters curved segments. Magnified trajectories in Figure 6.4b and 6.4c also show the difference of driving styles according to each autopilot mode. HG seems to follow the midline of the path more than RG, whereas RG seems to place the heading of vehicle more parallel to the path direction compared to HG.

The summarized results in terms of mean E_d, E_δ, and the mean vehicle velocity V are plotted in Figure 6.5. All the test-runs in every path satisfied maintaining the desired velocity. On every path, HG showed smaller distance errors, resulted in the better accuracy performance. In contrast to this, RG showed smaller angular errors, resulted in the better stability performance on every path. These results are in an agreement of the observation in Figure 6.3 and Figure 6.4.

To this end, we can summarize the findings of this experiment into: (1) The autopilot of pedaling implemented by PID control can effectively control a vehicle to maintain the same velocity on every path; (2) Both human-like haptic assistance (or, guidance) and robotic haptic assistance (or, guidance) also can effectively control a vehicle to stay in the same lane on every path; (3) Human-like haptic assistance has better accuracy performance compared to robotic haptic assistance on every path; (4) Robotic haptic assistance has better stability performance compared to human-like haptic assistance on every path.
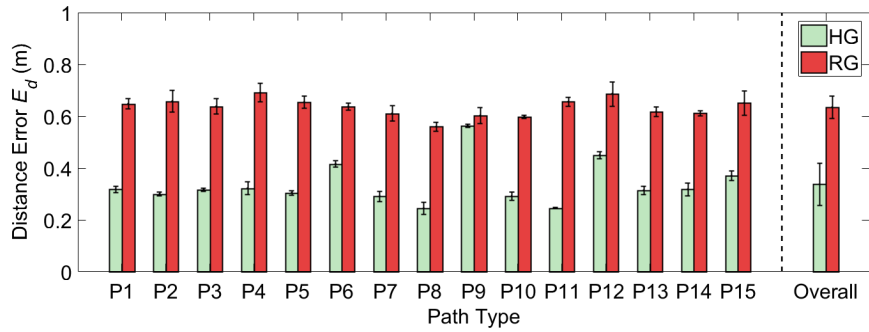
(a) Distance error E_d
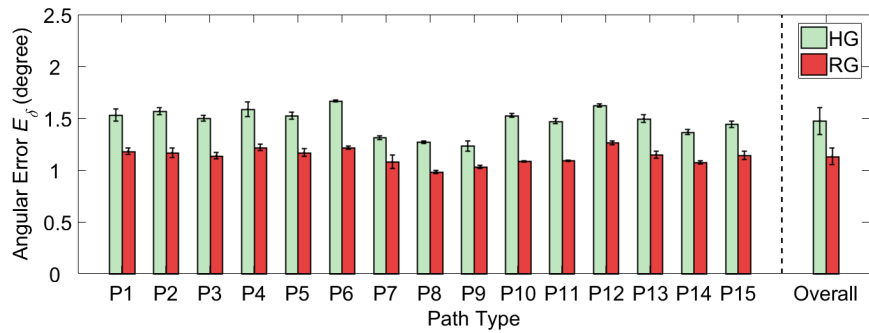
(b) Angular error E_δ
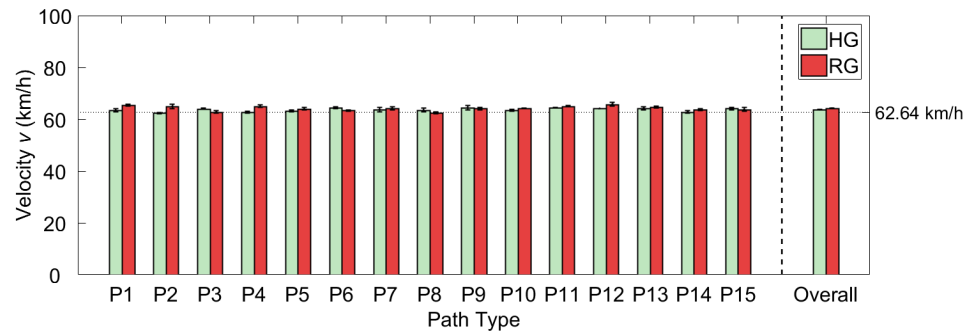
(c) Vehicle velocity v

Figure 6.5: Mean performance measures for autopilot runs. Error bars represent standard deviations.

6.3 Experiment II: Effectiveness of Human-like Haptic Assistance for Training on Car Steering Task

Because HG and RG have different driving styles, in this experiment, we hypothesized that the novice drivers who practiced with each haptic assistance method may develop a different driving behavior. Therefore, we finally tested the training effectiveness of different haptic assistance methods for steering, in this experiment. There were total three training conditions including HG, RG and the control condition of no guidance (NG).

6.3.1 Design of Score Map

We have introduced two error metrics (RMSEs in terms of distance error E_d and angular error E_δ), each of which reflects the performance of two sub-tasks, respectively. However, in this experiment, the overall performance score is required, as (1) the representative score given after each trial to promote learning as KR, and (2) the parametric function for gain increase in performance-based progressive algorithm (See 6.3.2). Because the dimensions of the two RMSEs are not compatible, we designed a mapping function which transforms RMSEs into score metrics that are summable to overall performance score, representing the performance of the overall steering skill.

In manual accuracy tasks to make a hit on a target in rapid movements under Fitt's law, human errors form a Gaussian distribution [75]. Inspired from this, we designed score functions which transform the distance error and the angular error into the accuracy score $S_d(\cdot)$ and the stability score $S_\delta(\cdot)$ are computed as

$$S_d(x) = 100\left(1 - \overline{\mathrm{erf}}\left(\frac{x - \mu_d}{\sqrt{2\sigma_d{}^2}}\right)\right), \tag{6.9}$$

and

$$S_\delta(y) = 100\left(1 - \overline{\mathrm{erf}}\left(\frac{y - \mu_\delta}{\sqrt{2\sigma_\delta{}^2}}\right)\right), \tag{6.10}$$

respectively. $\overline{\text{erf}}(\cdot)$ is a zero-bounded Gauss error function $\text{erf}(\cdot)$, defined as

$$\overline{\text{erf}}(z) = \begin{cases} \text{erf}(z) & \text{if } \text{erf}(z) > 0, \\ 0 & \text{otherwise.} \end{cases} \tag{6.11}$$

Finally, we can get the function of overall performance score by summing two score functions, i.e., $S_{all}(x, y) = S_d(x) + S_\delta(y)$. Because $0 \leq S_d \leq 100$ and $0 \leq S_\delta \leq 100$, $0 \leq S_{all} \leq 200$.
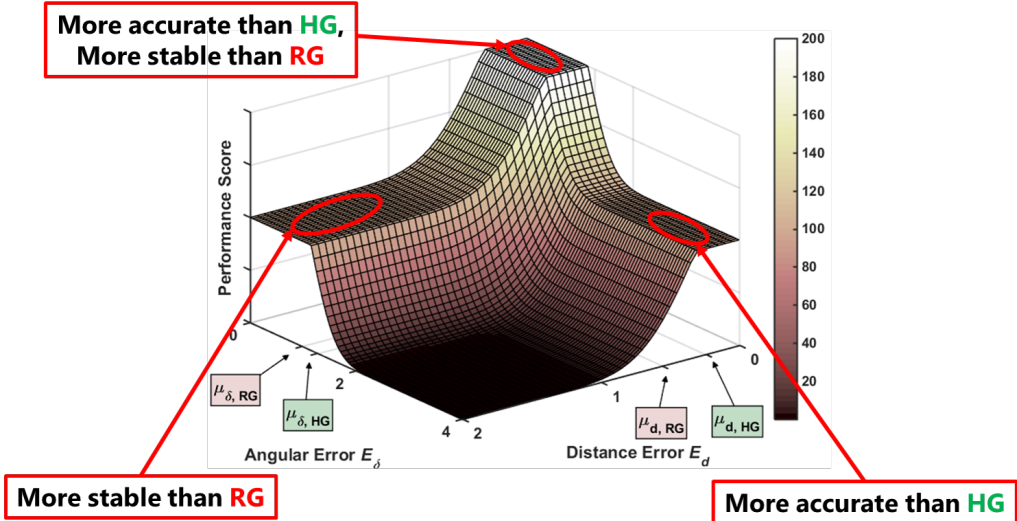
Figure 6.6: Example Score map (P8).

Because the task difficulty on each path cannot be identical, the four parameters (μ_d, μ_δ, σ_d, and σ_δ) are set with respect to the mean results of the autopilot test on each path. Because HG has better accuracy whereas RG has better stability, we set $\mu_d = \mu_{d,HG}$ and $\sigma_d = (\mu_{d,HG} - \mu_{d,RG})$ to compute the accuracy score; and $\mu_\delta = \mu_{\delta,RG}$ and $\sigma_\delta = (\mu_{\delta,RG} - \mu_{\delta,HG})$ to compute the stability score. Here, $\mu_{d,HG}$ and $\mu_{d,RG}$ are mean E_d of five respective autopilot test-run trials of HG and RG, respectively. $\mu_{\delta,RG}$, $\mu_{\delta,RG}$ are mean E_δ's of five respective autopilot test-run trials of HG and RG, respectively.

An example score map of S_{all} on P8 is depicted in Figure 6.6. By using these parameters, the overall performance score should cannot biased to either

sub-task. All autopilot test runs are similarly scored to $S_{all} \approx 130.1$, where the sub-scores of HG are $S_d \approx 100.0$ and $S_\delta \approx 30.1$ for HG and the sub-scores of RG are $S_\delta \approx 100.0$ and $S_d \approx 30.1$, respectively.

6.3.2 Autonomy Shift: Performance-based Progressive Algorithm

In every method, the accelerator pedal was automatically driven by the simulator to assess only the steering performance. In NG, only the simulated realistic steering torque (4.1) was delivered to the user. However, we applied the performance-based, progressive algorithm for HG and RG similarly in Chapter III. The performance-based, progressive (also called guidance-as-needed) algorithm often regarded as effective in the training of steering tasks [45]. This guidance-as-needed algorithm gradually shifts the autonomy of the task from machine-oriented control to human-oriented control, trying to overcome the guidance hypothesis that harms training effectiveness from unfamiliarity.

First, we consider the performance changes *within* a training trial. During each trial, the within-trial gain is updated at each sampling time $dt = 0.02\,\mathrm{s}$ (in $50\,\mathrm{Hz}$):

$$\alpha_{within}(t + dt) = f_{within} \cdot \alpha_{within}(t) + g_{within} \cdot \frac{200 - S_{all}(x, y)}{200}, \qquad (6.12)$$

where $x = e_d(t)$ and $y = e_\delta(t)$ are the current distance error and the current angular error, respectively. $\alpha_{within}(0) = 1.0$. f_{within} is the forgetting factor that decreases the guidance torque over time, and g_{within} is the learning factor that increases the guidance torque. From (6.12), the gain decreases as time goes on, but increases when the driver's accuracy/stability errors become larger. In the experiment, $f_{within} = 0.998$ and $g_{within} = 0.004$.

Second, we consider the performance variations *across* the training trials.

An across-trial gain $\alpha_{across}[j]$ of the j-th trial is computed as

$$\alpha_{across}[j+1] = f_{across} \cdot \alpha_{across}[j] + g_{across} \cdot \frac{200 - S_{all}(x, y)}{200}, \qquad (6.13)$$

where $x = E_d[j]$ and $y = E_\delta[j]$ are the mean distance and the mean angular error in the j-th trial, respectively. $\alpha[1] = 1.0$. f_{across} and g_{across} are the across-trial forgetting and learning factors and in the experiment, $f_{across} = 0.75$, and $g_{across} = 0.05$.
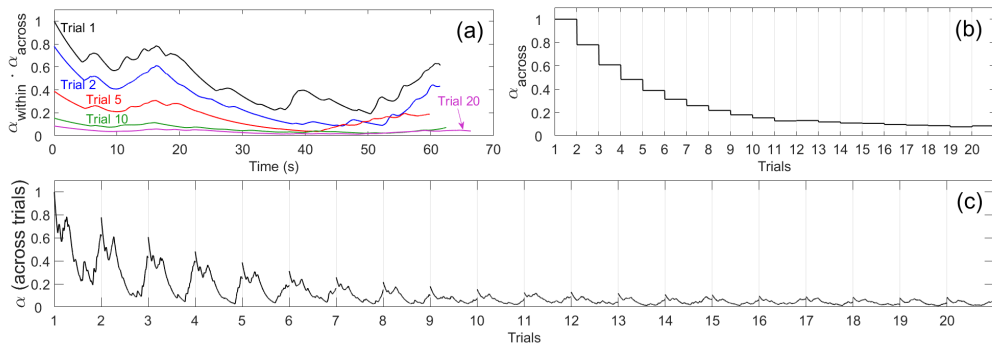
Figure 6.7: Guidance gains of one example participant. (a) Within-trial Gain α_{wihtin} over time (scaled by $\alpha_{across}[j]$), (b) Across-trial gain α_{across} over trials, and (c) Overall gain α.

The performance-based progressive algorithm returns the autonomy back from the training interface to the human learner at the latter trials of training. Therefore, the torque feedback in the latter trials should become similar to realistic steering torque. Let the overall gain α be the composition of α_{within} and α_{across} in a specific time, i.e., $\alpha = \alpha_{within} \cdot \alpha_{across}$. Then, we implemented the similar hybrid scheme as described in Chapter III, by combining the guidance torque and the realistic torque to deliver the final torque feedback T_{final} as

$$T_{final} = \alpha \cdot T_{assist} + \beta \cdot T_{real}, \qquad (6.14)$$

$$\beta = 1 - \alpha, \qquad (6.15)$$

where T_{assist} is the torque feedback T_s, which is determined from respective $\theta_d(t)$ in HG or RG. T_{real} is the realistic torque feedback (See T_s in Section 4.3).

The gains changes within and across trials are depicted in Figure 6.7. When the across-trial gain $\alpha[j]$ decreased to be lower than 0.1 at the later trials, such small gains do not result in perceptible assistance. Therefore, under (6.15), participants can feel similar perception to real steering in actual vehicles, in the later training trials.

6.3.3   Participants

To recruit eligible participants, we tried to control their gender, age, and driving skill level. Gender and age are regarded as important factors motor learning, especially for steering tasks [63]. Total 30 participants (15 males and 15 females) who did not have a driving license participated as learners in this experiment (19–25 years old; M 20.53; SD 1.68). Before the experiment, we requested them to have high motivations to learn. They were compensated KRW 20,000 ($\simeq$ USD 18) after the experiment. This experiment was approved by the Institutional Review Board at Pohang University of Science and Technology (PIRB-2018-E098).

6.3.4   Driving Environments

(a) Day-time Driving   (b) Night-time Driving

Figure 6.8: Two driving environments implemented for Experiment II.

To provide a minimized visual cue to prevent large errors due to unintended mistakes, small red-colored arrows were displayed on the screen to guide the heading direction to the midline of the path when the tire of the vehicle steps outside of the road boundary. The leftwards arrows were placed on the right side of the screen and the rightwards arrows were placed on the left side of the screen to minimize visual intervention.

For the experiment, we deployed two driving environments: day-time driving and night-time driving (Figure 6.8). The night-time driving is more difficult situation because the participants are not allowed to predict the future path, whereas the day-time driving is a usual driving situation.

The night-time driving was implemented using a black-colored exponential squared fog mode [3] in Unity3D. The fog density fd $(\cdot)$ over a distance d is:

$$\text{fd}\,(d) = \frac{1}{2^{(cd)^2}}, \tag{6.16}$$

where d is a distance between a driver's position and the position of a certain virtual environment. We set $c = \frac{1}{6}$ so the environments in $d = 6\,\text{m}$ was $50\,\%$ visible. In results, fd $(\cdot)$ falls down to almost 0 to the virtual environments in $d > 15\,\text{m}$; in other words, only the environments in a distance less than $15\,\text{m}$ can be only visible in this night-time driving.

6.3.5 Experimental Protocol

Ten participants (five males and five females) were randomly assigned into each of three groups, in a between-subjects design. The three groups were: no guidance (NG), human-like haptic guidance (RG), and robotic haptic guidance (HG). Because the degrees of learning were different among the three methods, within-subjects designs were not affordable.

The experiment was conducted on two consecutive days (See Figure 6.9 for detailed procedure), with one pretest and two post-training retention tests. On
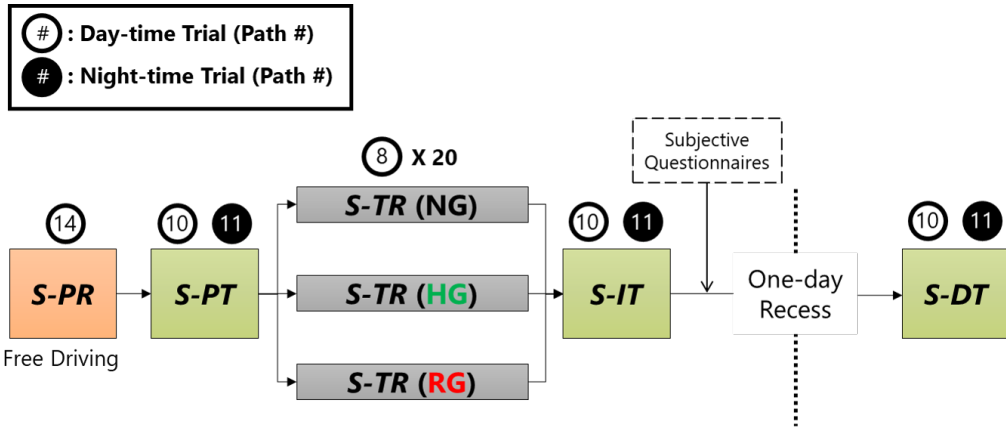
Figure 6.9: Experimental Procedures.

day 1, each subject finished four sessions of practice (S-PR), a pretest (S-PT), training (S-TR), and an immediate retention test (S-IT). On day 2, 24 hours after the onset of day 1, each participant conducted another session for a delayed retention test (S-DT).

To show only generalized improvement on motor skills without memorization of path shapes, for this experiment, we selected several 1 km-long paths whose autopilot performance are similar. In results, P8, P10, P11, and P14 were chosen.

In S-PR, the novice driver could freely drive the path P14 once in NG. The purpose was to familiarize the participant with our driving simulator and virtual environments. They completed driving using all the manipulators (a steering wheel, an accelerator pedal and a brake pedal). For several participants asked to conduct an additional practice trial, they were allowed to do so. After S-PR, the participant proceeded to S-PT.

From S-PT to S-DT, every participant was instructed to practice both accuracy and stability of their skill execution in every trial. In every trial, the accelerator pedal was automatically controlled to maintain the same velocity $v_d = 62.64$ km/h to let the novices focus on the training of their steering skill. Also, to motivate their own practice, the overall score of S_{all} was visually pro-

vided after the completion of each trial. However, the separated scores of S_d and S_δ were not provided to prevent biased learning of either sub-task.

S-PT was included to assess their performance improvement before training, which includes two consecutive trials in NG: a day trial and a night trial. In the day trial, the participant complete driving over the path P10 in the day-time environment. In the night trial, the participant complete driving over the path P11, in the night-time environment.

S-TR was for main training and consisted of 20 repeated driving trials in the day-time environment on the path P8. Steering torque feedback (with performance-based progressive algorithm) was provided according to the training method (NG, HG and RG) assigned to the participant.

After S-TR, the participant proceeded to S-IT that was included to assess their performance improvement immediately after training. It had the same procedure as S-PT.

After S-IT, the participant was asked to answer the following five questions on an 1 to 7 continuous scale (a neutral score of 4): (1) Was the training easy/difficult to follow? (Easiness); (2) Was the training effective? (Effectiveness); (3) Was the training comfortable/uncomfortable? (Comfort); (4) Was the training fun? (Fun); (5) Do you think the training helped to improve your skill of day-time steering? (Helpfulness - Day). (6) Do you think the training helped to improve your skill of night-time steering? (Helpfulness - Night). and (7) Did the score relevantly represent the performance of steering? The first-day experiment took about one and half hour per participant.

On day 2, S-DT was conducted. It had the same procedure as S-PT and S-IT. The purpose of S-DT was to evaluate long-lasting training effectiveness. This session took about 10 min for each participant.

Between each trial and each session, every participant could freely take a

break to prevent fatigue. After the break time, they requested for the initiation of the next training trial (or session) to the experimenter.

6.3.6 Results and Discussion

In this section, we report each measurement in performance scores (S_{all}, S_d, and S_δ) and RMSEs (E_d, and E_δ) as results of performance.

Learning Curves

Figure 6.10 and 6.11 shows the means of measurements that were averaged across the participants of each group for each experimental trial. The control condition NG, training with no haptic guidance, resulted in a typical learning curve for both accuracy and precision. However, in the most of trials, the stability score S_δ was lower than the accuracy score S_d. This means that the stable driving was more difficult and unnatural task for novice drivers than the accurate driving.

Compared to the NG group, the robotic haptic guidance group RG exhibited higher S_δ ($smaller E_\delta$) and lower S_d (larger E_d) during the early stage of training in S-TR, showing the steepest learning curves. In contrast, the human-like haptic guidance group HG showed a similar tendency to NG with slightly better scores and lower errors than NG. This tendency means the guidance feedback in HG did not harm the own nature of participants for the steering task. All of these tendencies clearly demonstrate each characteristic nature of assistance methods.

Quantitative Results

Here, we report only measurements in three test sessions (S-PT, S-IT and S-DT). To provide clear comparison, the results are depicted in Figure 6.12 and 6.13.

The stability score S_δ is nearly zero in the night trials. Thus, the major portion of overall score S_{all} in the night trials is the accuracy score S_d. The lack
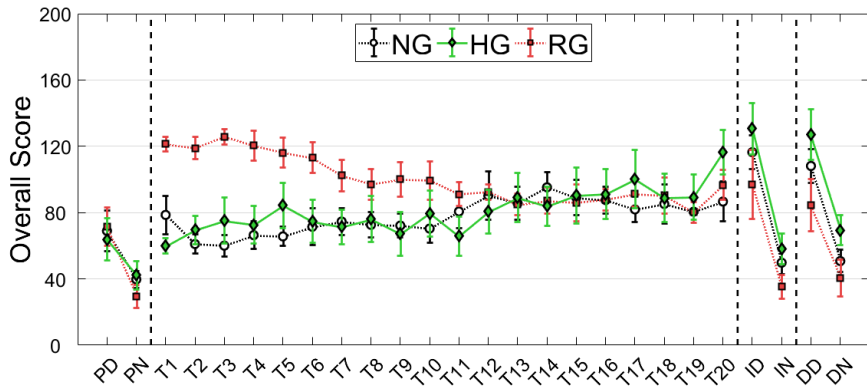
(a) Overall Score S_{all}
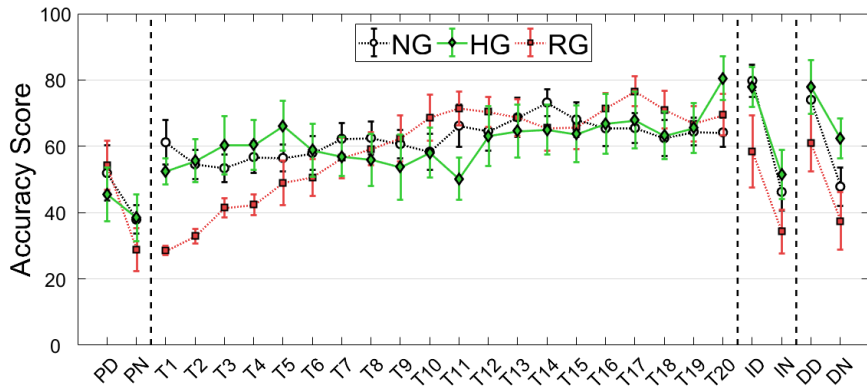
(b) Accuracy Score S_d
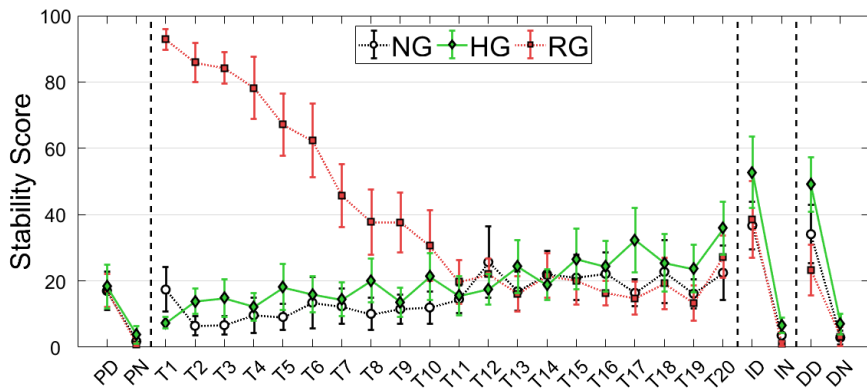
(c) Stability Score S_δ

Figure 6.10: Means of performance scores for each trial. T1–T20 denote the trials in the session S-TR. P–, I–, D– denote the session S-PT, S-IT, and S-DT, respectively. –D and –N denote the day/night trials, respectively.
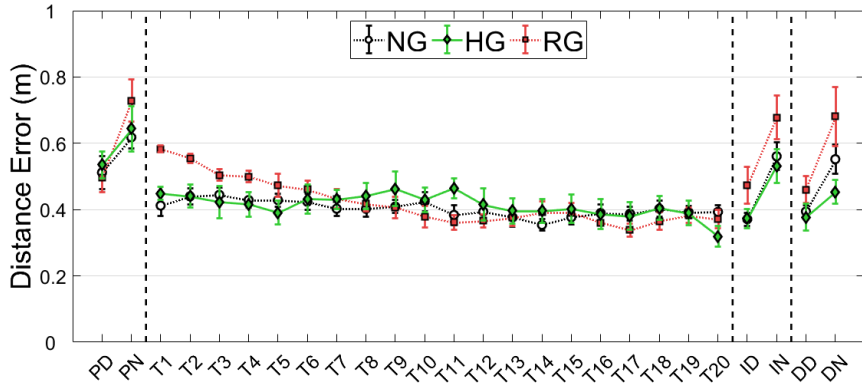
(a) Distance Error E_d
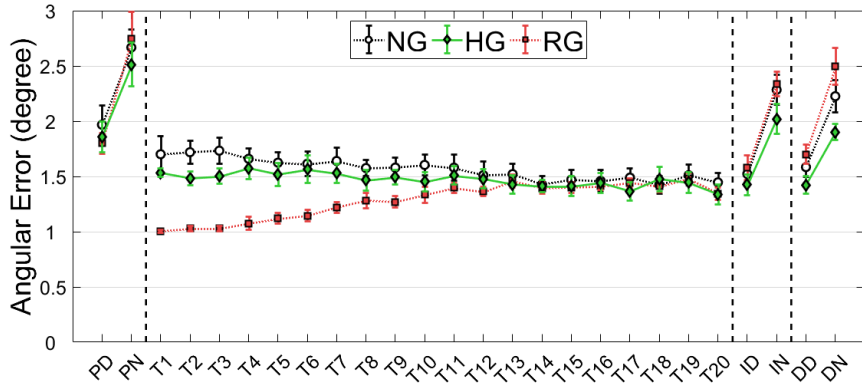
(b) Angular Error E_δ

Figure 6.11: Means of two RMSEs for each trial. T1–T20 denote the trials in the session TR. P–, I–, D– denote the session S-PT, S-IT, and S-DT, respectively. –D and –N denote day/night trials, respectively.
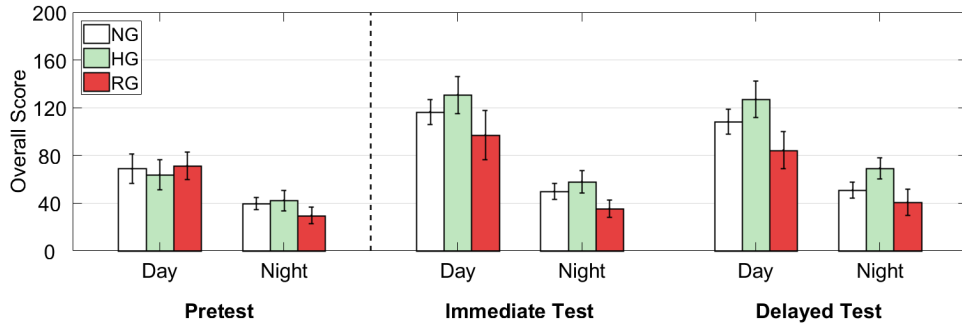
(a) Overall Score S_{all}
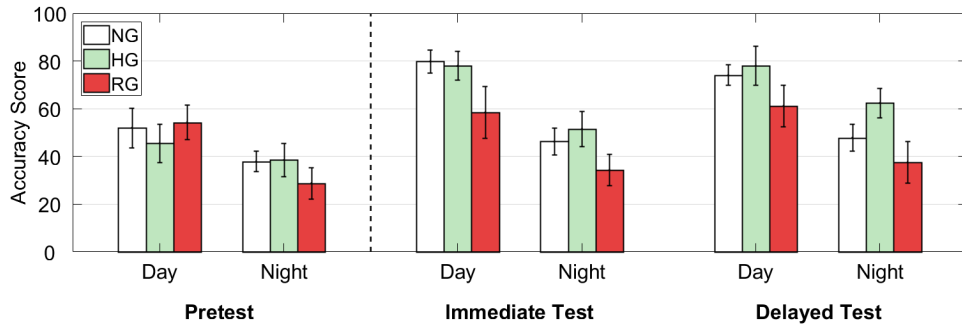
(b) Accuracy Score S_d
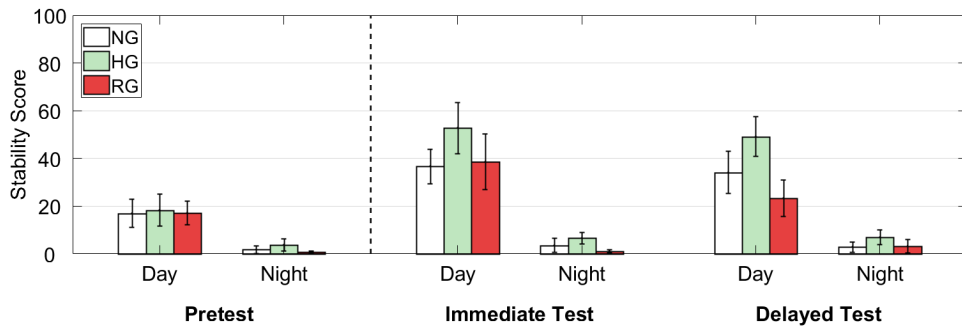
(c) Stability Score S_δ

Figure 6.12: Means of S_{all}, S_d and S_δ measured in the test sessions. Error bars represent standard errors.
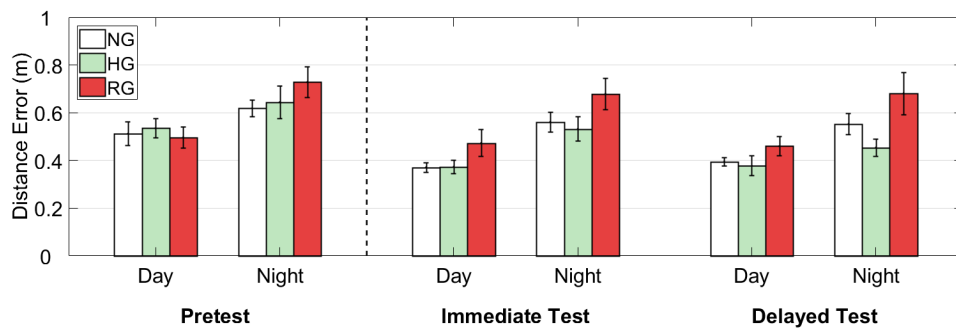
(a) Distance Error E_d
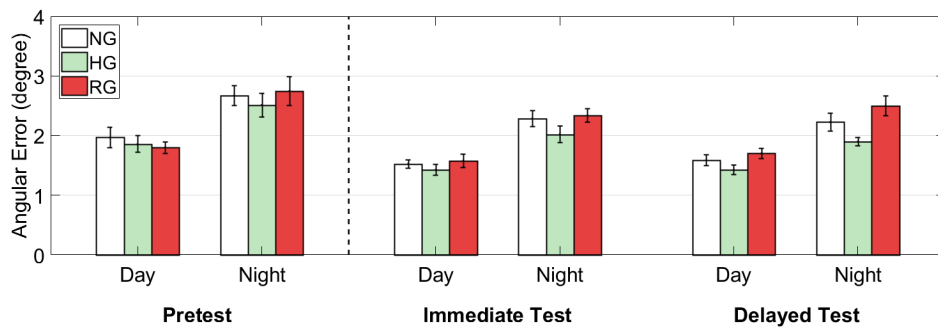
(b) Angular Error E_δ

Figure 6.13: Means of E_d and E_δ measured in the test sessions. Error bars represent standard errors.

of prediction affected a bias to the error canceling skill so resulted low stability of steering skill. This clearly reflects the previous definition of characteristics for the steering skill in Section 6.1:

All groups in S-IT and S-DT obtained improved mean scores and decreased mean RMSEs than S-PT. However, the amount of improvements is different according to assistant conditions and post-training test sessions. To clarify the results, a between-subjects one-way Analysis of Variance (ANOVA) and an one-way Anaysis of Covariance (ANCOVA) were conducted as statistical analyses.

Analysis of Variance

Because this experiment has a pretest-posttest experimental design, we considered three different approaches for ANOVA. First, we regarded all test measurements as independent variables in ANOVA: (X). Second, we regarded gain scores that is difference between pretest measurements and posttest measurements as independent variables: ($X - X_{S-PT}$). Third, we regarded normalized gain scores that is gain scores normalized by pretest measurements as independent variables: ($X - X_{S-PT})/X_{S-PT}$. All results of different approaches are summarized in Table 6.1.

In results, no statistically significant difference is observed in any measurements in S-PT; the initial skill levels of novice participants were homogeneous. There exists no significant difference in any measurements in S-IT, but there were significant differences in several measurements in S-DT.

Therefore, we observed their improvement of steering skills, in terms of gain scores, which represents learning effectiveness after the participants practiced with each training method. In results, S_{all}, S_d and E_d in the day trials in S-IT, S_{all}, S_d, S_δ, E_d, and E_δ in the day trials in S-DT, and S_d in the night trials in S-DT shows significant or marginally significant differences. We also analyzed

Table 6.1: Between-Subjects One-Way ANOVA

X			(1) X only		(2) $X - X_{\mathsf{S-PT}}$		(3) $\frac{X-X_{\mathsf{S-PT}}}{X_{\mathsf{S-PT}}}$	
			$F(2,27)$	p	$F(2,27)$	p	$F(2,27)$	p
$\mathsf{S-PT}$	Day	S_{all}	0.10	0.904				
		S_d	0.33	0.720				
		S_δ	0.02	0.984				
	Night	S_{all}	0.91	0.416				
		S_d	0.81	0.457				
		S_δ	0.68	0.516				
$\mathsf{S-IT}$	Day	S_{all}	1.11	0.345	2.80	0.079*	0.93	0.408
		S_d	2.33	0.116	3.34	0.051*	1.10	0.347
		S_δ	0.77	0.475	1.20	0.318	1.68	0.205
	Night	S_{all}	2.15	0.137	1.26	0.301	1.36	0.274
		S_d	1.79	0.186	0.93	0.407	1.21	0.314
		S_δ	1.58	0.225	0.57	0.572	-	
$\mathsf{S-DT}$	Day	S_{all}	2.33	0.117	5.19	0.012**	1.13	0.338
		S_d	1.44	0.255	3.58	0.042**	0.84	0.441
		S_δ	2.44	0.106	4.29	0.024**	0.67	0.519
	Night	S_{all}	2.59	0.094*	2.00	0.155	1.48	0.245
		S_d	3.20	0.057*	2.91	0.072*	1.40	0.264
		S_δ	0.67	0.519	0.13	0.879	-	
$\mathsf{S-PT}$	Day	E_d	0.19	0.825				
		E_δ	0.37	0.694				
	Night	E_d	1.02	0.376				
		E_δ	0.34	0.715				
$\mathsf{S-IT}$	Day	E_d	2.36	0.113	2.84	0.076*	2.37	0.112
		E_δ	0.71	0.499	1.40	0.265	1.12	0.342
	Night	E_d	2.11	0.141	0.93	0.407	0.98	0.388
		E_δ	1.71	0.199	0.16	0.850	0.44	0.650
$\mathsf{S-DT}$	Day	E_d	1.56	0.229	2.59	0.094*	2.54	0.098*
		E_δ	2.64	0.090*	2.62	0.092*	3.47	0.046**
	Night	E_d	3.50	0.044**	2.11	0.141	2.62	0.091*
		E_δ	4.90	0.153	0.99	0.384	1.54	0.232

-: not applicable because $^\exists X_{\mathsf{S-PT}} \approx 0$

**: significance less than $\alpha = 0.050$

*: significance less than $\alpha = 0.100$

the normalized gain scores, however, the statistical power was better in the gain scores.

Analysis of Covariance

Table 6.2: ANCOVA Assumption Tests

			Pre-post Correlation	Homogeneity of Variances (Levene's Test)		Homogeneity of Regression Slopes ($IV \times CV$)		Available (Pass /Marginal /Fail)
X			r	$F(2,27)$	p	$F(2,24)$	p	
S − IT	Day	S_{all}	0.599	3.73	0.037**	2.57	0.098*	F
		S_d	0.359	9.89	<0.001**	0.94	0.405	F
		S_δ	0.679	2.38	0.111	3.82	0.036**	F
	Night	S_{all}	0.829	2.28	0.122	0.20	0.821	P
		S_d	0.819	1.32	0.284	0.03	0.975	P
		S_δ	0.660	0.84	0.445	9.41	<0.001**	F
S − DT	Day	S_{all}	0.568	0.79	0.466	1.90	0.171	P
		S_d	0.524	1.92	0.167	2.98	0.067*	M
		S_δ	0.652	0.09	0.910	0.34	0.712	P
	Night	S_{all}	0.705	0.70	0.507	0.33	0.723	P
		S_d	0.718	1.25	0.303	0.26	0.773	P
		S_δ	0.315	0.19	0.825	3.95	0.033**	F
S − IT	Day	E_d	0.356	10.90	<0.001**	1.27	0.299	F
		E_δ	0.624	2.40	0.110	3.93	0.033**	F
	Night	E_d	0.806	2.01	0.153	1.22	0.313	P
		E_δ	0.734	0.30	0.747	1.29	0.294	P
S − DT	Day	E_d	0.484	1.81	0.184	2.41	0.111	P
		E_δ	0.534	0.08	0.925	1.01	0.379	P
	Night	E_d	0.602	2.81	0.078*	0.43	0.653	M
		E_δ	0.490	1.67	0.207	0.79	0.467	P

**: significance less than $\alpha = 0.050$

*: marginal significance less than $\alpha = 0.100$

However, an ANCOVA is the preferred method for analysis of pretest-posttest designs to reduce error variance and eliminate systematic bias [16], especially for learning experiments [57]. Therefore, we additionally conducted ANCOVA with two posttest measurements in S-IT and S-DT (X) as dependent variables, mea-

Table 6.3: One-Way ANCOVA

X			Available (Pass/Marginal/Fail)	Results	
				$F(2,26)$	p
S − IT	Day	S_{all}	F	2.59	0.094*
		S_d	F	3.39	0.049**
		S_δ	F	1.14	0.337
	Night	S_{all}	P	1.40	0.265
		S_d	P	1.16	0.328
		S_δ	F	0.85	0.438
S − DT	Day	S_{all}	P	4.97	0.015**
		S_d	M	3.35	0.051*
		S_δ	P	4.14	0.028**
	Night	S_{all}	P	2.09	0.144
		S_d	P	3.25	0.055*
		S_δ	F	0.37	0.693
S − IT	Day	E_d	F	3.34	0.051*
		E_δ	F	1.67	0.208
	Night	E_d	P	1.59	0.223
		E_δ	P	1.62	0.217
S − DT	Day	E_d	P	2.96	0.070*
		E_δ	P	4.70	0.018**
	Night	E_d	M	3.05	0.065*
		E_δ	P	4.59	0.020**

**: significance less than $\alpha = 0.050$

*: marginal significance less than $\alpha = 0.100$

surements in S-PT($X_{\mathsf{S-PT}}$) as covariates and the treatment type (NG, HG and RG) as independent variables.

Before conducting ANCOVA, we carefully checked each measurement can satisfy the assumptions of ANCOVA. To apply ANCOVA, (1) a correlation between measurements in the pretest and the posttest should be high enough; (2) Levene's test testing the homogeneity of variances should not be significant; and (3)the interaction between independent variable (IV) and the covariate (CV) in the standard GLM procedure should not be significant, to satisfy the homogeneity of regression slopes. Further, several other assumptions of ANCOVA were tested in a strict way, and all of them were suitable for ANCOVA. The important results of ANCOVA assumption tests are summarized into Table 6.2.

Finally, the results of ANCOVA are reported in Table 6.3. In results, the results of ANCOVA (Table 6.3) produced similar results than the results of gain scores in ANOVA (Table 6.1) in this experiment.

Only for the measurements having a significant (or marginally significant) effects which have passed the conservative assumption tests, Tukey's HSD multiple testing was conducted as a post-hoc analysis to compare adjusted means. The results of Tukey's test and the adjusted means (using the population means in S-PT) are described in Table 6.4.

The significant results can be observed in the measurements only in S-DT. In the day trial, the ranking of the overall score S_{all} is RG < NG < HG, and in the post-hoc test, RG < HG. The ranking of the accuracy score S_d is RG < NG < HG, and in the post-hoc test, RG < HG. The ranking of the stability score S_δ RG < NG < HG, and in the post-hoc test, RG < HG. In the night trial, the ranking of the accuracy score S_d is RG < NG < HG, and in the post-hoc test, RG < HG.

The error metrics have a consistent tendency. However, because the stability score in the night trial is reported to be so low. Therefore, we report an incon-

Table 6.4: Adjust Means and Tukey's HSD Tests on Significant Effects

X		Adjust Means $\pm$ SD	Tukey's HSD	
S − DT / Day / S_{all}	NG	107.49 $\pm$ 10.81	NG–HG	0.315
	HG	130.19 $\pm$ 10.83	NG–RG	0.234
	RG	81.87 $\pm$ 10.82	RG–HG	0.011**
S − DT / Day / S_d	NG	73.26 $\pm$ 5.98	NG–HG	0.655
	HG	80.77 $\pm$ 6.02	NG–RG	0.230
	RG	59.02 $\pm$ 6.00	RG–HG	0.044**
S − DT / Day / S_δ	NG	34.61 $\pm$ 6.06	NG–HG	0.268
	HG	48.24 $\pm$ 6.06	NG–RG	0.418
	RG	23.64 $\pm$ 6.06	RG–HG	0.021**
S − DT / Night / S_d	NG	45.48 $\pm$ 4.96	NG–HG	0.130
	HG	59.52 $\pm$ 4.97	NG–RG	0.920
	RG	42.69 $\pm$ 5.03	RG–HG	0.066*
S − DT / Day / E_d	NG	0.40 $\pm$ 0.03	NG–HG	0.794
	HG	0.37 $\pm$ 0.03	NG–RG	0.219
	RG	0.47 $\pm$ 0.03	RG–HG	0.066*
S − DT / Day / E_δ	NG	1.55 $\pm$ 0.07	NG–HG	0.454
	HG	1.43 $\pm$ 0.07	NG–RG	0.188
	RG	1.73 $\pm$ 0.07	RG–HG	0.014**
S − DT / Night / E_d	NG	0.58 $\pm$ 0.05	NG–HG	0.256
	HG	0.47 $\pm$ 0.05	NG–RG	0.700
	RG	0.64 $\pm$ 0.05	RG–HG	0.058*
S − DT / Night / E_δ	NG	2.22 $\pm$ 0.12	NG–HG	0.257
	HG	1.94 $\pm$ 0.12	NG–RG	0.337
	RG	2.46 $\pm$ 0.12	RG–HG	0.015**

**: significance less than $\alpha = 0.050$

*: marginal significance less than $\alpha = 0.0100$

sistent results which showed significance in the error metric. In the night trial in S-DT, the ranking of the angular error E_δ is HG < NG < RG, and in the post-hoc test, RG < HG.

Subjective Questionnaire
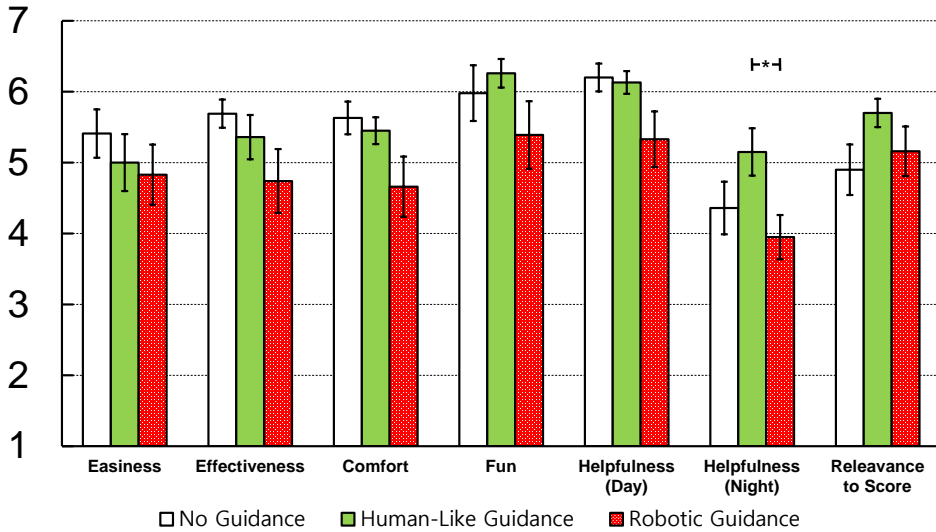
Figure 6.14: Subjective score responses obtained from questionnaires (1–7 continuous scale). Error bars represent standard errors. An asterisk indicates a marginal significant difference.

We computed the mean scores for each subjective question (Figure 6.14). For a statistical analysis, we applied the non-parametric Kruskal-Wallis test. Dunn's post-hoc nonparametric test was conducted as a post-hoc test to obtain significant (or marginally significant) effects. For the steering wheel, the rankings of the easiness, effectiveness, comfort, fun, helpfulness (day), helpfulness (night) and relevance scores are: RG < HG < NG ($\chi^2(2) = 0.63, p = 0.730$), RG < HG < NG ($\chi^2(2) = 2.25, p = 0.326$), RG < HG < NG ($\chi^2(2) = 4.26, p = 0.119$), RG < NG < HG ($\chi^2(2) = 1.06, p = 0.599$), RG < HG < NG ($\chi^2(2) = 3.06, p = 0.216$), RG < NG < HG ($\chi^2(2) = 5.63, p = 0.060$), and NG < RG < HG

$(\chi^2\,(2) = 3.69, p = 0.168)$, respectively. Only a marginal significant differences is the helpfulness (night) score. In the post-hoc test, the learners in HG reported higher helpfulness score for the night-time steering task, compared to the learners in RG.

Several noticeable results are summarized in the following for each training method. HG was ranked at the highest fun and helpfulness (night) and relevance. RG was ranked the lowest on all criteria except relevance. This may due to the lack of intrinsic human nature. NG was ranked the highest on easiness, effectiveness, and comfort, and helpfulness (day). NG was ranked the lowest on relevance; They were only learners who could not perceive haptic information about accurate/stable steering behaviors. Hence, they was not convinced to the performance score.

Summary

Even without haptic guidance, the accuracy and stability performance for steering can be improved in repeated practice. However, while human-like haptic guidance contributed to long-term learning, without haptic guidance and robotic haptic guidance failed to show long-lasting effects. Especially, the robotic haptic guidance resulted the worst performance improvement of training on the steering task; this can be another attribution to the *guidance hypothesis* [66, 68]: the excessive amount of feedback stimuli may reduce their focus during the training, rather interfering with retention of the learned skill. Even though we applied the performance-based progressive algorithm to our robotic haptic guidance, the unnatural haptic feedback to novice drivers hampered their focus of learning, leading to the ineffective retention performance.

However, the human-like haptic guidance under our framework (human-like haptic assistance), resulted in the best performance improvement on the steer-

ing task for a long term. Because our framework formulates the performance error based on the natural task executions of experienced human drivers, the guidance feedback was natural and comfortable for novice drivers and resulted a contribution to maintain the learned skill. Thus, we conclude that human-like haptic guidance has overcome the guidance hypothesis. To design haptic guidance (a representative example of haptic assistance) to induce better long-term skill improvement, the guidance feedback should necessarily consider the natural execution of humans. If this cannot be satisfied, the guidance feedback even can degrade learning effectiveness like robotic haptic guidance.

VII. General Discussion

In the human experiments, we used four measures for the analysis of the driving (both steering and pedaling) performance, and each measure is closely related to the ability to demonstrate corresponding sub-skills: E_δ for motion-initiating, E_d for fine-tuning (both for steering), E_v for motion-initiating, and Ω_a for fine-tuning (both for pedaling). The driving skill is a vague mixture of the sub-skills: two for steering and other two for pedaling.

The model f_s captured the experts' sub-skill of gross steering more effectively (Section 5.2). Usually, haptic guidance is effective at transferring gross skills by providing kinetic references with specific timing and force. Hence, haptic guidance could successfully transfer experts' steering behavior of gross motions (Section [44].

In contrast, f_a captured experts' sub-skill of fine pedaling more effectively (Section 5.2). Haptic guidance may not be effective in transferring experts' pedaling behavior of fine motions, which results in a failure of pedaling skill enhancement (Section 5.3). To this end, we established an improved pedaling skill model, $f_a^{(25)}$ using the configuration of $\tau = 25$ with the same data-set, and we could show that this model can conduct a nice adjustment of vehicle velocity in autopilot mode on the various types of paths (Section 6.2).

In the thesis, the training effectiveness of human-like haptic assistance utilizing NN-based steering skill model was proven (Section 6.3). Although we could not test human-like haptic assistance which utilizes an improved pedaling model with increased prediction time, we still believe that the improved model would induce a better training outcome.

Another remarkable statement in this thesis is that the human performance

error vector $\boldsymbol{e}_\theta$, which is formulated by NNs, may be employed to other types of haptic assistance, e.g., error amplification providing the haptic stimuli that increases the trajectory errors [18], or haptic disturbance (an extension of error amplification) providing random, unpredictable force fields [38].

Therefore, here, from the understandings in this thesis, we propose a simple way of designing performance-based haptic assistance for a trajectory-following task, including a vague task like steering a car in a wide-banded path. The main design issues can be twofolds: (1) modeling: how to model an optimized skill and (2) feedback: how to deliver the optimized model to learners.

In simple trajectory-following tasks, a current human performance error vector $\boldsymbol{e}$ can be defined as

$$\boldsymbol{e}\left(t\right) = \boldsymbol{\theta}\left(t\right) - \boldsymbol{\theta}_d\left(t\right), \tag{7.1}$$

where $\boldsymbol{\theta}$ is a current control vector and $\boldsymbol{\theta}_d$ is a deisred control vector at time t. $\boldsymbol{\theta}_d$ can be specified by the output of a particular model $f_1\left(\cdot\right)$ representing the optimized trajectory-following skill. However, all trajectory-following skills are sensorimotor skills based on dynamic human behavioral strategy in capable of any type of sensory feedback. Therefore, the optimized skill model can be regarded as a dynamic system which can be approximated using difference equations [51], with a number of inputs of control vectors (for its own movements), system-state vectors (for its own state) and exogenous environmental features.

Therefore, $\boldsymbol{\theta}_d$ can be simplified to

$$\boldsymbol{\theta}_d\left(t\right) = f_1\left(\boldsymbol{\theta}\left(t\right), \boldsymbol{x}\left(t\right), \boldsymbol{z}\left(t\right)\right), \tag{7.2}$$

where $\boldsymbol{x}\left(\cdot\right)$ is the a current system-state vector and $\boldsymbol{z}\left(\cdot\right)$ is a environmental feature vector.

For easy trajectory-following tasks providing noticeable visual reference, the optimized skill model f_1 can be simple so $\boldsymbol{\theta}_d$ is easily noticeable. Therefore, most

of previous skill training was only conducted on this kind of simple trajectory following tasks, with manual model-driven approaches for skill modeling.

The latter design issue of performance-based haptic assistance for trajectory following tasks is how to utilize the performance vector $\boldsymbol{e}$ to generate feedback vector $\boldsymbol{T}_{assist}$.

Let f_2 be a generalized method of haptic assistance, then

$$\boldsymbol{T}_{assist}\left(t\right) = f_2\left(\boldsymbol{e}\left(t\right)\right). \tag{7.3}$$

For example, the easiest form of haptic assistance is performance-based haptic guidance which utilizes PID control. The feedback vector for PID-based haptic guidance as an example of haptic assistance can be generated as:

$$\boldsymbol{T}_{assist,G}\left(t\right) = \boldsymbol{K}_{pid}\boldsymbol{e}\left(t\right) + \boldsymbol{I}_{pid}\int_{t_0}^{t}\boldsymbol{e}\left(t'\right)dt' + \boldsymbol{D}_{pid}\dot{\boldsymbol{e}}. \tag{7.4}$$

It intuitively generates $\boldsymbol{T}_{assist}$ almost proportional to $\boldsymbol{e}$. Hence, a learner can perceive his/her own performance error $\boldsymbol{e}$, intuitively in a form of kinesthetic feedback.

Using this framework, it is also feasible to generate error amplification methods [18, 59] with providing negative proportional gains to the proposed guidance. Although many types of haptic assistance can be implemented with the proposed design framework, the author suggests that the trainer should have great caution to design f_2 for learners to easily recover the performance error vector to understand the nature of the task.

VIII. Conclusions

In this thesis, the author proposes human-like haptic assistance, a novel data-driven framework for driving skill enhancement and training. Finally, in this chapter, we summarize our finding and propose future works that should be pursued.

8.1 Summary of Findings and Contributions

8.1.1 Hybrid Haptic Assistance

The author proposed hybrid haptic assistance for virtual steering task. In a hybrid way, two methods of haptic assistance (haptic guidance and haptic disturbance) have been combined into a performance-based, progressive scheme. The training effectiveness of hybrid haptic assistance was investigated in a human experiment. Even though the statistical significance was not supported due to large individual variance, the author could observe the learner's learning behavior to confirm that combining two augmented feedback can induce synergistic effect on the training the steering skill. In other words, by combining two different assistance methods, more effective training might be possibly promoted.

8.1.2 Haptic Driving Training Simulator

We developed a haptic driving training simulator that provides realistic experiences, to accomplish both modeling and driving skill training. In our simulator, performance-based haptic feedback can be delivered to a learner to assist with the training for the simultaneous manipulation of both a steering wheel and an accelerator pedal.

8.1.3   Driving Skill Modeling Using Neural Networks

To design proper haptic feedback for realistic driving skill of both steering and pedaling, an adequate optimized model of the skill is required. To this end, we used artificial neural networks to extract a driving expert's motor behavior when modeling the skill. We validated our proposed model with predictive errors, and objectively proved the performance of haptic guidance using the model by performing a human experiment. In results, our modeling approach showed an ability to capture specific behavior of experienced drivers, which indicates the validity of our modeling approach. Further, we implemented PID-based haptic guidance using the performance errors obtained by the neural-network-model of steering and pedaling, then demonstrated those errors to novice drivers to show applicability of our approach. In results, the transfer of performance errors significantly enhanced novice drivers' steering performance, whereas it failed to enhance pedaling performance. We conjecture the problem of pedaling skill recognition can be incurred due to the different cognitive capacity on steering and pedaling.

8.1.4   Human-like Haptic Assistance

To show that our framework can demonstrate the optimized skill execution of both steering and pedaling, we designed a generalized autopilot algorithm using PID control. In results, all the autopilot modes (implemented by the NN-based pedaling model) using our steering model and the conventional steering model can drive appropriately on different types of paths. However, their behavior of steering was meaningfully different; our framework steered the steering wheel more similar to humans. Therefore, we named our framework, human-like haptic assistance. The human-like haptic assistance can induce more accurate driving style but less stable driving style,compared to the conventional, robotic haptic

assistance. Therefore, we designed the final human experiment querying whether different styles of driving can be inherited after the training in two distinct haptic assistance methods (human-like and robotic), where the optimized skill model of steering is only different. In results, the novice drivers trained by human-like haptic assistance resulted more improved accuracy and stability performance. Because the driving style of human-like haptic assistance is more similar to humans, our results of the experiment indicate that to induce better training effectiveness (or, to overcome the guidance hypothesis), the design of haptic assistance should necessarily demonstrate natural execution of humans for a certain task.

8.2 Future Works

We should mention here is the feasibility of human-like haptic assistance for different kinds of trajectory-following tasks. The human-like haptic assistance outperformed the conventional haptic assistance in both terms of the accuracy and stability performance. The most obvious characteristic of the human-like haptic assistance is that because it its formulated by real humans, the final movements to control a certain target task become similar to real humans.

For haptic assistance designers, the conventional model-driven approach always require additional considerations and efforts to present a similar behavior to the nature of the task dynamics. However, using the neural networks as our approach, those considerations and efforts can be minimized and even the researchers might be convinced to achieve a better training effectiveness as a final outcome. Therefore, the author suggests that human-like haptic assistance using neural networks can be a feasible solution for future motor learning and rehabilitation studies targeting the training of composite continuous trajectory-following skills.

To this end, we note that there remain opportunities for the application of

other well-known approaches, such as Learning from Demonstration (LfD) [8], to realize efficient reference modeling for the driving skill to design an advanced version of human-like haptic assistance. Moreover, several machine-learning techniques that are based on a human decision behavior, such as the hidden Markov model (HMM) [55, 58], would be a novel extension to our data-driven modeling approach for more difficult, decision-based tasks.

요 약 문

운전 기능은 실용성 및 연구적 필요성이 높은 대표적인 감각운동 기능이다. 본 논문에서 저자는 운전 기능의 향상과 교육을 목적으로 하는 인간-유사 햅틱 어시스턴스를 제시한다. 인간-유사 햅틱 어시스턴스는 신경망 알고리즘과 성능-기반 햅틱 피드백을 사용하는 새로운 형태의 데이터 주도 햅틱 어시스턴스 프레임워크라고 할 수 있다.

사전 연구로 저자는 혼합형 햅틱 어시스턴스라고 부르는, 기존 두 가지의 성능-기반 햅틱 어시스턴스(햅틱 가이던스 및 디스터번스)를 혼합한 어시스턴스 방법을 개발하고 이를 이용하여 가상 조향 기능을 교육하는 실험을 진행하였다. 이 혼합형 방법은 교육 초반에는 햅틱 가이던스가 사용되지만 훈련자의 성능에 따라 점진적으로 햅틱 디스터번스로 변화하는 형태를 가지고 있으며, 실험 결과 해당 방법의 다양한 장점을 확인할 수 있었으나 통계적 유의성은 확보할 수 없었다.

저자는 이러한 사전 연구를 확장시켜 더욱 실제 상황과 유사한 운전 교육을 진행하고자 하였고, 이를 위해 실제와 유사한 시뮬레이션이 가능한 햅틱 운전 훈련 시뮬레이터를 개발하였다. 그리고 전문가 모델 수립을 목적으로 시뮬레이터를 통해 숙련된 운전자의 운전 데이터를 수집, 수집한 데이터로 인공 신경망을 훈련시켰다. 그 결과, 인공 신경망을 통해 전문가의 성공적인 운전 기능(조향 및 페달)을 예측 값을 제공할 수 있는 최적화된 기능 모델을 개발할 수 있었다. 수립한 기능 모델의 타당성 및 성능-기반 햅틱 피드백에의 적용 가능성을 확인하기 위한 사용자 실험을 진행한 결과, 우리의 방법이 전문가의 조향 및 페달 양상을 타당하게 추출하는 것을 확인하였다. 단, 성능-기반 햅틱 피드백의 적용 가능성에 대해서는 조향 모델에 대해서만 확보할 수 있었다.

이에 따라 저자는 해당 전문가 모델을 사용하여 성능-기반 햅틱 피드백이 아닌 자

율주행 알고리즘을 개발, 다양한 도로 상황에서의 자율주행 테스트를 진행하였다. 그 결과 우리의 기능 모델로 개발된 자율 주행 알고리즘이 모든 도로에서 성공적인 주행이 가능하다는 사실이 확인되었으며, 특히 시뮬레이터의 주행 자체가 인간 전문가에 의해 개발된 모델 덕에 인간과 유사한 조향 양상을 보인다는 사실을 확인하였다.

이에 따라 저자는 본 논문의 프레임워크를 인간-유사 어시스턴스로 명명하였고, 프레임워크를 충실하게 따르는 인간-유사 가이던스를 개발하였다. 그리고 대조군인 기존 로봇 가이던스에 대비하여 인간-유사 가이던스가 조향 기능 교육에 가지는 이점을 확인하기 위해 두 방법 각각에 성능-기반 점진적 알고리즘을 적용, 최종적인 조향 기능 교육 실험을 진행하였다. 실험 결과, 로봇 가이던스 교육 방법에 비해 인간-유사 가이던스 교육 방법이 조향의 정확성 및 안정성 모두를 더욱 높게 향상시킬 수 있다는 사실을 확인하였으며, 이는 인간-유사 가이던스가 인간의 자연스러운 조향 양상을 반영하기 때문으로 이해할 수 있다. 따라서, 저자는 우리의 인간-유사 햅틱 어시스턴스 방법이 운전 기능의 향상 및 교육에 모두 효과를 나타낸다는 사실을 입증할 수 있었으며, 궤도-추적과 같은 다른 감각운동 기능 교육에도 해당 프레임워크가 확장될 수 있을 것으로 기대한다.

References

[1] Vehicle Physics Pro (VPP). https://www.vehiclephysics.com/.

[2] Automobile-Catalog. https://www.automobile-catalog.com/.

[3] Catlike Coding: Unity Tutorials. https://www.catlikecoding.com/.

[4] D. A. Abbink and M. Mulder. Neuromuscular analysis as a guideline in designing shared control. In *Advances in haptics*, pages 499–516. InTech, Vienna, Austria, 2010.

[5] D. A. Abbink, M. Mulder, and E. R. Boer. Haptic shared control: Smoothly shifting control authority? *Cogn. Tech. Work*, 14(1):19–28, 2012.

[6] D. A. Abbink, M. Mulder, F. C. Van der Helm, and E. Boer. Measuring neuromuscular control dynamics during car following with continuous haptic feedback. *IEEE Trans. Syst. Man Cybern. B Cybern.*, 41(5):1239–1249, 2011.

[7] J. Accot and S. Zhai. Beyond Fitts' law: Models for trajectory-based HCI tasks. In *Proceedings of the ACM SIGCHI Conference on Human Factors in Computing Systems*, pages 295–302. ACM, 1997.

[8] B. D. Argall, S. Chernova, M. Veloso, and B. Browning. A survey of robot learning from demonstration. *Rob. Auton. Syst.*, 57(5):469–483, 2009.

[9] B. Bayart, A. Pocheville, and A. Kheddar. An adaptive haptic guidance software module for I-TOUCH: Example through a handwriting teaching simulation and a 3D maze. In *Proceedings of the IEEE International Workshop on Haptic Audio Visual Environments and their Applications*, pages 51–56, 2005.

[10] B. S. Bell and S. W. J. Kozlowski. Adaptive guidance: Enhancing self-regulation, knowledge, and performance in technology-based training. *Pers. Psychol.*, 55(2):267–306, 2002.

[11] T. L. Brooks. Telerobotic response requirements. In *Proceedings of the IEEE International Conference on Systems, Man and Cybernetics*, pages 113–120, 1990.

[12] E. Burdet and T. E. Milner. Quantization of human motions and learning of accurate movements. *Biol. Cybern.*, 78(4):307–318, 1998.

[13] H. Cai and Y. Lin. Coordinating cognitive assistance with cognitive engagement control approaches in human-machine collaboration. *IEEE Trans. Syst. Man Cybern. A Syst. Humans*, 42(2):286–294, 2012.

[14] V. Cavallo, M. Brun-Dei, O. Laya, and M. Neboit. Perception and anticipation in negotiating curves: The role of driving experience. In A. G. Gale, M. H. Freeman, C. M. Haslegrave, P. Smith, and S. P. Taylor, editors, *Vision in Vehicles II: Proceedings of the Second International Conference on Vision in Vehicles*, pages 365–374. Elsevier, 1988.

[15] B. Corteville, E. Aertbelien, H. Bruyninckx, J. De Schutter, and H. Van Brussel. Human-inspired robot assistant for fast point-to-point movements. In *Proceedings of the IEEE International Conference on Robotics and Automation*, pages 3639–3644, 2007.

[16] D. M. Dimitrov and P. D. Rumrill Jr. Pretest-posttest designs and measurement of change. *Work*, 20(2):159–165, 2003.

[17] M. A. Eid, M. Mansour, A. E. Saddik, and R. Iglesias. A haptic multimedia handwriting learning system. In *Proceedings of the International Workshop on Educational Multimedia and Multimedia Education*, pages 103–108, 2007.

[18] J. L. Emken and D. J. Reinkensmeyer. Robot-enhanced motor learning: Accelerating internal model formation during locomotion by transient dynamic amplification. *IEEE Trans. Neural Syst. Rehabil. Eng.*, 13(1):33–39, 2005.

[19] A. R. Ferber, M. Peshkin, and J. E. Colgate. Using kinesthetic and tactile cues to maintain exercise intensity. *IEEE Trans. Haptics*, 2(4):224–235, 2009.

[20] D. Feygin, M. Keehner, and F. Tendick. Haptic guidance: Experimental evaluation of a haptic training method for a perceptual motor skill. In *Proceedings of the International Symposium on Haptic Interfaces for Virtual Environment and Teleoperator Systems*, pages 40–47, 2002.

[21] B. A. C. Forsyth and K. E. MacLean. Predictive haptic guidance: Intelligent user assistance for the control of dynamic tasks. *IEEE Trans. Visual Comput. Graphics*, 12(1):103–113, 2006.

[22] G. Garimella, J. Funke, C. Wang, and M. Kobilarov. Neural network modeling for steering control of an autonomous vehicle. In *Proceedings of the IEEE/RSJ International Conference on Intelligent Robots and Systems*, pages 2609–2615, 2017.

[23] R. B. Gillespie, M. S. O'Modhrain, P. Tang, D. Zaretzky, and C. Pham. The virtual teacher. In *Proceedings of the ASME Dynamic Systems and Control Division*, pages 171–178, 1998.

[24] M. A. Goodrich, A. C. Schultz, et al. Human-robot interaction: A survey. *Foundations and Trends in Human-Computer Interaction*, 1(3):203–275, 2008.

[25] E. R. Guthrie. *Psychology of Learning*. Harper & Row, 1935.

[26] K. Henmi and T. Yoshikawa. Virtual lesson and its application to virtual calligraphy system. In *Proceedings of the IEEE International Conference on Robotics and Automation*, volume 2, pages 1275–1280, 1998.

[27] H. Heuer and J. Lüttgen. Robot assistance of motor learning: A neuro-cognitive perspective. *Neurosci. Biobehav. Rev.*, 56:222–240, 2015.

[28] T. Hiraoka, O. Nishihara, and H. Kumamoto. Steering reactive torque presentation method for a steer-by-wire vehicle. *Rev. Automot. Eng.*, 29:287–294, 2008.

[29] M. Hirokawa, N. Uesugi, S. Furugori, T. Kitagawa, and K. Suzuki. Effect of haptic assistance on learning vehicle reverse parking skills. *IEEE Trans. Haptics*, 7(3):334–344, 2014.

[30] S. Holland, A. J. Bouwer, M. Dalgelish, and T. M. Hurtig. Feeling the beat where it counts: Fostering multi-limb rhythm skills with the haptic drum kit. In *Proceedings of the ACM International Conference on Tangible, Embedded, and Embodied Interaction*, pages 21–28. ACM, 2010.

[31] J. C. Huegel and M. K. O'Malley. Progressive haptic and visual guidance for training in a virtual dynamic task. In *Proceedings of the IEEE Haptics Symposium*, pages 343–350, 2010.

[32] A. H. Jamson, D. L. Hibberd, and N. Merat. The design of haptic gas pedal feedback to support eco-driving. In *Proceedings of the International Driving Symposium on Human Factors in Driver Assessment, Training, and Vehicle Design*, pages 264–270, 2013.

[33] L. E. Kahn, M. L. Zygman, W. Z. Rymer., and D. J. Reinkensmeyer. Robot-assisted reaching exercise promotes arm movement recovery in chronic hemi-

paretic stroke: A randomized controlled pilot study. *J. NeuroEng. Rehabil.*, 3(12):1–13, 2006.

[34] J. A. S. Kelso. *Human motor behavior: An introduction.* Lawrence Erlbaum Associates, Hillsdale, NJ, 1982.

[35] A. Kumar, Y. Tanaka, A. Grigoriadis, J. Grigoriadis, M. Trulsson, and P. Svensson. Training-induced dynamics of accuracy and precision in human motor control. *Sci. Rep.*, 7(1):6784, 2017.

[36] H. Lee, G. Han, I. Lee, S. Yim, K. Hong, H. Lee, and S. Choi. Haptic assistance for memorization of 2D selection sequences. *IEEE Trans. Human-Mach. Syst.*, 2013.

[37] I. Lee and S. Choi. Vibrotactile guidance for drumming learning: Method and perceptual assessment. In *Proceedings of the IEEE Haptics Symposium*, pages 147–152. IEEE, 2014.

[38] J. Lee and S. Choi. Effects of haptic guidance and disturbance on motor learning: Potential advantage of haptic disturbance. In *Proceedings of the IEEE Haptics Symposium*, pages 335–342, 2010.

[39] Y. Lin, P. Tang, W. Zhang, and Q. Yu. Artificial neural network modelling of driver handling behaviour in a driver-vehicle-environment system. *Int. J. Veh. Des.*, 37(1):24–45, 2005.

[40] J. Liu, S. C. Cramer, and D. J. Reinkensmeyer. Learning to perform a new movement with robotic assistance: Comparison of haptic guidance and visual demonstration. *J. NeuroEng. Rehabil.*, 3(20):1–10, 2006.

[41] I. S. MacKenzie. Fitts' law as a research and design tool in Human-Computer interaction. *Hum-Comput. Interact.*, 7(1):91–139, 1992.

[42] R. A. Magill. *Motor Learning: Concepts and Applications*. McGraw-Hill, New York, NY, USA, 6th edition, 2000.

[43] L. Marchal-Crespo, J. Furumasu, and D. J. Reinkensmeyer. A robotic wheelchair trainer: Design overview and a feasibility study. *J. NeuroEng. Rehabil.*, 7(40):1–12, 2010.

[44] L. Marchal-Crespo, S. McHughen, S. C. Cramer, and D. J. Reinkensmeyer. The effect of haptic guidance, aging, and initial skill level on motor learning of a steering task. *Exp. Brain Res.*, 201(2):209–220, 2009.

[45] L. Marchal-Crespo and D. J. Reinkensmeyer. Haptic guidance can enhance motor learning of a steering task. *J. Mot. Behav.*, 40(6):545–556, 2008.

[46] L. Marchal-Crespo and D. J. Reinkensmeyer. Review of control strategies for robotic movement training after neurologic injury. *J. NeuroEng. Rehabil.*, 6(1):20, 2009.

[47] M.-H. Milot, L. Marchal-Crespo, C. S. Green, S. C. Cramer, and D. J. Reinkensmeyer. Comparison of error-amplification and haptic-guidance training techniques for learning of a timing-based motor task by healthy individuals. *Exp. Brain Res.*, 201(2):119–131, 2009.

[48] M. Mulder, D. A. Abbink, and E. R. Boer. Sharing control with haptics: Seamless driver support from manual to automatic control. *Hum. Factors*, 54(5):786–798, 2012.

[49] M. Mulder, D. A. Abbink, M. M. van Paassen, and M. Mulder. Design of a haptic gas pedal for active car-following support. *IEEE Trans. Intell. Transp. Syst.*, 12(1):268–279, 2011.

[50] M. Mulder, M. R. v. Paassen, and E. R. Boer. Exploring the roles of information in the manual control of vehicular locomotion: From kinematics and dynamics to cybernetics. *Presence-Teleop. Virt.*, 13(5):535–548, 2004.

[51] K. S. Narendra and K. Parthasarathy. Identification and control of dynamical systems using neural networks. *IEEE Trans. Neural Netw.*, 1(1):4–27, 1990.

[52] M. C. Nechyba. *Learning and validation of human control strategies.* Ph.d. thesis, The Robotics Institue, Carnegie Mellon University, 1998.

[53] M. C. Nechyba and Y. Xu. Human skill transfer: Neural networks as learners and teachers. In *Proceedings of the IEEE/RSJ International Conference on Intelligent Robots and Systems*, volume 3, pages 314–319, 1995.

[54] M. C. Nechyba and Y. Xu. On the fidelity of human skill models. In *Proceedings of the IEEE International Conference on Robotics and Automation*, volume 3, pages 2688–2693, 1996.

[55] M. C. Nechyba and Y. Xu. Human control strategy: Abstraction, verification, and replication. *IEEE Control Syst. Mag.*, 17(5):48–61, 1997.

[56] M. C. Nechyba and Y. Xu. Stochastic similarity for validating human control strategy models. *IEEE Trans. Robot. Autom.*, 14(3):437–451, 1998.

[57] S. Oh, H.-J. So, and M. Gaydos. Hybrid augmented reality for participatory learning: The hidden efficacy of multi-user game-based simulation. *IEEE Trans. Learn. Technol.*, 11(1):115–127, 2018.

[58] R. H. Osgouei, H. Lee, and S. Choi. Comparative evaluation of performance measures for human driving skills. *Intelligent Service Robotics*, 6(4):169–180, 2013.

[59] J. L. Patton, M. Kovic, and F. A. Mussa-Ivaldi. Custom-designed haptic training for restoring reaching ability to individuals with poststroke hemiparesis. *J. Rehabil. Res. Dev.*, 43(5):643–656, 2006.

[60] J. L. Patton, M. E. Stoykov, M. Kovic, and F. A. Mussa-Ivaldi. Evaluation of robotic training forces that either enhance or reduce error in chronic hemiparetic stroke survivors. *Exp. Brain Res.*, 168(3):368–383, 2006.

[61] S. M. Petermeijer, D. A. Abbink, M. Mulder, and J. C. de Winter. The effect of haptic support systems on driver performance: A literature survey. *IEEE Trans. Haptics*, 8(4):467–479, 2015.

[62] D. Powell and M. K. O'Malley. The task-dependent efficacy of shared-control haptic guidance paradigms. *IEEE Trans. Haptics*, 5(3):208–219, 2012.

[63] D. J. Reinkensmeyer. and J. L. Patton. Can robots help the learning of skilled actions? *Exerc. Sport Sci. Rev.*, 37(1):43–51, 2009.

[64] D. S. Reisman, R. Wityk, K. Silver, and A. J. Bastian. Locomotor adaptation on a split-belt treadmill can improve walking symmetry post-stroke. *Brain*, 130(7):1861–1872, 2007.

[65] L. Saleh, P. Chevrel, F. Claveau, J.-F. Lafay, and F. Mars. Shared steering control between a driver and an automation: Stability in the presence of driver behavior uncertainty. *IEEE Trans. Intell. Transp. Syst.*, 14(2):974–983, 2013.

[66] A. W. Salmoni, R. A. Schmidt, and C. B. Walter. Knowledge of results and motor learning: A review and critical reappraisal. *Psychol. Bull.*, 95(3):355–386, 1984.

[67] R. A. Schmidt. A schema theory of discrete motor skill learning. *Psychol. Rev.*, 82(4):225–260, 1975.

[68] R. A. Schmidt. Frequent augmented feedback can degrade learning: Evidence and interpretations. In J. Requin and G. E. Stelmach, editors, *Proceedings of the NATO Advanced Study Institute*, pages 59–75, 1990.

[69] R. A. Schmidt and T. D. Lee. *Motor Control and Learning: A Behavioral Emphasis.* Human Kinetics, Windsor, ON, USA, 4th edition, 2005.

[70] J. Solis, C. A. Avizzano, and M. Bergamasco. Teaching to write Japanese characters using a haptic interface. In *Proceedings of the International Symposium on Haptic Interfaces for Virtual Environment and Teleoperator Systems*, pages 255–262, 2002.

[71] D. Spelmezan, M. Jacobs, A. Hilgers, and J. Borchers. Tactile motion instructions for physical activities. In *Proceedings of the ACM SIGCHI Conference on Human Factors in Computing Systems*, pages 2243–2252. ACM, 2009.

[72] M. Steele and R. B. Gillespie. Shared control between human and machine: Using a haptic steering wheel to aid in land vehicle guidance. *Proc. Hum. Factors Ergon. Soc. Annu. Meet.*, 45(23):1671–1675, 2001.

[73] E. Velloso, D. Schmidt, J. Alexander, H. Gellersen, and A. Bulling. The feet in human–computer interaction: A survey of foot-based interaction. *ACM Comput. Surv.*, 48(2):21:1–21:35, 2015.

[74] R. Wallis, B. Elliott, and M. Koh. The effect of a fast bowling harness in cricket: An intervention study. *J. Sports Sci.*, 20(6):495–506, 2002.

[75] J. O. Wobbrock, E. Cutrell, S. Harada, and I. S. MacKenzie. An error model for pointing based on Fitts' law. In *Proceedings of the ACM SIGCHI Conference on Human Factors in Computing Systems*, pages 1613–1622. ACM, 2008.

[76] Y. Yokokohji, R. L. Hollis, and T. Kanade. WYSIWYF display: A visual/haptic interface to virtual environment. *Presence-Teleop. Virt.*, 8(4):412–434, 1999.

[77] Y. Zhang, W. C. Lin, and Y.-K. S. Chin. A pattern-recognition approach for driving skill characterization. *IEEE Trans. Intell. Transp. Syst.*, 11(4):905–916, 2010.

Publications

International Journals

1. **Hojin Lee**, Gabjong Han, In Lee, Sunghoon Yim, Kyungpyo Hong, Hye-seon Lee, and Seungmoon Choi. Haptic assistance for memorization of 2D selection sequences. *IEEE Transactions on Human-Machine Systems*, 43(6):643–649, 2013.

2. Reza Haghighi Osgouei, **Hojin Lee**, and Seungmoon Choi. Comparative evaluation of performance measures for human driving skills. *Intelligent Service Robotics*, 17(3):169–180, 2013.

3. **Hojin Lee**, Ji-Sun Kim, Jae-Young Kim, Seungmoon Choi, Jae-Hoon Jun, Jong-Rak Park, A-Hee Kim, Han-Byeol Oh, Jun-Hyeok Baek, Seung-Jin Yang, Hyung-Sik Kim, and Soon-Cheol Chung. Mid-air tactile stimulation using indirect laser radiation. *IEEE Transactions on Haptics*, 9(4):574–585, 2016.

International Conference: Papers

1. **Hojin Lee**, Gabjong Han, In Lee, Sunghoon Yim, Kyungpyo Hong, and Seungmoon Choi. Effect of active and passive haptic sensory information on memory for 2D sequential selection task. In *Proceedings of the International Symposium on Ubiquitous Virtual Reality (ISUVR)*, pages 52–54, 2011.

2. Sunghwan Shin, In Lee, **Hojin Lee**, Gabjong Han, Kyungpyo Hong, Sunghoon Yim, Jongwon Lee, YoungJin Park, Byeong Ki Kang, Dae Ho Ryoo, Dae Whan Kim, Seungmoon Choi, and Wan Kyun Chung. Haptic simulation

of refrigerator door. In *Proceedings of the IEEE Haptics Symposium*, pages 147–154, 2012.

3. **Hojin Lee** and Seungmoon Choi. Combining haptic guidance and haptic disturbance: An initial study of hybrid haptic assistance for virtual steering task. In *Proceedings of the IEEE Haptics Symposium*, pages 159–165, 2014.

4. Hoang Minh Phuong, Jaebong Lee, **Hojin Lee**, Kyusong Lee, Gary Geunbae Lee, and Seungmoon Choi. Haptic-enabled English education system. In *Lecture Notes in Electrical Engineering (AsiaHaptics 2014)*, 277:293–296, 2014.

5. **Hojin Lee**, Ji-Sun Kim, Seungmoon Choi, Jae-Hoon Jun, Jong-Rak Park, A-Hee Kim, Han-Byeol Oh, Hyung-Sik Kim, and Soon-Cheol Chung. Mid-air tactile stimulation using laser-induced thermoelastic effects: The first study for indirect radiation. In *Proceedings of the IEEE World Haptics Conference (WHC)*, pages 374–380, 2015.

6. Hojun Cha, **Hojin Lee**, Junsuk Park, Hyung-Sik Kim, Soon-Cheol Chung, and Seungmoon Choi. Mid-air tactile display using indirect laser radiation for contour-following stimulation and assessment of its spatial acuity. In *Proceedings of the IEEE World Haptics Conference (WHC)*, pages 136–141, 2017.

7. Yongjae Yoo, **Hojin Lee**, Hyejin Choi, and Seungmoon Choi. Emotional responses of vibrotactile-thermal stimuli: Effects of constant-temperature thermal stimuli. In *Proceedings of the International Conference on Affective Computing and Intelligent Interaction (ACII)*, pages 273–278, 2017.

8. Hyejin Choi, Seongwon Cho, Sunghwan Shin, **Hojin Lee**, and Seungmoon Choi. Data-driven thermal rendering: An initial study. In *Proceedings of*

the IEEE Haptics Symposium, pages 344–350, 2018.

International Conference: Demonstrations

1. **Hojin Lee**, Ji-Sun Kim, Seungmoon Choi, Jae-Hoon Jun, Jong-Rak Park, A-Hee Kim, Han-Byeol Oh, Sung-Jun Park, Hyung-Sik Kim, and Soon-Cheol Chung. Mid-air tactile stimulation using laser-induced thermoelastic effects: The first study for indirect radiation. Demonstrated in *the IEEE World Haptics Conference (WHC)*, 2015.

2. Hojun Cha, **Hojin Lee**, Junsuk Park, Hyung-Sik Kim, Soon-Cheol Chung, and Seungmoon Choi. Mid-air tactile application using indirect laser radiation for contour-following stimulation. Demonstrated in *the IEEE World Haptics Conference (WHC)*, 2017.

3. **Hojin Lee**, Hojun Cha, Junsuk Park, Seungmoon Choi, Hyung-Sik Kim, and Soon-Cheol Chung. LaserStroke: Mid-air tactile experiences on contours using indirect laser radiation. Demonstrated in *the ACM Symposium on User Interface Software and Technology (UIST)*, pages 73–74, 2016.

4. **Hojin Lee**, Hyoungkyun Kim, and Seungmoon Choi. Haptic assistance using neural networks for driving skill enhancement and training. Demonstrated in *the AsiaHaptics* (Video Demonstration), 2018.

International Conference: Abstracts/Posters/Presentations

1. Reza Haghighi Osgouei, **Hojin Lee**, and Seungmoon Choi. Haptic-enabled driving training system. In *Proceedings of the IEEE International Symposium on Robot and Human Interactive Communication (RO-MAN)*, pages 302–303, 2013 (Work-In-Progress).

2. **Hojin Lee**, Jongman Seo, and Seungmoon Choi. Psychophysical magnitude function of vibrotactile stimuli with similar physical characteristics to laser stimulus. At *the International Biomedical Engineering Conference (IBEC)*, 2014 (Special Session).

3. **Hojin Lee** and Seungmoon Choi. Physical analysis of indirect laser radiation for mid-air tactile stimulation. At *the International Biomedical Engineering Conference (IBEC)*, 2015 (Special Session).

Domestic Journals

1. Jaebong Lee, Kyusong Lee, Hoang Minh Phuong, **Hojin Lee**, Gary Geunbae Lee, and Seungmoon Choi. POMY: POSTECH immersive English study with haptic feedback. *Journal of Institute of Control, Robotics and Systems*, 20(8):815–821, 2014.
이재봉, 이규송, Hoang Minh Phuong, **이호진**, 이근배, 최승문. POMY: 햅틱 피드백을 적용한 몰입형 영어 학습 시스템. 제어 로봇 시스템 학회 논문지, 20(8):815–821, 2014.

Domestic Conference: Papers/Demonstrations

1. Gunhyuk Park, Seunghwan Oh, **Hojin Lee**, and Seungmoon Choi. Color information transfer with vibration feedback. In *Proceedings of KIISE Fall Conference*, pages 58–59, 2010.
박건혁, 오승환, **이호진**, 최승문. 진동을 통한 색상 정보 전달. 정보과학회 가을 학술발표논문집, pages 58–59, 2010.

2. **Hojin Lee**, Gabjong Han, In Lee, Sunghoon Yim, Kyungpyo Hong, and Seungmoon Choi. Effect of active and passive haptic sensory information on memory for 2D sequential selection task. In *Proceedings of the HCI*

Korea, pages 248–250, 2011.

이호진, 한갑종, 이인, 임성훈, 홍경표, 최승문. 이차원 순차 선택에서의 능동 및 수동 햅틱 정보 제공을 통한 기억력 향상. 한국 HCI 학술대회 논문집, pages 248–250, 2011.

3. **Hojin Lee**, Reza Haghighi Osgouei, In Lee, Sunghwan Shin, and Seung-moon Choi. Haptic accelerator pedal for providing force feedback in virtual driving environment. In *Proceedings of the 8th KROC*, pages 257–258, 2013.

   이호진, Reza Haghighi Osgouei, 이인, 신성환, 최승문. 가상 운전 환경에서의 힘 피드백 제공을 위한 햅틱 가속 페달. 제 8회 한국로봇종합학술대회 논문집, pages 257–258, 2013.

4. **Hojin Lee** and Seungmoon Choi. Hybrid assistance combining haptic guidance and disturbance for steering task. In *Proceedings of the HCI Korea*, pages 215–217, 2013.

   이호진, 최승문. 조향 교육을 위한 햅틱 유도와 방해의 혼합형 햅틱 도움 방법. 한국 HCI 학술대회 논문집, pages 215–217, 2013.

5. Kyusong Lee, Jaebong Lee, Nohkyung Lee, Chiyoung Lee, Hoang Minh Phuong, Sangdo Han, and **Hojin Lee**. POMY: POSTECH immersive English study with haptic feedback. Demonstrated in *the HCI Korea (HCI KIDS)*, 2014.

   이규송, 이재봉, 이노경, 이치영, Hoang Minh Phuong, 한상도, **이호진**. POMY: 햅틱 피드백을 적용한 몰입형 영어 학습 시스템. 한국 HCI 학술대회 - HCI KIDS, 2014.

6. Hyejin Choi, Seongwon Cho, Sunghwan Shin, **Hojin Lee**, and Seungmoon Choi. Data-driven thermal rendering. In *Proceedings of the 13th KROC*, 2018.

   최혜진, 조성원, 신성환, **이호진**, 최승문. 데이터 기반 온감 렌더링. 제 13회

한국로봇종합학술대회 논문집, 2018.

7. **Hojin Lee**, Hyongkyun Kim, and Seungmoon Choi. Driving skill modeling using neural networks for robot-mediated haptic training. In *Proceedings of the 13th KROC*, 2018.

   이호진, 김형균, 최승문. 로봇 중재를 활용한 햅틱 훈련을 위한 운전 기능의 신경망 기반 모델링. 제 13회 한국로봇종합학술대회 논문집, 2018.

Acknowledgements

오랜 기간의 여정이 일단락되고 있습니다. 처음 햅틱스 및 가상현실 연구실의 신입생으로 들어온 2010년의 저, 처음 포항공대 학부생으로 입학했을 때의 2006년의 저에 비해 지금의 저는 얼마나 변화했을까요? 제 연구의 주된 내용 또한 배움에 대한 것이었습니다. 배움이라는 것은 변화와 향상을 의미합니다. 현역에서 교육계에 몸담고 계신 부모님의 의지가 투영된 것이었던, 들어오고 처음 한국연구재단의 감각운동 기능의 모델링 및 전수 과제를 처음 맡게 되었을 때 해당 연구를 마무리하고 싶었던 생각에서 시작한 제 연구가 결국 뜻있는 결과를 남기고 졸업하게 되는 것에서 큰 뿌듯함과 후련함을 느끼고 있습니다. 이에 제 연구에 도움을 주신 많은 분들께 이 지면을 빌어 감사의 말씀을 올리고자 합니다.

부모님, 동생, 할머니, 할아버지, 여러 친지분들의 응원과 격려가 없었다면 이 연구 여정을 중도에 포기했을지도 모릅니다. 객지 포항에서의 여정이 끝나기를 기다려 준 가족과 친지 여러분께 항상 감사드리며, 이 은혜 반드시 보답하도록 하겠습니다. 함께 입학한 경표 형, 명찬이 형은 떠나면서 호진이 너는 박사를 해야 한다고 말씀하셨습니다. 형들의 격려 덕에 무사히 졸업합니다. Reza, thank you. You were a truly nice mentor for me. 대학원에서 제일 오랜 시간을 함께한 두 사람, Friendly한 룸메이트 성환, 그리고 며칠 빨리 태어난 용재. 항상 고마운 마음 뿐이다. 앞으로도 오래오래 보자. 최근 연구에 여러 도움을 준 승재, 덕분에 무사히 졸업하니 너도 어서 여정을 마치고 좋은 연구 결과로 졸업하기를. 파이오니어 과제를 함께한 호준, 현대 운전 과제를 함께한 인석, 고맙다. 두 사람의 무궁무진한 잠재력은 이미 믿고 있으니 그 잠재력이 어서 피어나기만 기다릴게. 함께 졸업하게 되는 혜진이, 선웅이. 졸업 너무너무 축하하고, 두 사람 앞날에도 언제나 희망이 가득차기를 바랄게. 대학원에서 제일 중요한 시기에 있는 상윤이, 성원이, 겨레, 성호, 그동안 함께 생활하면서 너무 즐거웠고, 많은 부분에서 도와주고 도움을 받을 수 있어 다행이었다고 생각해. 각자 하는 일들 또한 최고의 실력으로 마무리을 수 있을 거라 믿어 의심치 않는

다. 앞으로의 미래가 기대되는 효승이, 채용이, 지완이, 어려운 일 없이 모든 일들을 해결하길 바라고, 또 함께 웃도록 하자. Amit, thank you. It was a short but really valuable experience with you. 대학원에서 함께 동고동락한 적 있는, 그리고 또 뵙게 될 연구실의 모든 분들, 석희 형, 종현이 형, 성훈이 형, 재봉이 형, 갑종이 형, 인이 형, 인욱이 형, 건혁이 형, 종만이 형, Phuong, 한슬이, 준석이, 종호에게도 감사의 말을 전합니다. 여러분 모두와의 수많은 경험, 연구실에서의 생활은 제가 졸업의 소중한 밑바탕이 되어 주었다고 생각합니다. 그리고 너무나도 많은 것을 또한 배우게 해준 레이저 촉감에 대한 파이오니어 과제 교수님들과 학생들에게도 감사의 말씀을 드립니다.

송황준 교수님, 학부 때부터 어리디 어렸던 제자를 줄곧 지켜봐주셔서 감사하고, 기꺼이 박사과정 심사까지 해 주셔서 너무나 감사드립니다. 더불어 제 박사과정 심사를 진행해 주신, 한성호 교수님, 조민수 교수님, (그리고 석희 형)께도, 주셨던 여러 조언의 말씀에 감사의 말씀을 올립니다.

그리고 마지막으로 교수님, 최승문 교수님께서 제 박사과정 생활 중 해주셨던 수많은 조언은 제자의 피가 되고 살이 되었습니다. 교수님과 함께한 지난 9년간은 제 인생에 있어 어느 때라도, 언제까지라도 기억에 남을 것입니다. 배움이라는 행복 아래 저를 다시 태어나게 해 주신 분께 감사의 말씀을 전합니다.

지면은 너무 좁고 감사의 마음은 끝이 없습니다. 여기서 언급하지 못한- 제 여정에 도움을 주신 모든 분들께도 감사 드립니다. 이외에 하고 싶었던 수많은 말은 잠시 미뤄 두고, 여러분들을 다시 직접 뵙고 전해드리도록 하겠습니다. 부디 앞으로도 저를 비롯한 우리 모두의 앞날이 화창하게 피어나기를 바랍니다.

2018. 12. 31.

Curriculum Vitae

Name   : **Hojin Lee**   (Ho-Jin Lee; 이 호진; 李 鎬津)

Education

2006. 3. – 2010. 2.   **B.S.**,
Department of Computer Science and Engineering, POSTECH.

2010. 3. – 2019. 2.   **M.S. & Ph.D. Integrated (Direct Ph.D.)**,
Department of Computer Science and Engineering, POSTECH.
Thesis Title:
Human-like Haptic Assistance: Performance-based Haptic Assistance
Using Neural Networks for Driving Skill Enhancement and Training
Advisor: Prof. Seungmoon Choi

Research Experiences

Grants

2010. 3. – 2013. 3.   Haptics Technology for Modeling and Transfer of Sensorimotor
Skills, National Research Laboratory (NRL), National Research
Foundation (NRF).

2010. 3. – 2011. 12.   Immersive Haptic Media Technology, Information Technology Research Center (ITRC), National IT Industry Promotion Agency
(NIPA).

2013. 9. – 2015. 8.   Research Laboratory for Natural Language-Based Immersive English Tutoring System, Basic Research Laboratory (BRL), National Research Foundation (NRF).

2014. 3. – 2017. 2.   Touch Technology Based on Laser, Pioneer Program, National
Research Foundation (NRF).

<div align="center">**Contracts**</div>

2010. 6. – 2010. 11.	Development of a Simulation System for Refrigerator Door Opening/Closing Sensations, LG Electronics.
2016. 9. – 2016. 10.	Development of Interfaces for VR Ship Cabin Design System, Samsung Heavy Industry.
2017. 1. – 2017. 2.	Design and Development of a VR Object Manipulation and Simulation System for Naval Material Handling, Samsung Heavy Industry.
2017. 4. – 2018. 3.	Haptic Technology Research for Improving NVH Emotional Quality, NGV (Hyundai Automobile Company).

Teaching Experiences

Teaching Assistant (TA)

2010 Fall	CSED103: Introduction to Programming. Undergraduate Course, Full-time.
2013 Spring	EECE511: Introduction to Virtual Reality. Graduate Course, Part-time Guest Lecturer.
2013 Fall	CSED490J: Human-Computer Interaction. Undergraduate Course, Full-time.
2013 Fall	EECE517: Introduction to Haptics. Graduate Course, Full-time.

Supervising Assistant (Mentor) for Undergraduate Research Projects

2013 Fall	Moonhyun Jung. Haptic Fluid Rendering with Force-Feedback Device.
2014 Spring	Moonhyun Jung. Virtual Frottage Simulation with Haptic Device.
2015 Spring	Beomseok Kim. Hand-Tracking and Its Application for Secondary Task Execution in Virtual Driving Environment.
2015 Fall	Beomseok Kim. Effective Secondary-Function Execution During Driving Based on Gesture Recognition.
2015 Fall	Daeyoun Kim. Image-Based Virtual Driving System Using Google Street View Images.

2016 Spring	Sangyoun Han. Authoring of Interactive and Immersive 4D content Using Actual Vehicle Motion.
2016 Spring	DongChul Kim. Mid-air Surround Haptic Interaction in Virtual Environment Using Grid-Type Tactile Glove.
2016 Fall	Deukryeol Yoon. Haptic Alarm System for Hearing Impaired by Detecting Ambient Car Sound.
2018 Spring	Hanseoup Byun. VR Umbrella: Multimodal Virtual Simulation Using Haptic Feedback on Umbrella in Rainy Day.

" Be the kind of person you wish to attract into your life."